Permeability Measurement Experiments for Fabric Preforms Used in LCM Processes

by

Ayşen Sarıoğlu

A Thesis Submitted to the

Graduate School of Engineering

in Partial Fulfillment of the Requirements for

the Degree of

Master of Science

in

Mechanical Engineering

Koc University

August, 2012

Koc University

Graduate School of Sciences and Engineering

This is to certify that I have examined this copy of a master's thesis by

Ayşen Sarıoğlu

and found that it is complete and satisfactory in all respects,

and that any and all revision required by the final

examining committee have been made.

Committee Members:

E. Murat Sözer, Ph. D.

B. Erdem Alaca, Ph. D

Seda Kızılel, Ph.D

Date: 28.08.2012

ABSTRACT

Liquid Composite Molding (LCM) processes are commonly used in the composite manufacturing industries by impregnating a stationary fiber preform placed in the mold cavity. However, to produce fully impregnated high quality end products, and provide a repeatable process, process parameters such as injection gate and vent locations and conditions, and fill time should be designed by using a process model instead of trial-and-error approach commonly used in the industry. Reliability and accuracy of the process model requires correctly measured permeability data. It is very common to see that the permeability data in the literature has a large scatter; and there is no universal agreement among the modelers about which characterization procedure (unsteady versus steady; 1D versus 2D; constant injection pressure versus constant injection flow rate) should be used for permeability measurement. Permeability measurement experiments have some issues about accuracy, repeatability and the error sensitivity as studied in this study. To investigate the sources of errors and propose methods to minimize these errors, four different types of experimental procedure for three different fabric types were performed. Non-repeatable specimen preparation, deflection of mold parts and expansion of injection equipment and tubing were observed to be the main sources of the error. Results showed that the unsteady permeabilities of the fabric preforms were up to 91% higher than the steady permeabilities. For the same fabric type, it was observed that different characterization procedures resulted in more than one order of magnitude variation. Besides constructing a permeability database, the suggestions given in this study are beneficial to minimize the anticipated sources of error and they give guidance to the experimenters to obtain more reliable and accurate results.

ÖZET

Sıvı Kompozit Kalıplama, kompozit üretim endüstrisinde yaygın olarak kullanılan, kalıp boşluğu içinde sabit duran elyafın reçine ile ıslatılmasına dayalı bir üretim yöntemidir. Ancak, tam ıslatılmış, yüksek kaliteli nihai ürün üretmek ve sürecin tekrarlanabilirliğini sağlamak için, enjeksiyon giriş ve çıkış noktaları, dolum süresi gibi süreç parametreleri endüstride sıklıkla kullanılan deneme yanılma yönteminin yerine süreç modelleri kullanılarak belirlenmelidir. Modelin güvenilirliği ve doğruluğu düzgün olarak ölçülmüş geçirgenlik verisi gerektirmektedir. Literatürdeki geçirgenlik verileri çoğunlukla büyük varyasyonlara sahiptir; ve modelleyiciler arasında hangi karekterizasyon yönteminin (kararsız, kararlı, 1 boyutlu, 2 boyutlu, sabit basınç ya da sabit akış debisi sınır koşulu kullanarak) geçirgenlik ölçümlerinde kullanılması gerektiği konusunda bir mutabakat yoktur. Geçirgenlik ölçüm deneylerinin, bu çalışmada gösterildiği gibi, doğruluk, tekrarlanabilirlik ve hata hassasiyeti konusunda sorunları vardır. Hataların kaynaklarını araştırmak ve bu hataları en aza indirebilmek için, üç farklı elyaf türünde dört farklı deney prosedürü uygulanmış ve gözlemler yapılmıştır. Tekrarlanamayan numune hazırlama süreci, kalıp parçalarında meydana gelen esneme, enjeksiyon parçalarında ve borulama sisteminde meydana gelen genleşmelerin başlıca hata kaynağı olduğu gözlemlenmiştir. Kararsız geçirgenlik değerlerinin kararlı geçirgenlik değerlerinden % 91 ’e varacak kadar yüksek olduğu gözlenmiştir. Aynı elyaf türü için, karekterizasyon yönteminin on kattan daha fazla varyasyona sebep olduğu gözlenmiştir. Bu çalışmada verilen öneriler, öngörülen hataların kaynaklarının etkilerinin en aza indirilmesinde faydalı olacaktır; ve deneycinin daha güvenilir ve doğru sonuçlar elde etmesi için rehberlik edecektir.

ACKNOWLEDGEMENTS

I owe my deepest gratitude to my advisor Murat Sözer for his continuous support, patience, and immense knowledge. His guidance helped me in all the time of my research and writing of this thesis. Furthermore, I would like to thank the rest of my thesis committee Assoc. Prof Erdem Alaca and Assist. Prof. Seda Kızılel for their participation with their invaluable comments.

I am indebted to my colleagues, Bekir Yenilmez, Barış Çağlar, Mehmet Akif Yalçınkaya, Mustafa Reşit Haboğlu and Talha Akyol and part time students Benay Uzer and Tuğçe Öztürk who never begrudged their help, support and friendship during my study in Koç University.

Many thanks are also for my friends, Sıdıka Mine Toker, Berkay Gümüş, Orkun Önal and Işınsu Baylam who have made my life in Koç University unforgettable with their friendship.

I cannot find words to express my gratefulness to my mother Perihan Sarıoğlu, my father Kurtaran Sarıoğlu, my sister Ayşin Sarıoğlu Kuzeci, my uncle Şakir Gürel and my uncle's wife Naciye Gürel for their endless love, confidence and support during whole part of my life.

NOMENCLATURE

ρ_{sup}	Superficial (surface) density of fabric per layer [kg/m^2]
ρ_f	Density of glass fibers [kg/m^3]
V_f	Fiber volume fraction
$\emptyset$	Porosity
h	Thickness of the fabric perform [m]
w	Width of the fabric preform [m]
L	Length of the fabric preform [m]
μ	Viscosity of the test fluid [mPa.s]
V_{total}	Total volume of the fabric preform [cc]
V_{pore}	Volume of porosity inside the fabric preform [cc]
$t_{fill(expected)}$	Expected fill time of fabric preform [min]
$t_{fill(experimental)}$	Experimental fill time of fabric preform [min]
Q	Volumetric flow rate (cc/min)
$\bar{K}$	Permeability tensor
K_{uns}	Unsteady permeability [m^2]
K_s	Steady permeability [m^2]
Pin	Injection pressure [Pa]
$Pvent$	Pressure at ventilation port [Pa]

x_f	Flow front position [m]
ρ_f	Density of test fluid [kg/m^2]
dP_{in}/dt	The rate of change of compaction pressure [Pa/s]
dm/dt	The rate of change of mass of test fluid [kg/s]
R_{in}	Radius of the inlet hole [m]

TABLE OF CONTENTS

LIST OF FIGURES

LIST OF TABLES

CHAPTER 1

INTRODUCTION

Composite manufacturing industries suffer from the inconsistent mold filling and/or mechanical properties of the part induced by inherent process variations such as material, material preparation (cutting, stacking and placement) and nonrepeatable mold filling. Nonrepeatable mold filling is typically induced by issues such as racetracking channels between the fabric preform and mold walls, dual scale flow through a porous fabric preform and incomplete mold filling due to premature gelation. Thus, engineers will benefit from a reliable process modeling in LCM processes which may simulate mold filling and fiber compaction so that they can make some control actions to correct the process parameters (such as opening/closing inlet or exit ports, adjusting the boundary conditions, applying resin bleeding, and so on) to completely fill the mold cavity and/or reduce the tolerances in the part dimensions (especially in the thickness direction in VI). Permeability is a key parameter used in Darcy's Law, which will be discussed in detail later in this chapter, to relate the pressure gradient and resin velocity. That law is the replacement of the conservation of momentum in fluid mechanics, and commonly applied in LCM processes assuming that the flow is approximated as flow through a porous medium. In this thesis, different permeability measurement techniques will be reviewed; and then used in the determination of the permeability of three different fabric types (random, woven and biaxial). The main aim is to discuss the issues involving in these techniques, and how to deal with those.

Another important part is to discuss the advantages of using a continuous set of measurement by using something called “continuous permeability measurement experiments” using a single specimen. One issue that is not still too clear in the literature, and among the industrial users of the flow models, is that which permeability should be used in the flow models: unsteady or steady? By using 1D experiments or radial? There are many studies at the center of these discussions; but no common decision or approach is accepted by all the participants of this field. This thesis aims to highlight the causes of the errors in typical experiments, and their discussions. Statistical analysis is given to support that a significant scatter in the results is very typical; but a consistent shift between the types of measurement techniques is observed. A guideline for the experimenters is also given so that the modelers are aware of the deviation between the simulated results and the actually monitored flow.

In this chapter; general information about polymer composites, liquid composite molding (LCM) processes, permeability measurement methods and their issues are discussed.

1.1 Composite Materials

Composite materials can be defined as the heterogeneous combination of at least two different types of material that result in better properties than when the components are used individually. Polymer composites are made of fiber reinforcements which are embedded in a polymer material known as resin. In the past few decades, fiber reinforced composite materials have became important engineering materials used in the main structural component of aerospace, marine, automobile and civil industries. This is due to their outstanding mechanical, physical and electrical properties such as high specific strength and

stiffness, high corrosion resistance, low thermal and electrical conductivity and additionally ease of fabrication. The properties of a composite part strongly depend on the properties of the constituent materials, for this reason, additional care should be given during material selection.

Figure 1. 1 Use of polymer composite materials in different engineering fields [1-5]

1.1.1 Fabrics and Mats

Fabrics and mats are used as reinforcement material in polymer composite materials. A fabric is produced by weaving, braiding, knitting or stitching of the continuous fibers, and a mat is produced by binding or stitching of the chopped (short or long) fibers [6]. A reinforcement is responsible for carrying majority of structural loads and providing stiffness and strength to the end product. Because of this important role, type and structure of the reinforcement material are very effective parameters on mechanical properties of the composite materials.

Glass, carbon and Kevlar (aramid) are the most commonly used raw materials in fabrics and mats manufacturing. Detailed information for mechanical properties of fabric types and most frequently used engineering materials are given in Table 1.1 for comparison purpose. In this study, Fibroteks E-glass random mat, woven fabric and METYX stitched (biaxial) fabric are used (seen in Appendix C). Random mats are assumed to be isotropic both in their structural and flow properties. Their mechanical properties are generally lower than stitched and woven fabrics, so that they are generally preferred for low strength applications.. Fiber volume fraction, which is the ratio of the fiber volume to the total volume and calculated with Equation (1) given below, is another constitutive parameter on the determination of the mechanical properties of the composite materials.

$$V_f = \frac{N\ (\rho_{sup})}{h\ (\rho_f)} \tag{1.1}$$

where V_f is the fiber volume fraction, N is the number of the layers in the preform, h is the thickness of the mold cavity, ρ_{sup} and ρ_f are the superficial density of the preform per layer and density of the fiber, respectively. For random mats, even at high compaction pressures, low fiber volume fraction (typically less than 40-50 %) is obtained because of non structured ply. Woven and biaxial fabrics may have as high as 65-70% V_f value in RTM applications.

Table 1. 1 Mechanical properties for different engineering materials [6].

Material	**Modulus of Elasticity, E [GPa]**	**UltimateTensile Strength, UTS [MPa]**
Aluminum	69 -79	60-900
Steel	190 – 200	415-1750
Titanium	1.4 – 3.4	20 -120
Thermoplastic polymer	2 – 50	20 – 120
Thermoset polymer	3.5 -17	35 -170
Glass fiber	73 – 85	3500 – 4600
Carbon fiber	275 – 415	2000 – 3000
Kevlar (aramid)	62 – 117	2800

1.1.2 Resin

Resin is polymeric material (thermoset in LCM processes) composed of main monomer and curing agent. After its cure, resin functions as the matrix to hold fibers at fixed positions. Transmission of stresses between matrix and fibers under loading, protection of fibers against environmental conditions (heat, moisture and chemicals) can be listed as other functions of the matrix material.

Polymers can be classified into three subgroups according to their thermophysical properties . These are; (i) thermoplastic, (ii) thermoset and (iii) elastomers. Thermosets and thermoplastics are most widely used matrix materials in polymer composite materials manufacturing. They have some characteristic properties which make them preferential for some particular application. Thermoset materials are liquid and they have low viscosity (typically 0.1- 0.5 Pa.s) at room temperature. They are not postformable because of an irreversible curing reaction of the polymers. On the other hand, the thermoplastic materials are reformable, that means processing of them is reversible to reshape. Unlike thermosets, thermoplastic materials are generally solid and have much higher (typically hundreds to millions times higher) viscosity at room temperature. Furthermore, thermoplastics usually exhibit low mechanical and chemical properties, electrical and thermal stability when compared with thermosets [7]. For LCM (Liquid Composite Molding) processes, thermosets are more appropriate matrix material because of their low viscosity which enables easier impregnation of a fabric preform during mold filling.

In this study, instead of polymeric resin, glucose syrup diluted with water is used as test fluid. Detailed information about glucose syrup used in this study is given in Appendix C. The reason of using glucose syrup is that in the scope of this study, no investigation is made on the final product after completing its curing reaction. Furthermore, corn syrup has easy cleaning characteristics and no harmful volatile emission when compared with polymeric resin.

1.2 Liquid Composite Molding Process (LCM)

The liquid composite molding (LCM) processes are the most common thermoset composite manufacturing processes. They are based on impregnation of a fabric preform (previously placed in the mold cavity) with resin. The main goal of LCM processes is to obtain composite part which is fully saturated with resin both in macro and micro scales (i.e., without any resin starved region in the finished part). One of the advantages of the LCM processes is the ability to tailor the preform exactly to the needs of the part. RTM (Resin Transfer Molding), VARTM (Vacuum Assisted Resin Transfer Molding), which is also named as VI (Vacuum Infusion), SCRIMP (Seeman's Composites Resin Infusion Molding), SRIM (Structural Reaction Injection Molding), RRIM (Reinforced Reaction Injection Molding) and Light RTM are examples of LCM processes. VARTM and RTM are the basis of the others listed above; and they are widely used in industry. The most distinct difference between these two LCM processes is that the two sided rigid mold in RTM process is replaced with one sided rigid mold in VARTM process which is covered with flexible vacuum bag and sealed to the mold surface using tacky tape.

The main advantageous of the RTM process are (i) manufacturing near net shape products, (ii) having high fiber volume content, (iii) having good dimensional tolerances and surface finish on both sides of the product, (iv) achievement of good mechanical properties by tailoring stacked assembly of fabric layers. Besides these advantageous, the followings are the main disadvantageous of RTM processes: (i) high mold cost, (ii) long cycle time, (iii) higher clamping force compared to VARTM and (iv) high injection pressure.

In VARTM process, vacuum is applied in the mold cavity using a vacuum pump at the exit side which causes the compaction of fabric preform between vacuum bag and a rigid lower mold. Vacuuming not only allows compaction of the preform, but it also drives resin from a reservoir to mold cavity to fill the empty spaces between the fibers of the preform. Advantageous of the VARTM process compared to RTM process are (i) one sided mold and simple injection system, (ii) flow front can be observed visually due to transparent vacuum bag, (iii) complex and large parts can be manufactured easily. On the other hand, the following can be listed as the main disadvantageous of the process: (i) thickness variation due to non uniform compaction pressure, (ii) low fiber volume fraction as a result of low compaction pressure (around 1 atm), and (iv) being labor intensive.

The success of the LCM processes depends on understanding physic of the process. Instead of trial and error approach, which is time and cost consuming method, an appropriate computer simulation program based on constitutive law related with physic of the process can be used to determine (i) flow front propagation with time, (ii) injection gate and vent locations (for optimal mold design), (iii) thickness of the final product, (iv) fill time of the mold and cycle time. Thus, mold filling is achieved completely and micro and macro void formation is reduced to minimum. Otherwise, it may seriously degrade the strength and quality of the part. The reliability of the simulation programs depend on the accurate input data. Permeability is one (and the major one) of these crucial input material data used in numerical mold filling simulations in LCM processes.

1.3 Permeability

Permeability of a porous medium (fabric preform) is related to the inverse of resistance to the resin flow through the medium. It can be characterized using one of these approaches: (i) by using a flow model applied on a unit cell with periodic boundary conditions and solving the velocity field numerically and (ii) conducting experimental techniques that we will discuss and then applied in this thesis. Permeability strongly depends on the fiber volume fraction of the fabric preform and fabric architecture. Its unit is either cm^2 or m^2.

The flow of a resin through a porous medium is modeled by using empirical Darcy's Law;

$$Q = -\frac{K\ A}{\mu}\frac{dP}{dx} \tag{1.2}$$

where, Q is the flow rate across the cross-section A, μ is the fluid viscosity, $\frac{dP}{dx}$ is the pressure gradient and K is the permeability of the porous medium in x direction [8,9,10]. This equation macroscopically relates flow rate and the pressure gradient. In fluid mechanics, velocity and pressure distributions are solved by using conservation equations of mass and momentum. However in this particular case (flow of liquid resin through empty spaces between the fibers of a porous medium), it requires to describes the solution domain which is a very complicated channel network. But it is hard to solve momentum equation for each channel inside the network. Permeability term in Darcy's Law (Eq 1.2) is key empiric material parameter while relating pressure gradient and the flow rate [9].

Since fiber reinforced composite materials are anisotropic medium, three principal permeability values are necessary to model 3D flow inside the mold cavity. Hence, Darcy's Law is written as in the following tensorial form (3);

$$\bar{u} = -\frac{\bar{K}}{\mu}.\nabla \mathrm{P} \tag{1.3}$$

where $\bar{u}$ is the volume averaged Darcy's velocity, μ is the viscosity of the fluid, ∇P is the pressure gradient and $\bar{K}$ is the permeability tensor.

$$\bar{K} = \begin{pmatrix} K_{xx} & K_{xy} & K_{xz} \\ K_{yx} & K_{yy} & K_{yz} \\ K_{zx} & K_{zy} & K_{zz} \end{pmatrix} \tag{1.4}$$

Equation 1.3 can be rewritten as;

$$\begin{pmatrix} \bar{u}_x \\ \bar{u}_y \\ \bar{u}_z \end{pmatrix} = - \frac{1}{\mu} \begin{pmatrix} K_{xx} & K_{xy} & K_{xz} \\ K_{yx} & K_{yy} & K_{yz} \\ K_{zx} & K_{zy} & K_{zz} \end{pmatrix} \begin{pmatrix} \frac{\partial P}{\partial x} \\ \frac{\partial P}{\partial y} \\ \frac{\partial P}{\partial z} \end{pmatrix} \tag{1.5}$$

Permeability tensor has nine components; however it is assumed that the $K_{ij} = K_{ji}$ which reduces the number of unknown components to six. By selecting x and y axes as the principal directions of the fabric preform (thus $K_{ij} = 0$ for $\mathrm{i} \neq \mathrm{j}$), Eq 1.5 reduces to;

$$\begin{pmatrix} \bar{u}_x \\ \bar{u}_y \\ \bar{u}_z \end{pmatrix} = - \frac{1}{\mu} \begin{pmatrix} K_{xx} & 0 & 0 \\ 0 & K_{yy} & 0 \\ 0 & 0 & K_{zz} \end{pmatrix} \begin{pmatrix} \frac{\partial P}{\partial x} \\ \frac{\partial P}{\partial y} \\ \frac{\partial P}{\partial z} \end{pmatrix} \tag{1.6}$$

To use Darcy's Law for porous media flows and thus calculation of the permeability, the following conditions must be satisfied during experiments [12];

- The fluid used in experiments must be Newtonian that means the relation between shear stress and viscosity is linear.
- The fluid used in the experiments is chemically inert and incompressible.
- Solid matrix of the porous medium must be rigid and stationary.
- Flow assumed to be laminar and Reynolds number (which is the ratio of inertial force over viscous force of test fluid) is small enough ($0<Re<1$).

1.4 Experimental Methods for Permeability Measurement and Their Issues

In an anisotropic medium like fiber reinforced composites, three principal permeability values are required to model 3D flow inside the fabric preform. Two of these principal permeability values lie in the fabric plane, while the third one is perpendicular to it. The majority of the permeability measurement studies in the literature focused on the in-plane permeability components and ignore the transverse permeability component due to the lack of significant transverse pressure gradient and smaller thickness value than in-plane dimensions in typical RTM and VARTM applications. But, this 2D flow assumption is not valid under the following conditions [7]:

- If thickness of the mold cavity alters significantly in the mold,
- If the in-plane permeability components of each layer in the fabric preform have orders of magnitude variations,
- If core material into the plies to increase the effective permeability of the fabric preform is embedded into the plies.

Permeability measurement experiments for in-plane permeability components of a porous preform can be classified based on;

- *Flow geometry*: it can be either 1D (unidirectional-linear) or 2D (radial).
- *Injection boundary condition:* They can be performed under constant flow rate or constant pressure boundary conditions.
- *Saturation state of the experiments:* Saturated or steady case, preform is already impregnated with the resin and new arrival resin replaces with previous one. In unsaturated (which is also called unsteady or transient) resin impregnates the dry preform.

1.4.1 1D (Linear or Unidirectional) Permeability Measurement Experiments

1D permeability measurement experiments are performed by driving test fluid through a fabric specimen which is placed and compressed in the mold cavity before the injection. 1D test setup is a straightforward setup consisting of a metallic mold part and a transparent mold part (usually made of acrylic or glass to monitor 1D flow for validation) This mold must prevent any leakage during injection. Injection is done from an injection hole (inlet) located at an empty region before the fabric specimen to obtain 1D resin flow before resin impregnates the fabric preform. Procedures of several different permeability measurement experiments are described in the following sections.

1.4.1.1 1D Continuous (Unsteady – Steady) Permeability Measurement Experiments with Constant Flow Rate Boundary Condition

A 1D continuous permeability measurement experiment allows measuring one unsteady and a set of steady permeabilities at different fiber volume fractions using a single preform specimen. Constant flow rate injection is achieved by constant flow rate injection machine. In the unsteady part of the experiment, injection pressure P_{in} is expected to increase linearly with respect to time. Numerically evaluated slope, $\frac{dP_{in}}{dt}$ is substituted to Eq 1.7 given below and unsteady permeability of the fabric preform in the flow direction is calculated. Note that Eq 1.7 is derived from Darcy's law for transient resin flow with a constant flow rate boundary condition [7].

$$K_{uns} = \left(\frac{Q}{wh}\right)^2 \frac{\mu}{\emptyset} \frac{1}{\frac{dP_{in}}{dt}} \tag{1.7}$$

Where Q is volumetric flow rate, w and h are the width and thickness of the preform respectively, μ is viscosity of test fluid, Ø is the porosity of the preform. Top and side view of the mold during filling period and anticipated P_{in}, vs time profile can be found in Figure 1.2 for unsteady part of 1D permeability measurement experiment with constant flow rate boundary condition.

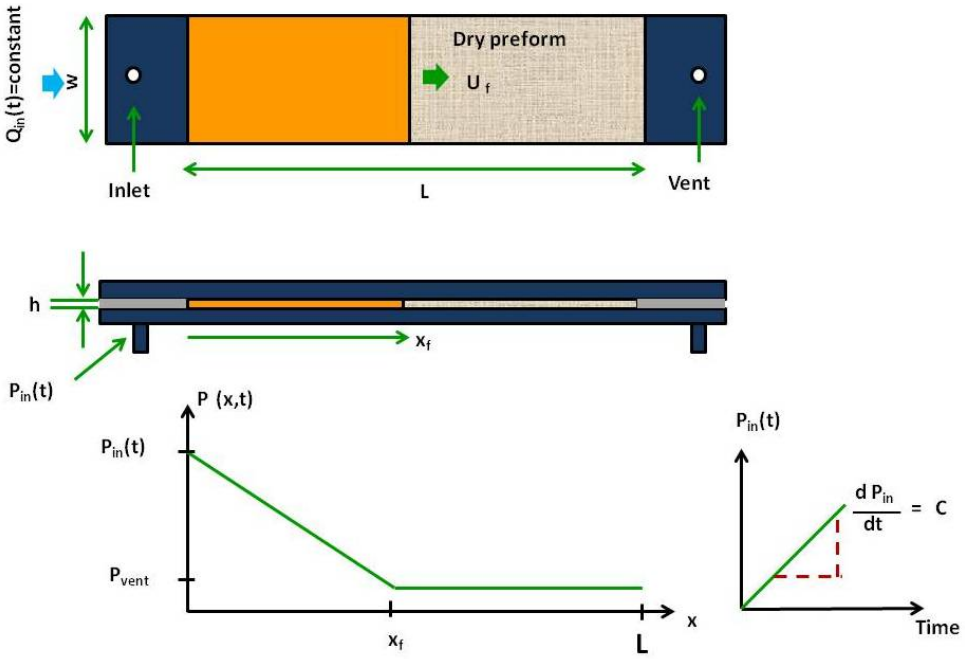

Figure 1.2 Schematic representation of top and side views of the mold, pressure distribution along mold cavity and graphical representation of P_{in} versus time during unsteady part of 1D continuous permeability measurements experiments with constant flow rate boundary condition. The figure was redrawn by adapting it from [7].

When the mold is completely filled and steady flow is achieved, the resin pressures are recorded at both the inlet and the vent; and they are expected not to change anymore. If micro voids are present in the specimen, steady state may not be achieved instantaneously. Hence $\frac{dP}{dx}$ can also be assumed to be constant and written as

$$\frac{dP}{dx} = \frac{\Delta P}{L} = \frac{P_{vent} - P_{in}(t_{fill})}{L} \tag{1.8}$$

Steady permeability can be calculated by using Darcy's Law [7].

$$K_s = \frac{Q\,\mu}{w\,h} \quad \frac{1}{\frac{P_{in-}\,P_{vent}}{L}} \tag{1.9}$$

Steady part of the experiment can be repeated at different thickness values using a single preform by adjusting mold gap and calculating K_s by using Eq (1.9) for each of thickness values separately. In Figure 1.3, top and side views of the mold and pressure distribution along the mold cavity during fully saturated stage of 1D permeability measurement experiment with constant flow rate can be seen.

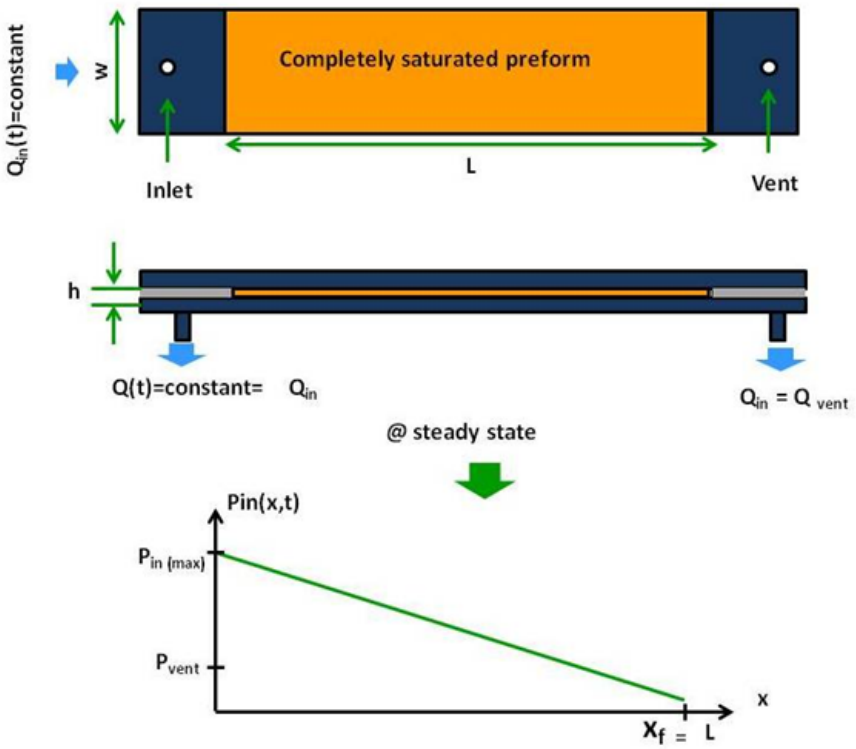

Figure 1.3 Schematic representations of top and side views of the mold and pressure distribution during steady part of a 1D continuous permeability measurement experiment with constant flow rate boundary condition. The figure was redrawn by adapting it from [7].

1.4.1.2 1D Continuous Permeability Measurement Experiment with Constant Pressure Boundary Condition

In 1D constant pressure permeability measurement experiments, injection is done under constant pressure which is provided using either a constant pressure injection machine or a resin tank open to atmosphere at the inlet and a vacuum pump at the exit. Resin flow in the mold cavity is achieved by the pressure difference between inlet and vent ports.

During unsteady part of the 1D constant pressure permeability measurement experiment, the flow front position $x_f(t)$ is monitored and plotted with respect to time. The data processing for permeability calculation along the flow direction is based on the integration of Darcy's Law under constant pressure boundary condition.

$$x_f(t) = \sqrt{\frac{2\ K_{uns}\ \Delta P\ t}{\mu\ \emptyset}} \tag{1.10}$$

here x_f is the flow front position, K_{uns} is the unsteady permeability of the preform along flow direction, $\Delta P \equiv P_{in} - P_{vent}$ is the pressure difference between the inlet and exit ports, μ is viscosity of test fluid, Ø is the porosity of the preform. When K_{uns} is left alone, the following is obtained.

$$K_{uns} = \frac{C\ \mu\ \emptyset}{2\ \Delta P} \tag{1.11}$$

where C is determined by using $x_f\,(t) = \sqrt{C\,t}$; and thus using first order curve-fit to the x_f vs $\sqrt{t}$ data. In Figure 1.4, schematic representation of top and side views of the mold and graphical representation of x_f versus time during unsteady part of 1D permeability measurement experiments with constant pressure boundary condition are illustrated. When the mold is filled and unsteady part of the experiment is completed, mass of the test fluid exiting from ventilation port is recorded with time for steady permeability calculation. The slope of $\frac{dm}{dt}$ is numerically calculated, and it is divided by density of the test fluid (ρ) in Eq 1.12 to calculate the flow rate which is assumed to be constant during steady part of the experiment for any constant thickness value.

$$Q = \frac{1}{\rho}\frac{dm}{dt} \tag{1.12}$$

Q substituted in the Eq 1.13 which is derived from Darcy's law for constant pressure boundary condition at steady state:

$$K_s = \frac{Q\,\mu\,L}{w\,h\,\Delta P} \tag{1.13}$$

Then, the thickness is changed, and the steady permeability at the new thickness value is measured using the same specimen, and using the same procedure explained above (i.e using the new h and dm/dt data in Eq(1.13)). In Figure 1.5 a 1D steady constant pressure permeability experiment is schematically illustrated.

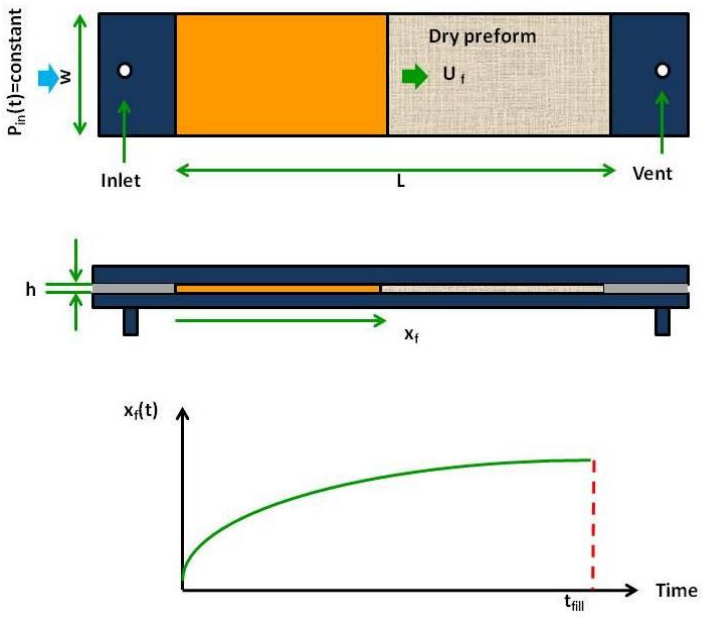

Figure 1.4 Schematic representation of top and side views of the mold and graphical representation of x_f versus time during unsteady part of 1D continuous permeability measurement experiments with constant pressure boundary condition. The figure was redrawn by adapting it from [7].

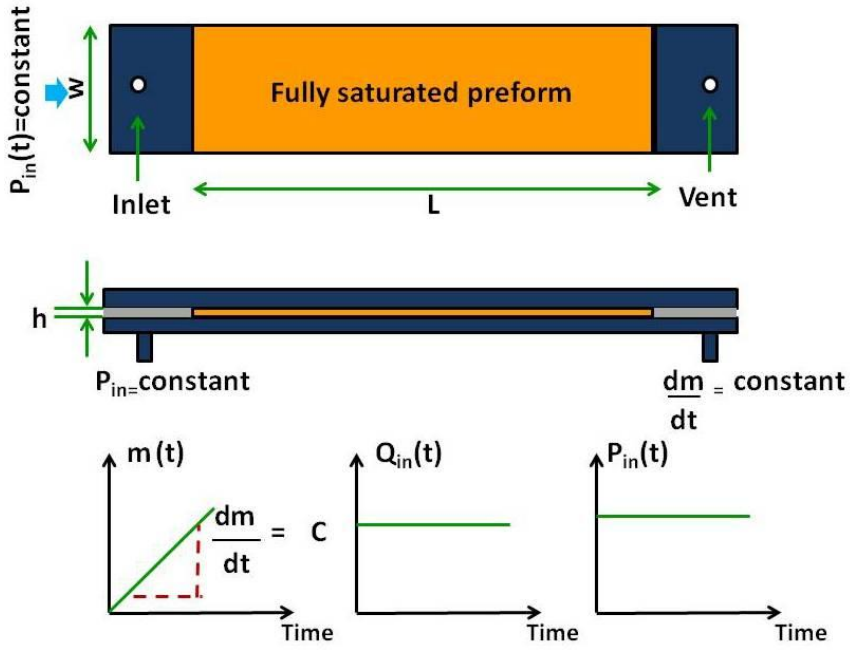

Figure 1.5 Schematic representation of top and side views of the mold and graphical representation of m, Q_{in}, x_f versus time during steady part of a 1D continuous permeability measurement experiments with constant pressure boundary condition.

1.4.2 2D (Radial) Permeability Measurement Experiments with Constant Flow Rate Boundary Condition

A 2D (radial) permeability measurement experiment setup typically consists of a metallic half of the mold which includes an injection hole in the middle, and a transparent half of the mold to monitor the flow front propagation. Injection is initiated from this hole and the specimen should have a central hole with the same or a little bigger than a radius of R_{in}. This is to ensure two dimensional flow generated from a circular gate (not a point); and also not to cause resin flow in the thickness direction near the gate.

In 2D (radial) injection, an elliptical flow front (as seen in Figure 1.7 with major $R_{f1}(t)$ and minor $R_{f2}(t)$ axes) is observed for an anisotropic preform. If the fabric preform is isotropic, the flow front would be circular which means ($R_{f1}(t) = R_{f2}(t) \equiv R_f(t)$), and $K_{11} = K_{22}$. 2D (radial) permeability measurement experiments allow measuring two in-plane principal permeabilities by performing only one experiment. It means that the 2D experiments are less time consuming when it is compared with 1D experiments. Additionally, principal axes are determined easily in radial experiments. These are the main advantages of 2D permeability measurement experiments. Another advantage is that the racetracking which is the most serious issue that occurs in 1D (linear) experiments, and explained later in detail is not encountered in 2D experiments. The required data to be collected and equations used in 2D unsteady permeability measurement experiments are given below.

An injection machine with flow rate control is used to adjust and then keep flow rate constant at the inlet boundary. Injection pressure P_{in} and flow front position (both major R_{f1} and minor axes R_{f2}) should be recorded with time during injection. Solution of the Darcy's law for polar coordinates as follows.

$$P_{in} = \frac{\mu Q_{in}}{4\pi h\sqrt{K_{11}\,K_{22}}}\, ln\left(1 + \frac{Q_{in}\,t}{\pi\, hR_{in}^2 \emptyset}\right) \tag{1.13}$$

Here P_{in} is injection pressure, μ is the viscosity of the test fluid, Q is volumetric flow rate, h is thickness of the fabric preform, R_{in} is the radius of inlet hole, $\emptyset$ is porosity of the fabric preform, and K_{11} and K_{22} are the principal permeability components along major and minor axes, respectively. The aspect ratio of the ellipse (the ratio of the major and minor axes) is

equal to the square root of the permeability components in those principle directions as seen below [7].

$$\frac{R_{f1}}{R_{f2}} = \sqrt{\frac{K_{11}}{K_{22}}} \tag{1.14}$$

Principal unsteady permeabilities are calculated using the equation below where D is obtained by curve fitting to the data using Eq 1.16.

$$K_{uns} \equiv \sqrt{K_{xx}\, K_{yy}} = \frac{\mu Q}{4\pi h D} \tag{1.15}$$

$$P_{in}(t) = D\ ln\left(1 + \frac{Q\, t}{\pi h R_{in}^2 \emptyset}\right) \tag{1.16}$$

In Figure 1.6, schematic representation of the mold during injection and graphical representation of important process parameters are shown. Detailed description of experimental procedures, the mold configuration and its boundary conditions, which equipment to be used (an injection machine or vacuum pump), sensors, data acquisition system and also schematic of setup used in this study are given in Chapter 3 and Appendix C.

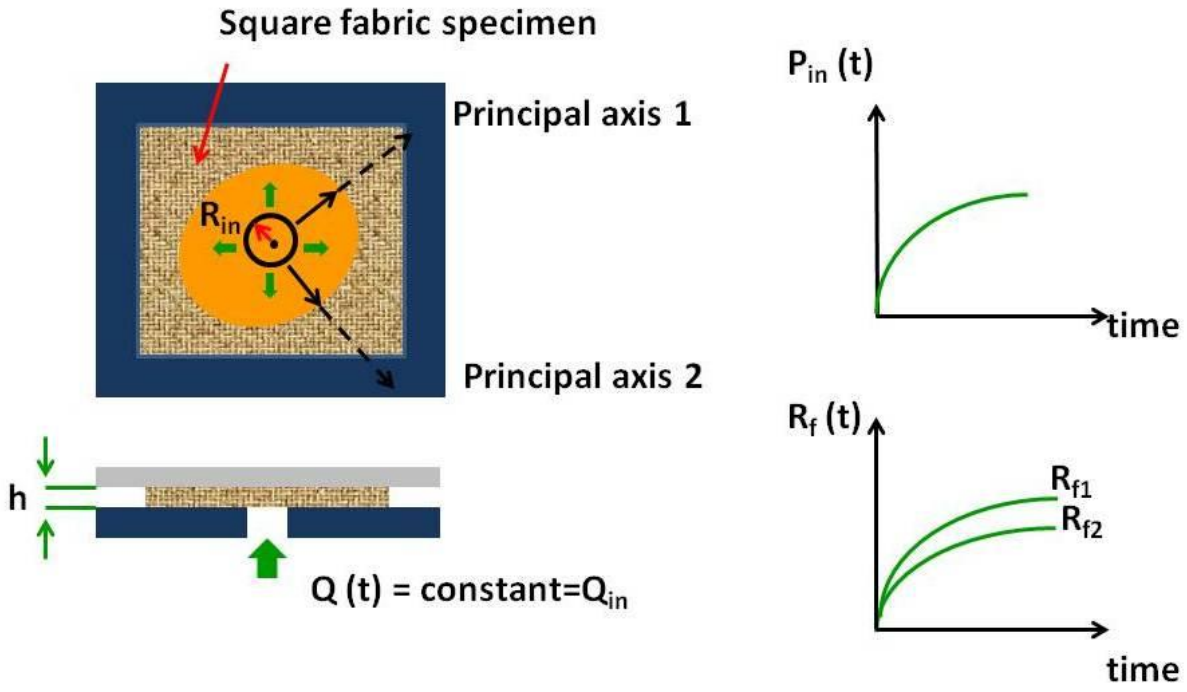

Figure 1.6 Schematic representations of top and side views of the mold, anticipated P_{in}, R_{f1} and R_{f2} versus time plots during unsteady part of 2D radial permeability measurements experiments with constant flow rate boundary condition. The figure was redrawn by adapting it from [7].

1.4 Issues of Experimental Permeability Measurement Methods

Permeability measurement experimental techniques have some issues about accuracy and repeatability. These experiments are easily affected from the variability of the specimen, cutting operations, skill of the experimenter, inappropriate choice of equipment and its components (injection machine, injection tube, sealant and vacuum pump), evaluation of measured raw data, and racetracking (fast flow of resin along preform – mold edge) high permeable region exists and causing deviation from 1D flow). In Figure 1.8, 1D experiments with and without racetracking is represented. One more noteworthy thing is

mold deflection which is one of the main sources of error, and it occurs because of high injection pressure plus compaction stress on the preform inside the mold cavity. If the injection equipment is not stiff enough, it may contribute to experimental error. Hence it can be easily said that, permeability of the fiber preform at particular thickness cannot be characterized by performing a single experiment. It is better to repeat the experiments many times and construct a statistical distribution of them to obtain more reliable results [12].

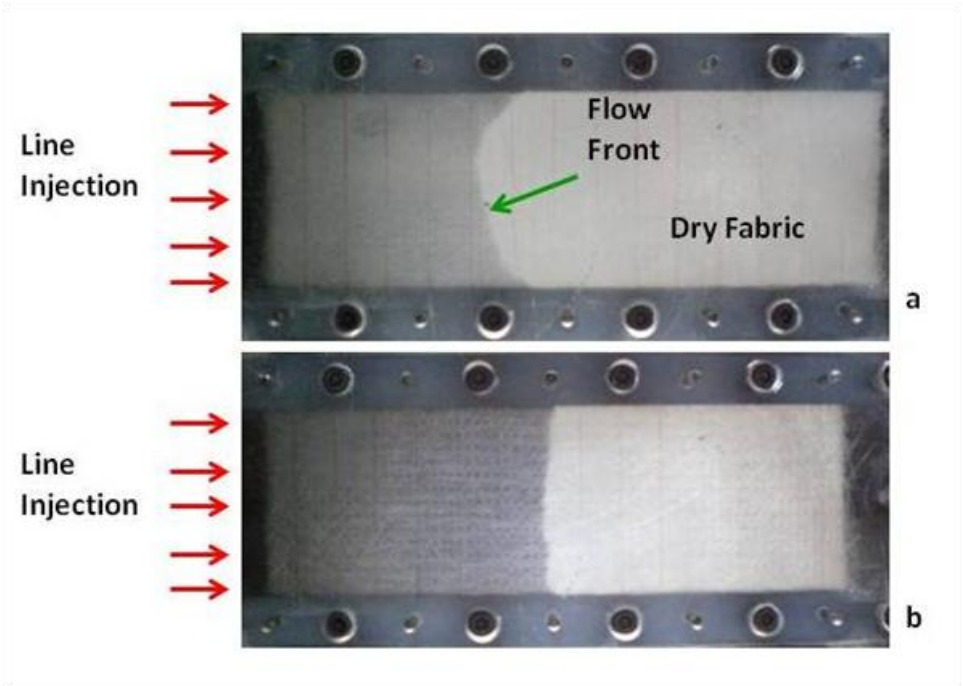

Figure 1. 7 Two flow front propagations during permeability measurement experiments a**)** the experiments is not valid because the flow front deviates from 1D flow probably due to racetracking channels between the specimen and the mold walls; **b)** the experiment is valid to be used for permeability measurement because almost a linear flow front is observed (as a sign of 1D flow).

1.5 Objectives

In the scope of this study, the followings are achieved;

- Both 1D continuous (unsteady and steady) permeability measurement experiments with constant flow rate boundary condition and 1D continuous (steady and unsteady) permeability measurement experiments with constant pressure boundary condition are performed by using three different fabrics.
- During steady part of the 1D permeability measurement experiments with constant pressure boundary condition, a new method is used to calculate steady permeability along the flow direction. This new method enables us to measure several steady permeability values on single specimen by changing thickness value. For each thickness value, mass of test fluid exiting from the ventilation port is weighted and recorded with time and the slope of $\frac{dm}{dt}$ is used in Darcy's law to calculate steady permeability values.
- A new mold with a practical design was produced for 1D experiments [26]. The most important part of this mold is thickness adjustment system. Two wheels are fixed at the two sides of the mold, and one turn of each wheel corresponds to 1 mm change in the mold cavity thickness which makes thickness adjustment during continuous experiments easy, reliable and consistent. Thickness adjustment system can work between 2 and 10 mm with 0.1 mm precision. The other characteristics of the mold are listed as follows: (i) perfect sealing up to 6 bar, (ii) easy open and close system which is operated by four latches on the four side of the mold, and (iii) acrylic lower mold that allows us monitoring flow front propagation.

- Mold deflection is observed by using two dial gages fixed at inlet and vent sides of the mold during each experiment. If any deflection is read on the screen, four latches which are fixed externally on the four corners of the mold are used to eliminate this deflection. In order to reduce the sudden deflection that occurs during thickness reduction in continuous experiments, an experiment starts with the lowest thickness value and continues with increasing thicknesses.
- Anticipated sources of error are analyzed comprehensively to reveal their contribution to the total error; and suggestions are proposed to minimize their effect on measured permeability.
- Comparison between steady and unsteady permeabilities and the methods used are discussed in the following sections.

This study is designed to be a useful guide for permeability measurement experimenters investigating all steps of each experimental method. It gives advices and makes some reminders to minimize the experimental errors. It is not possible to completely eliminate all of errors; but it is possible to take precautions against to those errors.

CHAPTER 2

LITERATURE SURVEY

2.1. Previous Studies

There are many researches that focused on the permeability measurement experiments and their issues given in Chapter 1. These studies and their crucial points are discussed below.

Parnas et al. [13] constructed a database for the most commonly used fabric types in LCM by conducting 1D saturated, radial unsaturated and through the thickness saturated flow methods. The compressibility of the fibers which determines the fiber volume fraction was also investigated. Mold deflection, racetracking and incomplete saturation because of entrapped residual gas inside the fabric preform were listed as main sources of the error encountered in permeability measurement experiments. Commonly, permeability measured by radial unsaturated flow was found higher than the permeability measured by unidirectional saturated flow. This discrepancy was explained by the capillary forces which were not taken into account during permeability calculation for unsaturated radial flow experiments.

The variation in the measured permeability was 20% for woven, unidirectional and stitched fabrics; and it was more than 50% for random mat and it was explained to be caused by large nonuniformities observed in the random fabric. Lundström et al. [14] presented a study which focused on reproducibility and stability of the three different permeability measurement methods: unsaturated 1D flow, saturated 1D flow, and unsaturated radial flow which were conducted at different laboratories. The anticipated sources of errors were investigated comprehensively. All three methods were consistent between each other. Sample preparation process was indicated as the main reason of a large scatter; and one of the suggestions given to reduce this scatter is stamping the specimen rather than cutting them. It was also observed that applied injection pressure during experiments which were conducted with constant pressure boundary condition has small influence on the measured permeability. The best repeatability was obtained in the unsaturated 1D flow technique. It was also recommended that in order to obtain more reliable results, the length to width ratio must be larger than the ratio between principal permeability components for 1D flow experiments. Gebart et al. [15] also analyzed the saturated and unsaturated 1D flow and unsaturated radial flow techniques. The purpose of that investigation was to compare different permeability measurement experiments and make theoretical error analysis before experiments and then compare both experimental and theoretical results in order to find which method is more sensitive to experimental errors. According to the theoretical error analysis which was done using standard error formula for these three experimental methods separately, none of the experimental method is superior to the other in terms of error sensitivity.

But, this result is not surprising because during theoretical error analysis, it was assumed that each parameter for these three experimental methods had a relative error of 2% which is not a realistic assumption and thus may result in a misleading conclusion. The contribution of individual error in each parameter is related to its sensor or data acquisition system. Thus, experimental methods using different sensors/DAQ systems may have different levels of errors contributing to the total error of the system. Their experimental studies induced higher variations between different types of experimental procedures than their theoretical correspondences. Large scatter was observed in the radial flow experiments because of deflection of the mold. In the permeability benchmark exercise [16], comprehensive study was done by the contribution of twenty institution and industrial users from twelve countries. Permeability of two types of fabrics roughly at 50% fiber volume fraction was measured using four methods: (i) unsaturated 1D flow; (ii) saturated 1D flow; (iii) unsaturated radial, and (iv) saturated radial flow, and two types of boundary conditions: (a) constant flow rate or (b) constant pressure. They used eight different test fluids. The results of this study showed that permeability values for each experimental setup were consistent in each other, but up to one order of magnitude scatter was observed between different experimental procedures. Human factor was indicated as the most significant factor that causes this high scatter. The other reasons of scatted are listed as; nonuniformities in a fabric roll, and setup component selection which are not stiff enough to work under such a high pressures encountered in experiments. Another review of the permeability measurement methods for fiber reinforced composites was presented by Sharma et al. [11]. As discussed in the previous section, racetracking is a major problem that is observed in 1D permeability measurement experiments.

According to Parnas et al. [17], the sensitivity of the 1D permeability measurement experiments on the edge effect or racetracking was a function of mold width. To minimize the error that occurs because of the edge effect, Parnas et al. [18], and Lekakou et al. [19] applied a sticky band between mold wall and fabric specimen edge. Furthermore Lawrance et al. [20] presented a method which enables to calculate the bulk permeability of the preform, when racetracking is present. This method requires using a mold filling simulation to investigate the deviation in the injection pressure caused by the racetracking channel, and then match the simulated and experimental results. Approximate equivalent isotropic scaling was used and a table which gives correction factor for different racetracking strength along top and bottom edges in the flow direction was constructed. This approach was validated by comparing it with virtual and real permeability measurement experiments which has no racetaracking along both edges. Strong consistence was observed.

Different dummy test fluids such as silicon oil, corn syrup, mineral oil and motor oil are used instead of polymeric resin in permeability characterization experiments because of their easy handling, low volatile emission and easy to clean behavior. But, it must be investigated under what conditions; the test fluid can be used in a permeability measurement experiment. Luo et al. [21] used silicon oil and diluted corn syrup as test fluids. They conducted unsaturated radial flow permeability measurement experiments. It was revealed that, at low fiber volume fractions, the two fluids resulted in identical permeabilities; but at high fiber volume fractions, the permeability measured silicon oil was slightly higher than with diluted corn syrup. This kind of scatter was observed especially when the fiber volume fraction was high and the wetting and surface tension properties of fluids have great difference.

Nevertheless, it was also specified that this scatter is insignificant when compared with experimental error that was encountered during permeability measurement experiment. Hammond et al. [22] also did not find any considerable effect of test fluid on the results of measured permeability. On the other hand, Steenkamer et al. [23] performed permeability measurement experiments at different fiber volume fractions by using 3 different test fluids (motor oil, diluted corn syrup and RTM resin) with several textile fabrics. Considerable influence of the test fluid on the permeability measurement results was observed. William et al. [24] also found dependency of measured permeability on the surface tension of the test fluid. Both Steenkamer et al. [23] and William et al. [24] agreed that better wetting result in higher permeability.

CHAPTER 3

EXPERIMENTAL SETUPS AND PROCEDURE

In this chapter, experimental procedures, schematics of experimental setups and sample calculations can be found for all types of experiments.

3.1 1D Permeability Measurement Experiments

In this study, all of the 1D permeability measurement experiments are performed with (i) 1D unsteady with Q_{in} = constant, (ii) 1D steady with Q_{in}= constant, (iii) 1D unsteady with P_{in} = constant, (iv) 1D steady with P_{in} = constant, for [8R], [$8W_{warp}$], [$8W_{weft}$] and [8B] fabric performs where 8R, 8W and 8B denote eight layer of random, woven and biaxial fabrics. Only for woven fabric, experiments are conducted in both warp and weft directions because of the anisotropic nature of the fabric structure. In Figure 3.1 weft and warp directions of E-glass woven (plain) fabric used in this study is presented. For each fabric type, at any thickness value, three continuous 1D permeability measurement experiments (unsteady) and several steady experiments are performed both under constant flow rate and constant pressure boundary condition.

Thickness ranges were extracted for each fabric type from the unloading (decompaction) and fiber relaxation characterization database briefly presented in Table 3.1 .[25] .

Table 3. 1 Thickness domains for three different fabric types for 1D permeability measurement experiments [25].

Type of Fabric	**Thickness domain[mm]**	**Increment [mm] with Constant Q**	**Increment [mm] with Constant P**
Random	3 – 6	0.5	0.5
Biaxial	5 – 8	0.5	0.5
Woven	2 – 4	0.25	0.25

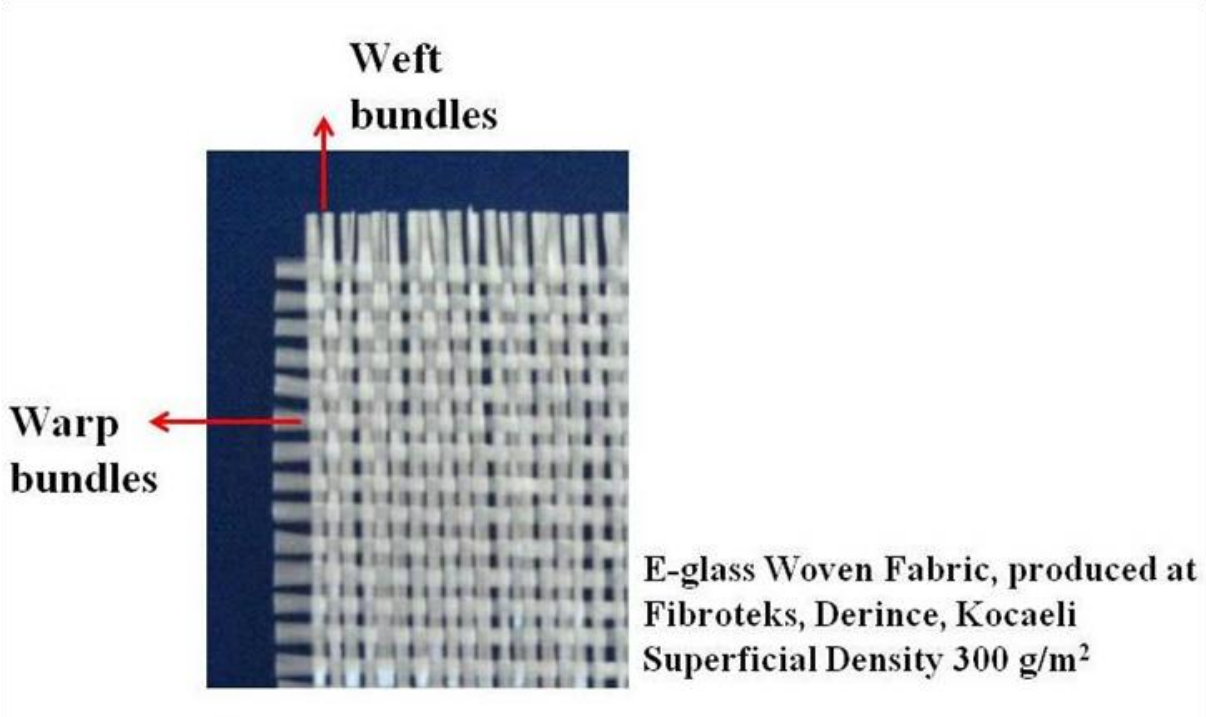

Figure 3. 1 Weft and warp directions of the plain (woven) E-glass fabric. Warp direction is along the rolling direction for all fabrics and weft direction is perpendicular to it.

A mold with a novel thickness adjustment system is used for both 1D constant pressure and 1D constant flow rate permeability measurement experiments. This mold was designed and manufactured for performing 1D continuous permeability measurement experiments; and also producing rectangular composite panels. Its cavity width is 100 mm and length is 400 mm. This mold (seen in Figures 3.2 and 3.3) consists of stainless steel upper plate, an acrylic lower plate and a moving male part which is attached to upper plate and perfectly fits the mold cavity. As mentioned above, the novel side of this mold is its thickness adjustment system which enables setting the initial thickness readily and changing the thickness during different stages of a continuous permeability measurement experiment accurately. Two thickness adjustment wheels are located on the upper metallic part and the connection between the wheels and the movable part of the upper mold is provided by nuts. The details of the molds and working mechanism are given inYalçınkaya's thesis [26].

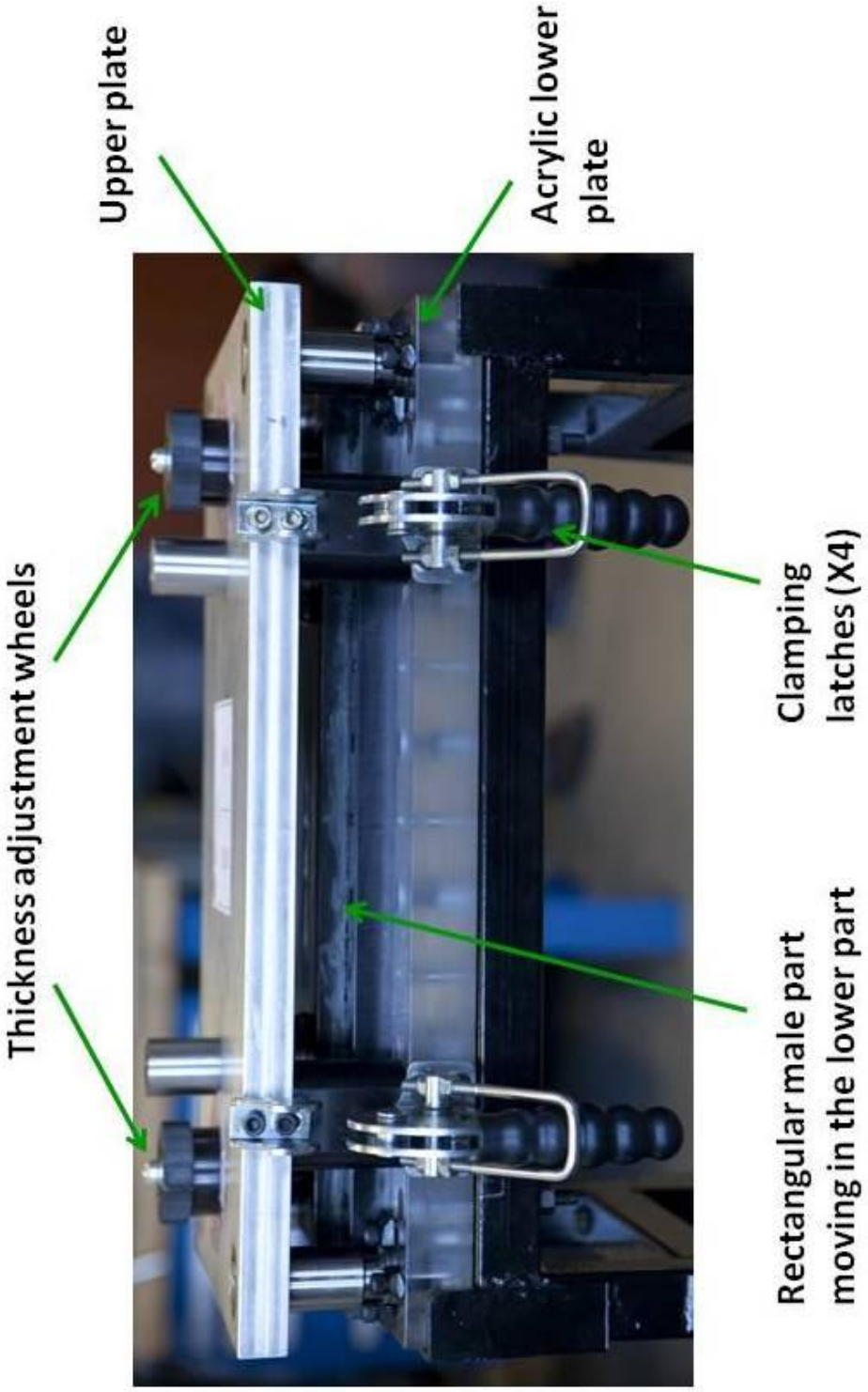

Figure 3. 2 Side view of the mold used for c1D continuous permeability measurement experiments.

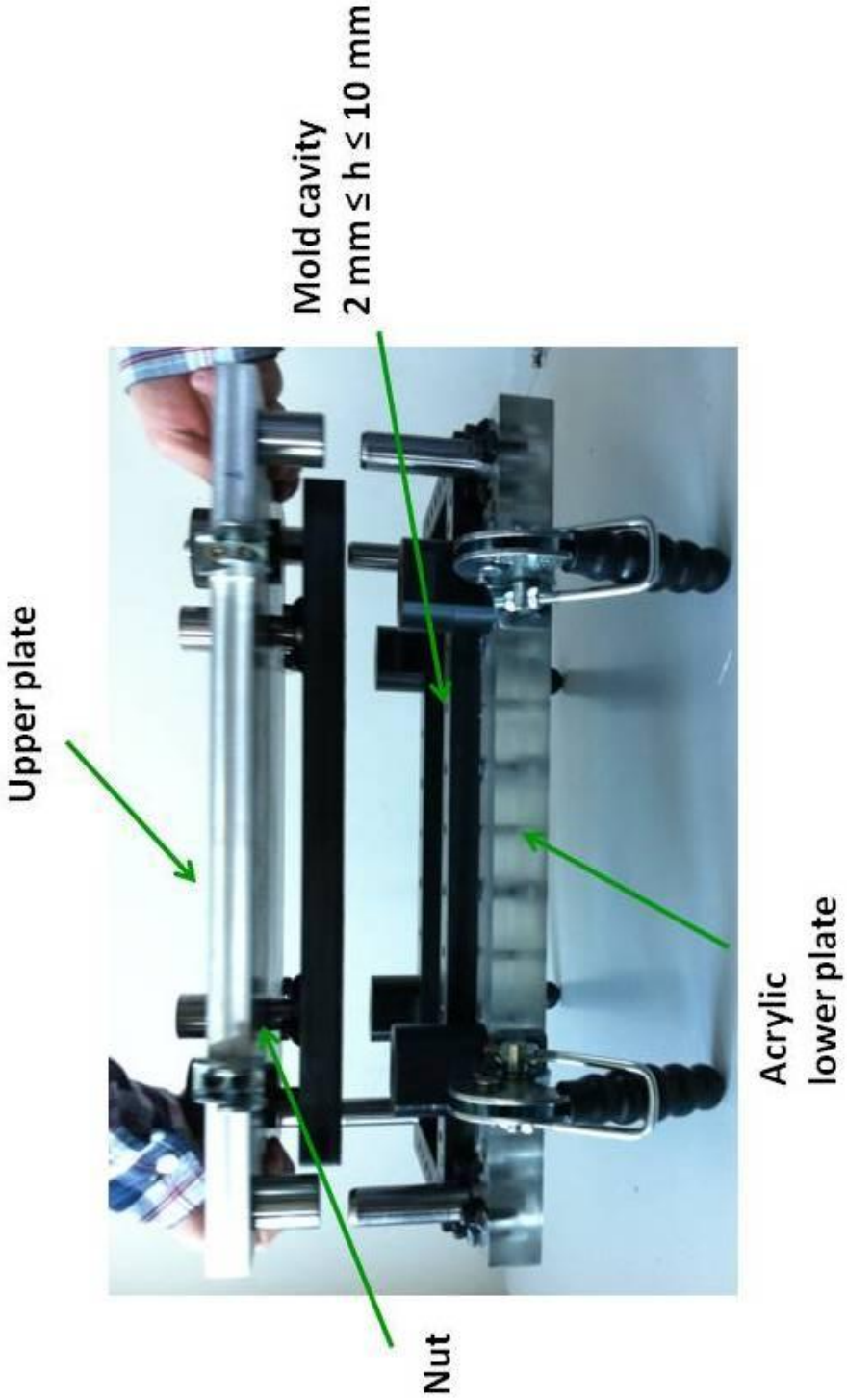

Figure 3. 3 Side view of the mold used in 1D contunious permeability measurement experiments.

By the help of force arms seen in Figure 3.4, the wheels are rotated. This rotation allows moving the rectangular male part inside the mold cavity; and hence it allows adjusting the thickness. A full rotation in clockwise direction corresponds to 1 mm increase in the mold cavity (h); and one full rotation in counterclockwise direction corresponds to 1 mm decrease in h. The distance between the upper metallic mold plate and the male part (L) is measured through the hole drilled on the metallic upper part using a vernier caliper as seen in figure 3.4. The thickness of the mold cavity is determined by using a look up table which is constructed to explain the relation between L and mold cavity thickness (h). An O-ring with a diameter of 2 mm is used around the male part of the upper mold to ensure perfect sealing up to 6 bars. Four latches are mounted on the two sides of the metallic upper plate to provide easy opening and closing. 3D visualization of the mold and detailed information of the mold parts can be found in Appendix C.

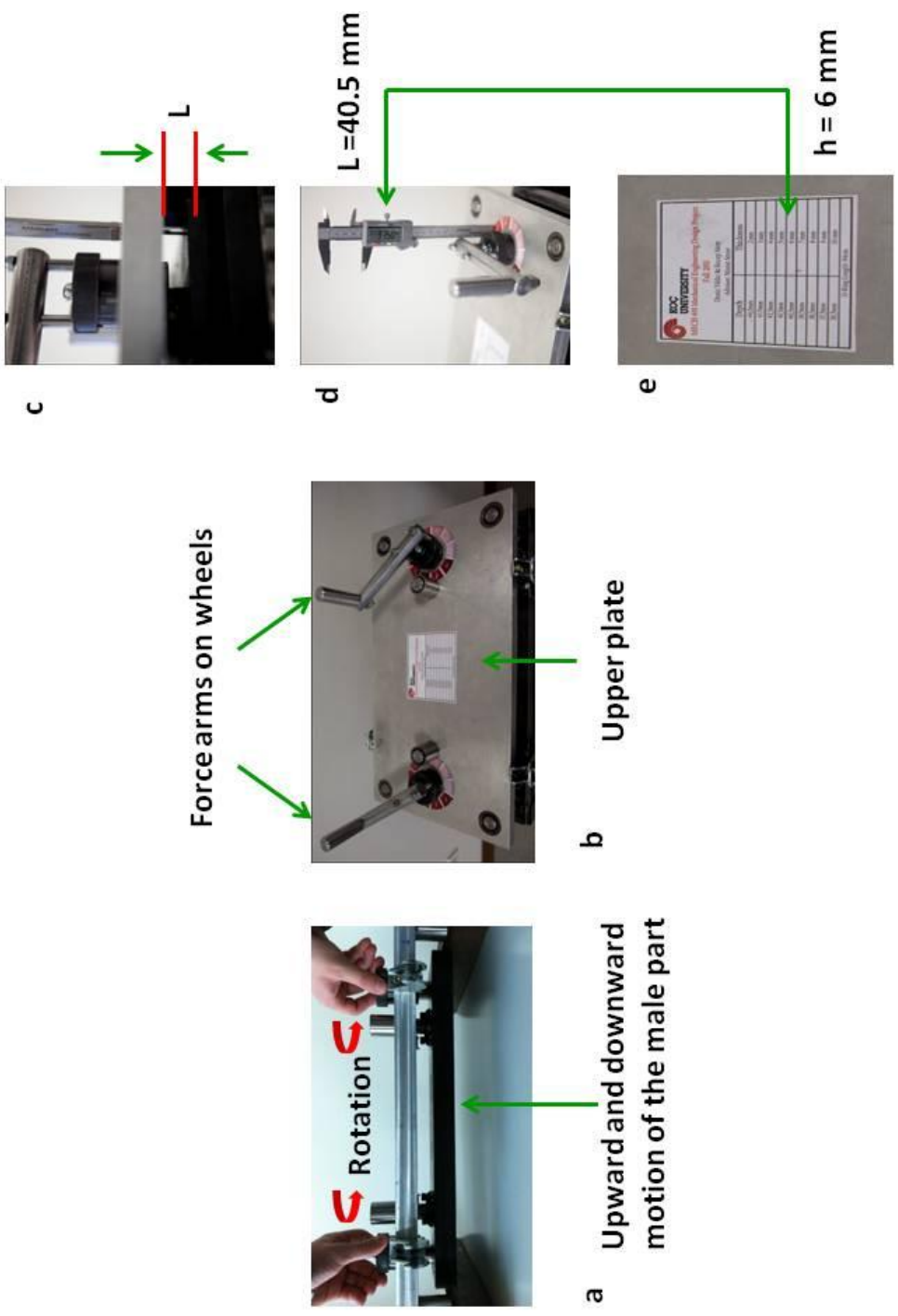

Figure 3. 4 Thickness adjustment system of the mold. a) Movement of the male part, b) force arms are used to make rotation easier, c) distance (L) between the male part of the upper mold and metallic upper plate, d) measuring L by using a vernier calipper, e) using ta look up able to find cavity thickness corresponding to this measured L.

The specimens are prepared by cutting eight layers of fabric with a width of 100 mm wide and a length of 300 mm for all 1D experiments. Before each experiment, the test fluid viscosity is measured and the specimen is weighted to calculate superficial density to reveal probable variation which directly affects the fiber volume fraction and also measured permeability. Statistical values for measured viscosities (μ) and calculated superficial densities (ρ_{sup}) for 1D experiment are listed in Table 3.2.

Table 3. 2 Test fluid and fabric properties for 1D experiments.

Type of Exp	**1D Continuous Permeability Measurement Experiments with Constant Flowrate**				**1D Continuous Permeability Measurement Experiments with Constant Pressure**			
Fabric Type	Superficial density, ρ_{sup} [$^{g}/_{m^2}$]							
	min	max	mean	σ	min	max	mean	σ
Woven (Warp)	273	292	285	5.3	260	286	275	6.2
Woven (Weft)	275	290	283	36	258	288	277	8.1
Biaxial	842	863	852	6.2	833	879	856	10.6
Random	395	435	418	13.1	415	479	445	18.0
Fabric Type	Viscosity [mPa.s]							
	min	max	mean	σ	min	max	mean	σ
Woven (Warp)	185	210	197	6.5	180	215	191	6.7
Woven (Weft)	190	200	196	3.7	180	205	190	6.2
Biaxial	190	200	194	3.7	190	215	196	7.3
Random	190	200	193	3.3	190	210	195	4.5

3.1.1 1D Continuous Permeability Measurement Experiments with Constant Flow Rate Boundary Condition

The experimental set up is schematically shown in Figure 3.5. RTM Radius Engineering flow rate-controlled, 2100 cc injection machine is used in this study. To avoid fiber wash (fabric movement inside the mold cavity) because of high pressure, the flow rate is set to a low value of 10 cc/min. During these experiments Dynisco Instruments pressure sensors (ranges 0 – 500 psig) are used to record P_{in} versus time.

Experimental procedure is detailed below;

1) ***Specimen preparation***: Initially, fabric layers are cut and stacked very carefully. The fabric specimen is weighted and ρ_{sup} (superficial density) is calculated before placement. Test fluid viscosity is measured before each experiment. Detailed calculation of superficial density is given in the sample calculation section.
2) ***Placement of the specimen and thickness adjustment***: The fabric specimen is placed in the mold cavity, and the mold is clamped. It is ensured that the fabric specimen should perfectly fit the mold cavity, otherwise racetracking occurs during injection. Thickness is adjusted by using wheels located on the upper mold part.
3) ***Zeroing dial-gages:*** After the mold is closed, the dial gages are set to zero if no mold bending is observed (i.e, if all gages measure the same thickness). If deflection is observed, the latches, which are located around the periphery of the mold, are fine adjusted to minimize this deflection (see Figure 3.5)

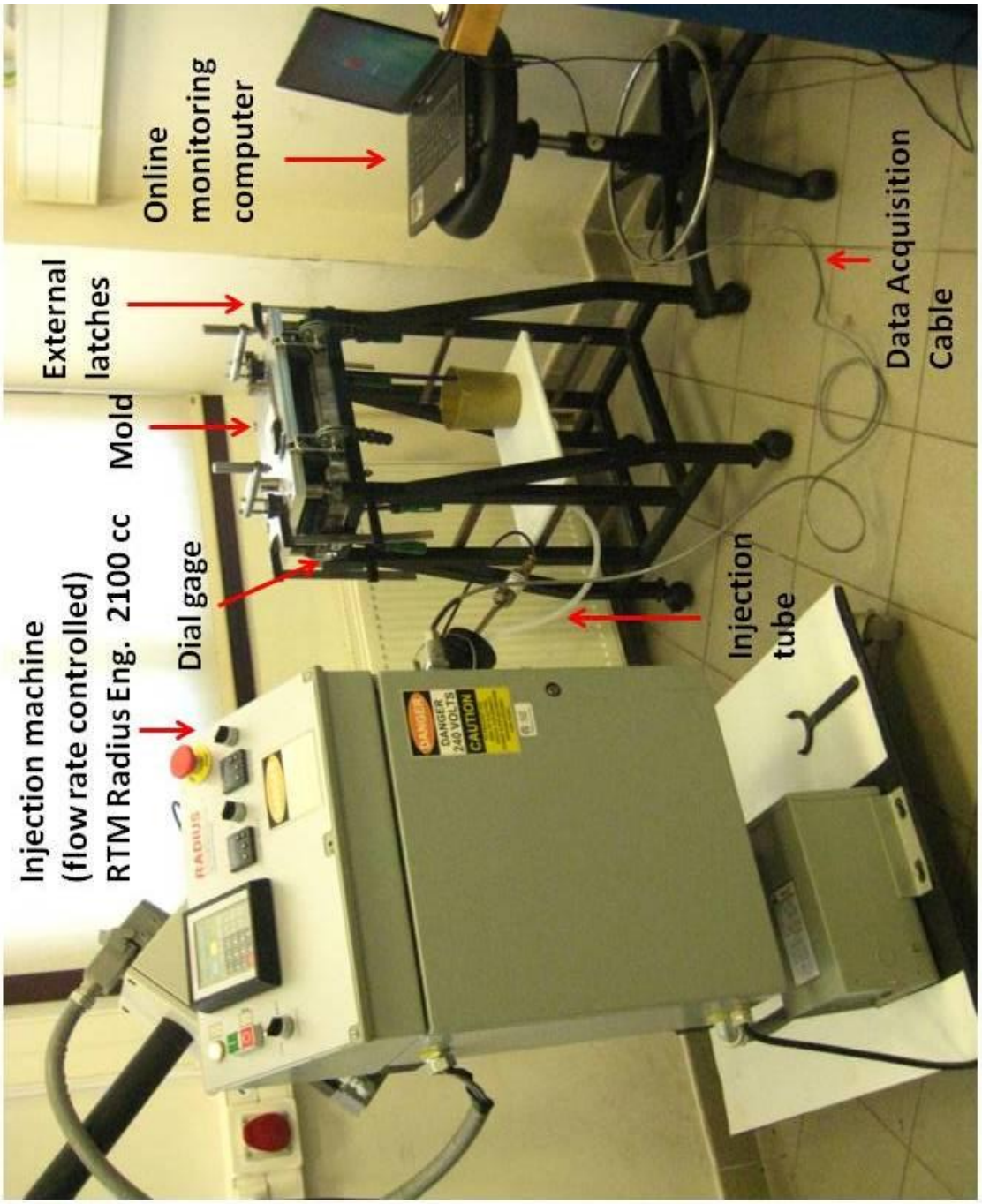

Figure 3. 5 Setup for 1D continuous permeability measurement experiment with constant flow rate boundary condition.

4) ***Operate injection machine:*** Software of the injection machine is run, and the necessary input data (flow rate set point, pressure set point, name of the experiment and frequency of the data acquisition) are entered. After zeroing the piston position, the test fluid is transferred into the cylinder.

5) ***Running online monitoring system:*** Online drawing of the injection pressure (P_{in}) versus time (t) data is achieved by running a Matlab code, which was specially prepared for this set up, just before the injection.

6) ***Injection:*** After the tube connection between the mold, and injection machine (RTM Radius Engineering 2100); and the connection between the pressure sensor and the computer are totally checked, the injection is started. Before starting the injection, the followings must be done: (i) The pressure sensor should be set to zero. (ii) All entrapped gas inside the cylinder and/or injection pipe should be removed; otherwise, it can cause deviation from the flow rate set point and underestimation of permeability.

7) ***Adjustment of new thickness***: When the mold is completely filled, approximately three or four minutes should be waited to achieve steady flow which means P_{in} is constant with respect to time. Then the thickness is changed to its new value in the domain of this particular fabric; and the experiment waits for the flow becomes steady again. Typical P_{in} versus time graph for [$8W_{warp}$] is seen in Figure 3.6 and Figure 3.7. In Figure 3.6, the experiment starts at the highest thickness value and continues towards to the lowest ones. Conversely, in Figure 3.7, the experiment is initiated at the lowest thickness value and continues towards the highest ones to observe whether there is any difference between these two approaches in terms of mold deflection, and/or very sudden peak in pressure. Its results are discussed in Chapter 5 in detail.

8) ***Data Processing:*** Data processing is explained in detail in sample calculation section of the 1D permeability measurement experiments with constant flow rate boundary condition.. Matlab codes for online monitoring of injection pressure (P_{in}) versus time (t) and calculation of unsteady (K_{uns}) and steady (K_s) permeability for 1D continuous permeability measurement experiments with constant flow rate are given in Appendix B.

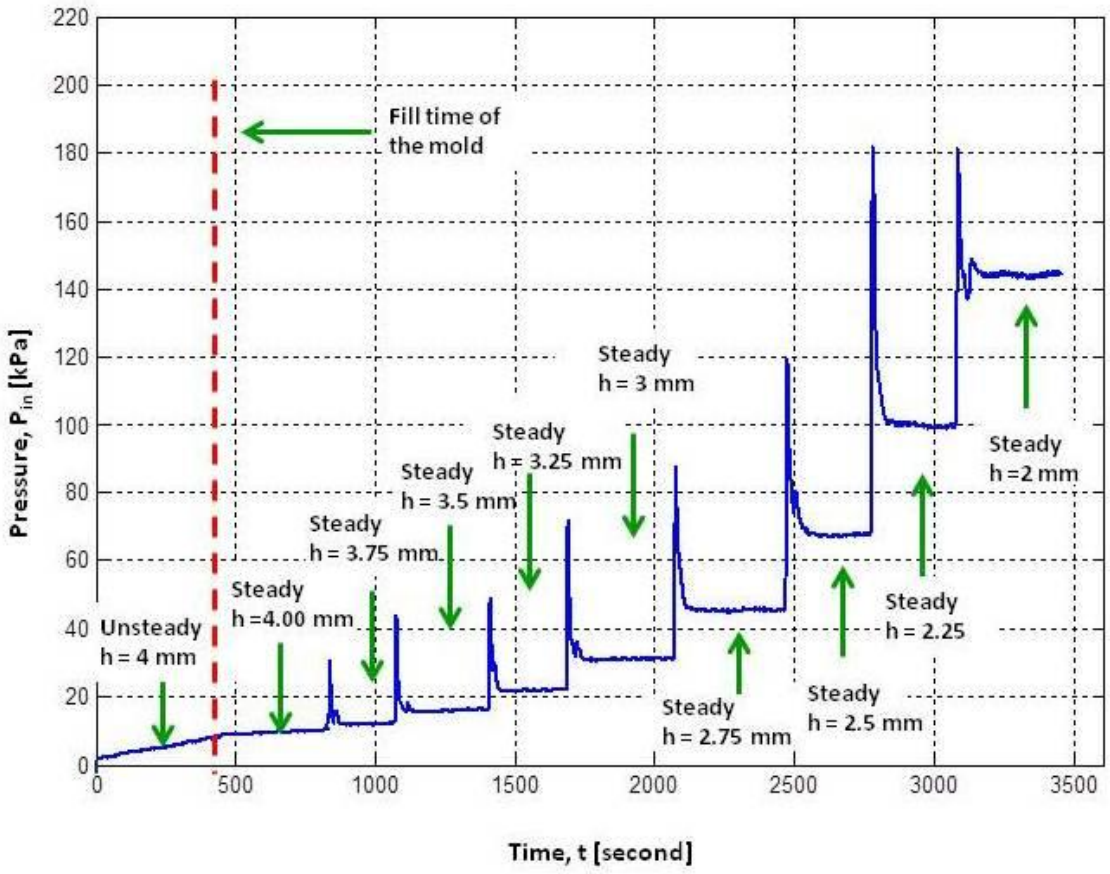

Figure 3. 6 Injection pressure (P_{in}) versus time (t) graph for a typical 1D continuous permeability measurement experiment with constant flow rate boundary condition for [$8W_{warp}$] at h = 4, 3.75, 3.5... , 2 mm.

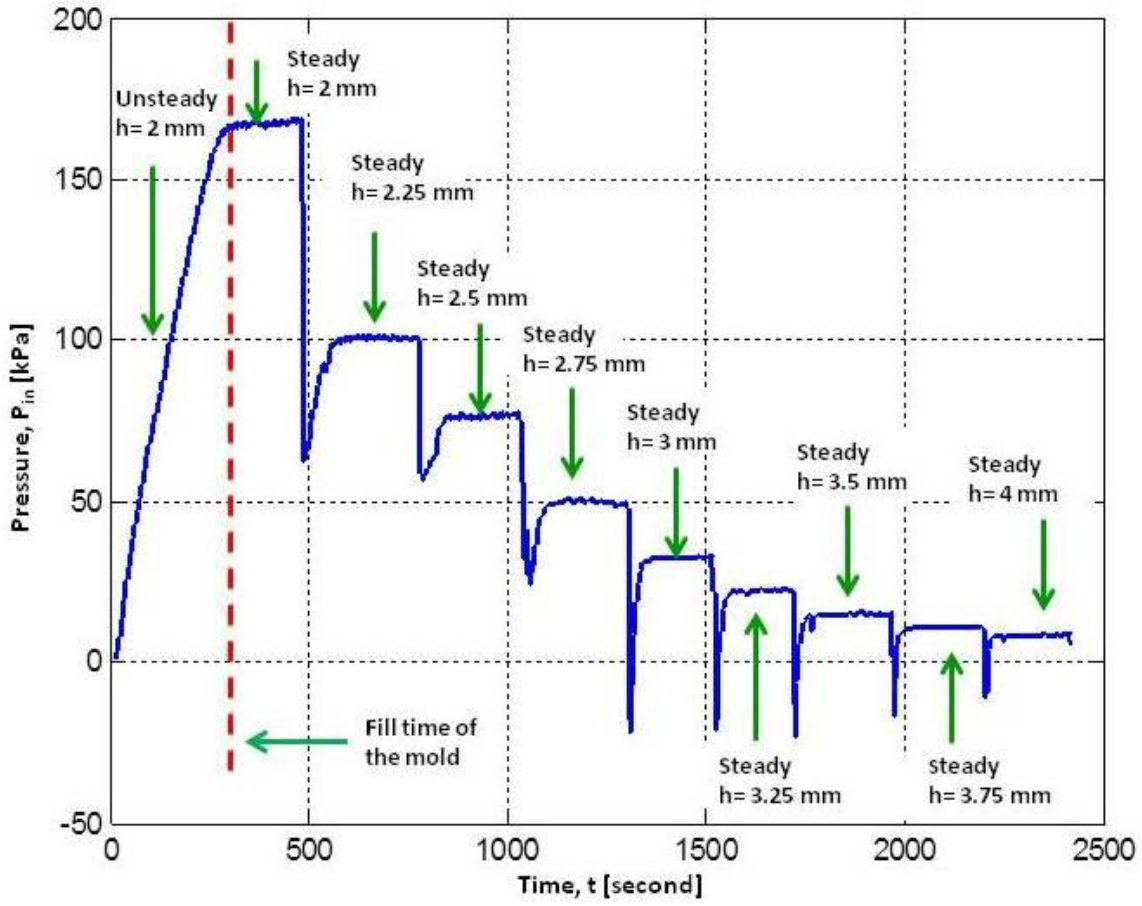

Figure 3. 7 Injection pressure (P_{in}) versus time (t) graph for a typical 1D continuous permeability measurement experiment with constant flow rate for [$8W_{warp}$] at h = 2, 2.25, 2.75... , 4 mm

3.1.1.a Sample Calculation for 1D Continuous Permeability Measurement Experiment with Constant Flow Rate Boundary Condition

In this case study, sample calculations are given for the experiment given in Figure 3.7 which for [$8W_{warp}$] fabric which starts with h =2 mm and terminates at h = 4 mm. K_{uns} and K_s of the specimen at 2 mm are calculated as follow.

Input data for this experiment are given below.

N = 8	Number of layers
m = 69.7	[g], (mass of the fabric preform)
h = 2	[mm], (thickness of the fabric preform in the mold cavity)
$\mu = 0.200$	[Pa.s], (viscosity of the test fluid)
Q = 10	[cc/min], (flow rate set point)
$l =$ 300	[mm], (length of the fabric preform)
w = 100	[mm], (width of the fabric preform)
ρ_f = 2540	[kg/m^3], (density of the glass fiber)
P_{vent} = 0	[kPa], (Pressure at the ventilation port = atmospheric gage pressure)

- Superficial density of the fabric (i.e., per layer) is calculated as:

$$\rho_s = \frac{m}{N\,w\,l} \tag{3.1}$$

$$\rho_s = \frac{(0.0697)}{(8)(0.1)(0.3)} = 0.290 \text{ kg/m}^3$$

- Fiber volume fraction (V_f) is calculated as:

$$V_f = \frac{N\,\rho_{sup}}{h\ \rho_{fiber}} = \frac{(8)(0.290)}{(0.002)(2540)} = 0.457 = 45.7\,\% \tag{1.1}$$

- Porosity of the preform is:

$$\emptyset = 1 - V_f = 0.543 = 54.3\,\%$$

- Total volume of the fabric preform at h = 4 mm:

$$V_t = (10\,)(30)(0.2) = 60\ cm^3 = 60\ cc$$

- Volume of the porosity inside the fabric preform:

$$V_p = (60)(0.543) = 32.6\ cc$$

- Expected fill time of this fabric preform:

$$t_{fill(expected)} = \frac{V_P}{Q} = \frac{32.6}{10} = 3.26\ \text{min} = 196\ second$$

- For unsteady permeability (K_{uns}) calculation at h= 4 mm, Eq (1.7) in Chapter 1 is used. The slope of $\frac{dP_{in}}{dt}$ = 0.514 kPa/s is found by using a first order polynomial fit to P_{in} (t) at unsteady region as seen in Figure 3.8.

$$K_{uns} = \left(\frac{Q}{wh}\right)^2 \frac{\mu}{\phi} \frac{1}{\frac{dP_{in}}{dt}} \tag{1.7}$$

$$K_{uns} = \left(\frac{(1.67\times10^{-7})}{(0.1)(0.002)}\right)^2 \left(\frac{(0.200)}{(0.543)}\right)\left(\frac{1}{514}\right) = 4.99 \text{ x } 10^{10}\ \text{m}^2$$

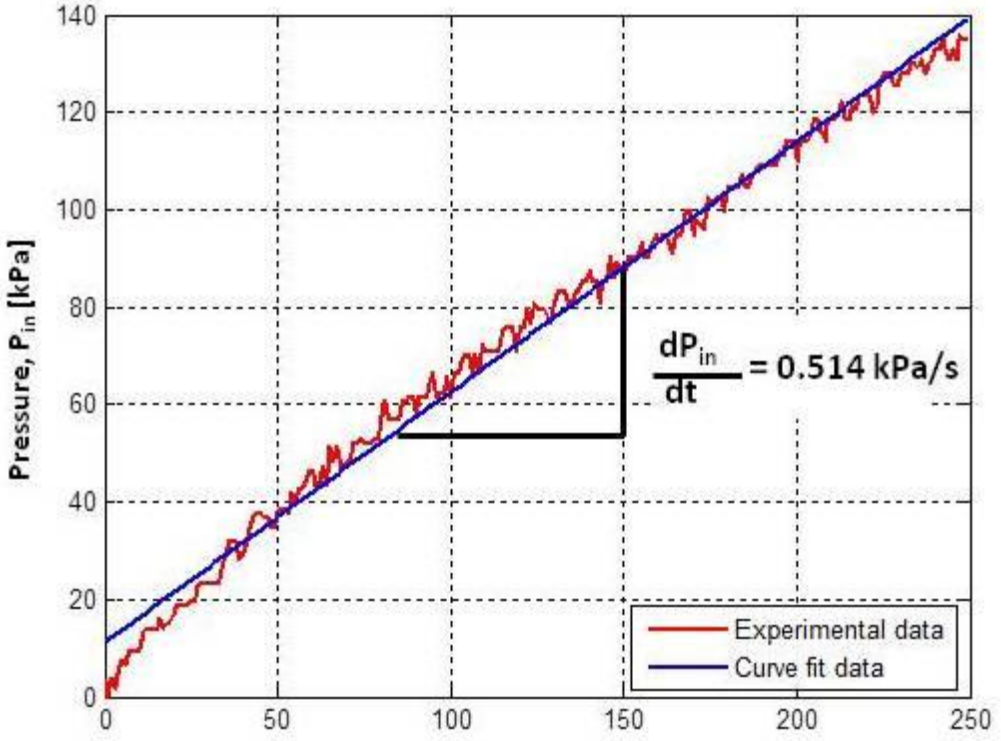

Figure 3.8 Injection pressure (P_{in}) versus time (t) graph for unsteady region of [$8W_{warp}$] at h= 2 mm.

- For steady permeability (K_s) calculation at h = 2 mm, Eq (1.9) in Chapter 1 is used. At that thickness, when the mold is completely filled, the injection pressure becomes constant at 135 kPa and does not change anymore.

$$K_s = \frac{Q\,\mu}{w\,h}\frac{1}{\frac{P_{in} - P_{vent}}{L}} \tag{1.9}$$

$$K_s = \left(\frac{(1.67\times10^{-7})\,(0.200)}{(0.1)(0.002)}\right)\left(\frac{(0.3)}{1.35\text{x}10^{5}}\right) = 3.71\,x\,10^{-10}m^2$$

3.1.2 1D Continuous Permeability Measurement Experiments with Constant Pressure Boundary Condition

1D continuous permeability measurement experiment setup consists of a mold, a vacuum pump, digital balance, a regulator and a camera. The experimental set up is seen in Figure 3.9. Detailed information about parts of experimental setup is given in Appendix C. Injected amount of test fluid is weighted by digital weighting using the digital balance during unsteady and steady parts of an experiment In Figure 3.10, mass of the injected test fluid (m) versus time (t) graph, is seen for both unsteady and steady parts of a typical 1D continuous permeability measurement experiment with constant pressure boundary condition. Flow rate of the test fluid exiting from the ventilation port gets too small when the thickness is set too thin during continuous experiments. The slope of m versus time graph also becomes too small; and therefore the precision of the balance is not small enough to get the desired level of accuracy to determine K_s at these very low h values. Because of that, steady part of 1D continuous permeability measurement experiments with constant pressure are not performed at whole the thickness domains given in Table 3.1.

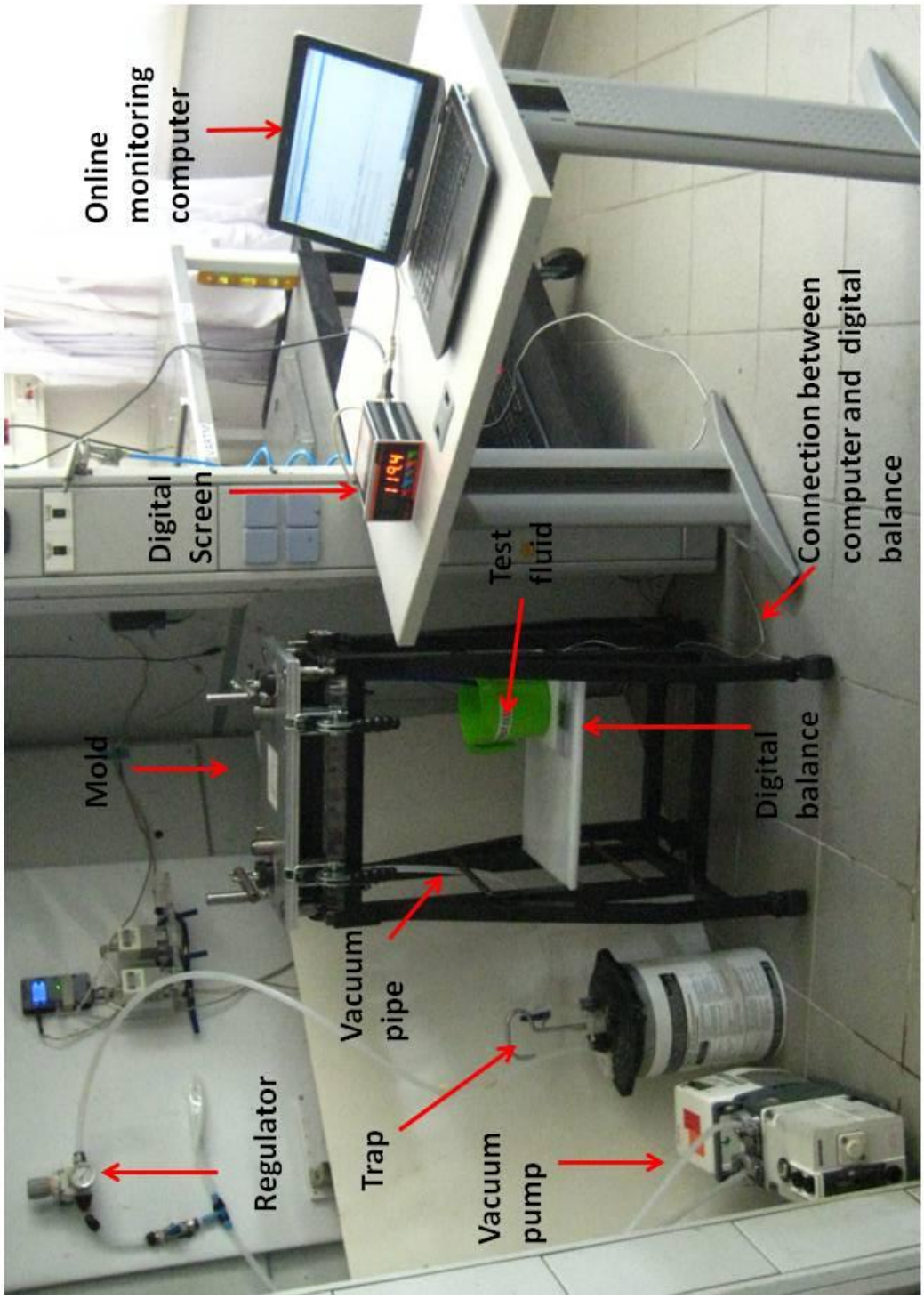

Figure 3. 9 Set up for 1D continuous permeability measurement experiment with constant pressure boundary condition.

First three stages of the experimental procedure for 1D continuous permeability measurement experiments with constant pressure boundary condition are the same as 1D continuous permeability measurement experiment with constant flow rate.

Experimental Procedure;

4) ***Operate vacuum pump:*** After the connection between the vacuum pump and the mold is completed, the vacuum pump is turned on and pressure is set to the selected value by using the regulator. To be sure that the pressure is equal to the set point, the pressure value on the regulator should be observed for awhile before starting the injection. For [8R] configuration P_{in} is set to 100kPa, for the other configurations P_{in} set as 20 kPa.
5) ***Connection between computer and digital balance:*** Digital balance is placed under the inlet port, and the resin reservoir is put on it. After it is connected to a computer, a Matlab code is run to record and online monitor m versus t.
6) ***Injection:*** Before starting the injection, a camera is placed underneath the mold to record the flow front position (x_f) versus time (t) during unsteady part of the experiment.
7) ***Changing of thickness:*** When the mold is completely filled and the resin starts exiting from the ventilation port, roughly seven minutes should be waited for collecting enough m versus t data which is sufficient to observe explicit slope dm/dt to calculate K_s at that thickness value. Then, the thickness is changed with the thickness domain of the fabrics given in Table 3.1.
8) ***Data Processing:*** Data processing is detailed in the sample calculation section. A Matlab code for data transfer of m (mass of test fluid) and time (t) from, the digital balance to the computer.

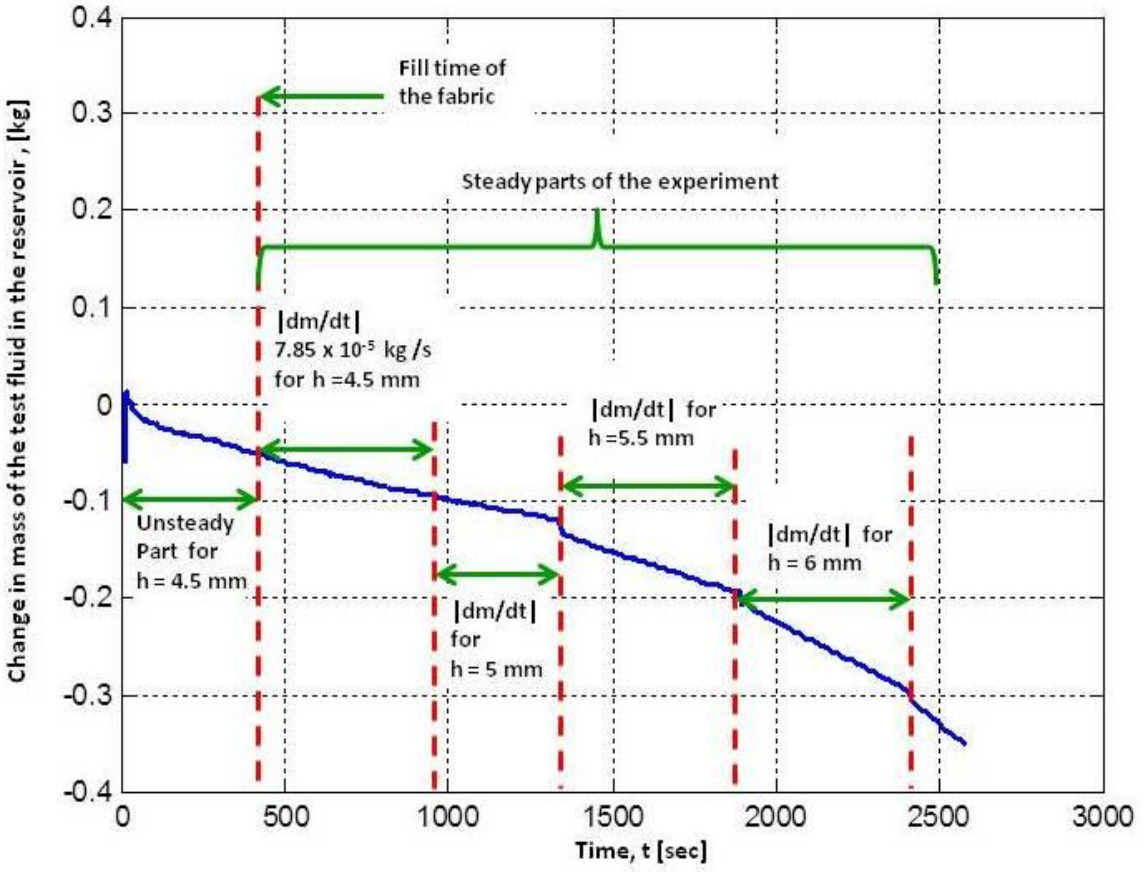

Figure 3. 10 Typical mass of injected test fluid (m) versus time (t) graph for a typical 1D continuous permeability measurement experiment with constant pressure boundary condition for [8R] fabric preform at h = 4.5, 5, 5.5 and 6 mm. Notice that change in mass of the test fluid in the reservoir is negative; and the mass flow rate is the absolute value of it.

Sample Calculation for 1D Continuous Permeability Measurement Experiment with Constant Pressure Boundary Condition

In this case study, a sample calculation is given for the experiment shown in Figures 3.10 and 3.11 which represent a [8R] fabric preform starting at h = 4.5 mm and ending at h= 6 mm with an increment of $\Delta h = 0.5$. Calculation of K_{uns} and K_s permeability values are demonstrated below for h = 4.5 mm.

Input data for this experiment are listed below**:**

N = 8 (Number of layers)

m = 107 [g] , (weight of the fabric preform)

h = 4.5 [mm], (thickness of the fabric preform in the mold cavity)

μ = 0.190 [Pa.s], (viscosity of the test fluid)

l = 300 [mm], (length of the fabric preform)

w = 100 [mm], (width of the fabric preform)

ρ_f = 2540 [kg/m^3], (density of the glass fiber)

P_{in} = 100 [kPa], (injection pressure)

ρ = 1250 [kg/m^3], (density of the test fluid corresponding to 0.190 Pa.s)

- Superficial density (ρ_{sup}), fiber volume fraction (V_f) and also porosity (∅) of the fabric preform at h = 4.5 mm are calculated.

$$\rho_{sup} = \frac{(0.107)}{(8)(0.1)(0.3)} = 0.446\ k\text{g/m}^2 \text{ (per layer)}$$

$$V_f = \frac{N\,\rho_{sup}}{h\,\rho_f} = \frac{(8)(0.446)}{(0.0045)(2540)} = 0.312 \;=\; 31.2\,\%$$

$$\emptyset = 1 - V_f = 0.688 = \; 68.8\,\%$$

- Unsteady permeability (K_{uns}) of this specimen at h = 4.5 mm is calculated by using Eq (1.11) where C is determined by using x_f curve-fit to the data as seen in Figure 3.11.

$$K_{uns} = \frac{\mu\,\emptyset}{2\,CP_{in}} = \frac{(0.190)(0.688)}{2(4868)(100000)} = \; 1.34\text{x}10^{-10} \;\; \text{m}^2 \qquad (1.11)$$

- In order to find the steady permeability (K_s) of the same fabric preform at h = 4.5 mm, the slope dm/dt = 7.85 x 10^{-5} kg/s is obtained from the first order polynomial curve fit. Eq (1.12) is used to calculate, the flow rate.

$$\text{Q} = \frac{1}{\rho}\frac{\text{dm}}{\text{dt}} = \frac{1}{1250}(7.85 \text{ x } 10^{-5}) = \; 6.28 \text{ x } 10^{-8}\text{m}^3 / \text{s} \qquad (1.12)$$

- This calculated flow rate then implemented into the Eq (1.13) from chapter 1 to calculate K_s at h = 4.5 mm.

$$K_s = \frac{Q\,\mu\,L}{w\,h\,\Delta P} = \frac{\left(6.28\,x\,10^{-8}\right)(\,0.190)(\,0.3)}{(0.1)\,(\,0.0045)\,(100000)} = \; 7.95 \text{ x } 10^{-11}\text{ m}^2 \qquad (1.13)$$

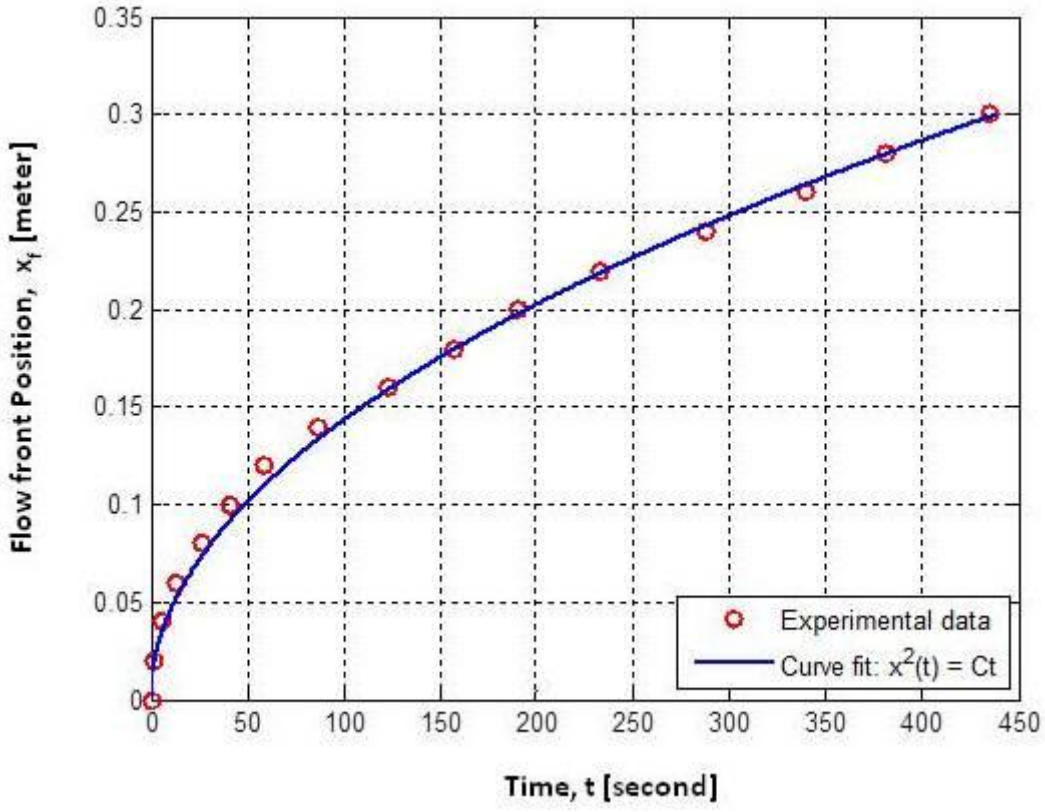

Figure 3. 11 Flow front position x_f versus time, t for a typical 1D unsteady permeability measurement experiment with constant pressure boundary condition for [8R] fabric at h = 4.5 mm. The curve fit constant C = 4868 m^2/s by using least square method.

Matlab code for DAQ of m and time (t) from digital balance to the computer and steady (K_s), unsteady (K_{uns}) permeability calculation for 1D continuous permeability measurement experiments with constant pressure are given in Appendix B.

3.2 2D (Radial) Permeability Measurement Experiments

Radial, unsteady permeability measurement experiments at constant flow rate are performed for [8R], [8S] and [8W] fabric preform. Thickness ranges of the experiments are decided from unloading (decompaction) and fiber relaxation stages of VI characterization experiments, for each fabric type as given in Table 3.3. For each thickness, three experiments are performed.

Table 3. 3 Thickness domains for three different fabric types in 2D permeability measurement experiments [25].

Type of Fabric	Domain [mm]	Increment [mm]
Random	3 – 6	1
Biaxial (Stitched)	5 – 8	1
Woven	2 – 4	0.5

The set up consists of a stainless steel lower plate and a glass upper plate which allows monitoring flow front progression. The plates are in 50 cm in width and 50 cm in length. The metallic lower plate is thick enough (5 mm) to prevent bending which may arise because of the high injection pressure during experiments. The thickness is adjusted by placing spacers between two plates which can be set to a particular thickness value by increasing or decreasing number of spacer layer, and its reliability is checked by using vernier caliper. Injection is done through a hole with a radius of 10 mm which was opened in the middle of the metallic plate. The specimens are cut with in-plane dimensions of 300 x 300 mm with the

same hole diameter of (20 mm) at the center. The hole allows obtaining 2D flow. The injection is carried out by RTM Radius Eng 2100 cc flow rate-controlled injection machine which was also used in 1D experiments. Injection pressure (P_{in}) versus time (t) data is recorded by the same sensor and data acquisition system that were also used in 1D experiments. A digital camera is used to record flow front position both along major (R_{f1}) and minor axes (R_{f2}) with to time during injection to calculate K_{uns}. The experimental set up for typical radial unsteady permeability measurement experiment is seen in Figure 3.12.

Experimental Procedure;

Almost all stages except DAQ of the 2D unsteady permeability measurement experiments are similar to the stages of 1D unsteady permeability measurement experiments. Some minor differences exist in specimen preparation and thickness adjustment as discussed below. Data processing for 2D experiments is given in sample calculation section.

1) ***Specimen preparation***: Eight layers of fabric are cut with an inlet hole which is opened in the middle of it by using a punch. For each experiment, superficial density is calculated and viscosity is measured.
2) ***Placement of the specimen and thickness adjustment***: It is placed on the metallic plate; it should be provided that the two holes both on the specimen and the plate must overlap each other. Requirements for operation of injection machine and precautions that should be taken during preparation of injection machine in 1D experiments are valid in 2D case. During injection the flow front progression with time is recorded by using camera. In Figure 3.10, flow front position at two different time for [8R] fabric during 2D permeability measurement experiment is demonstrated.

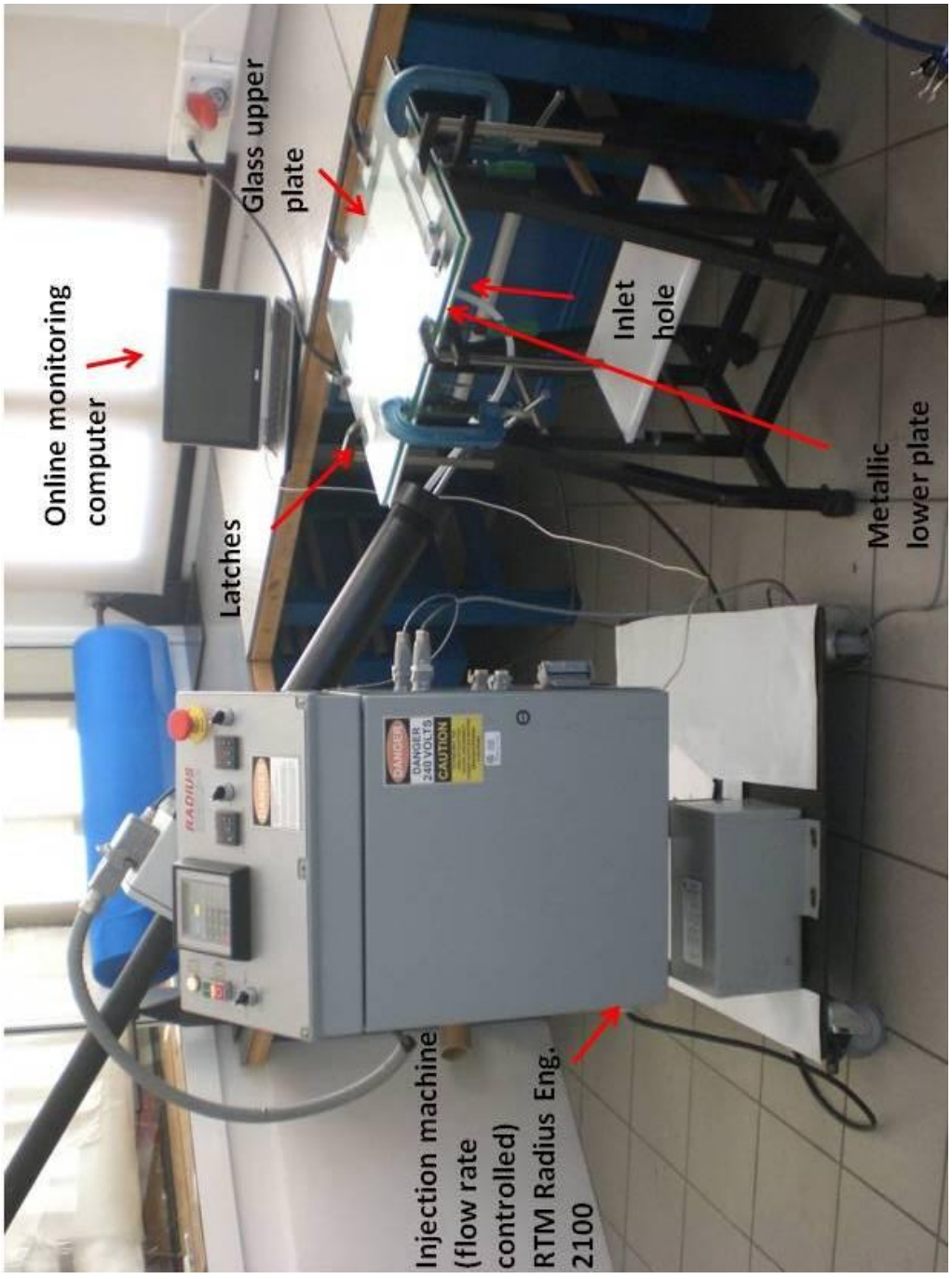

Figure 3. 12 Setup for 2D (radial) permeability measurement experiment with constant flow rate boundary condition.

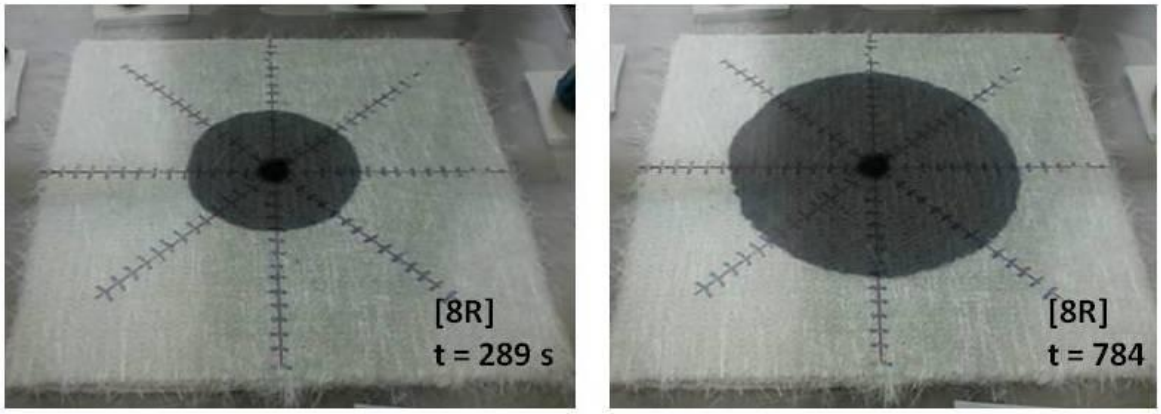

Figure 3.13 Flow front position at two different time for [8R] fabric during 2D permeability measurement experiment.

Sample calculation for 2D permeability measurement experiment with constant flow rate boundary condition

Sample calculation is done for [8R] fabric configuration.

Input data;

N = 8	Number of layers
m = 339	[g], (mass of the fabric preform)
h = 6	[mm], (thickness of the fabric preform)
$\mu = 0.191$	[Pa.s], (viscosity of the test fluid)
Q = 10	[cc/min], (flow rate set point)
$l =$ 300	[mm], (length of the fabric preform)
w = 300	[mm], (width of the fabric preform)
ρ_f = 2540	[kg/m^3], (density of the glass fiber)
R_{in} = 1	[cm], (diameter of the inlet hole)

- Superficial density, fiber volume fraction are calculated as follows.

$$\rho_{sup} = \frac{(0.3\ 39)}{(8)(0.3)(0.3)} = 0.471\ kg/m^2\ \text{(per layer)}$$

$$V_f = \frac{N\ \rho_{sup}}{h\ \rho_f} = \frac{(8)(0.471)}{(0.006)(2540)} = 0.247\ 24.7\ \%$$

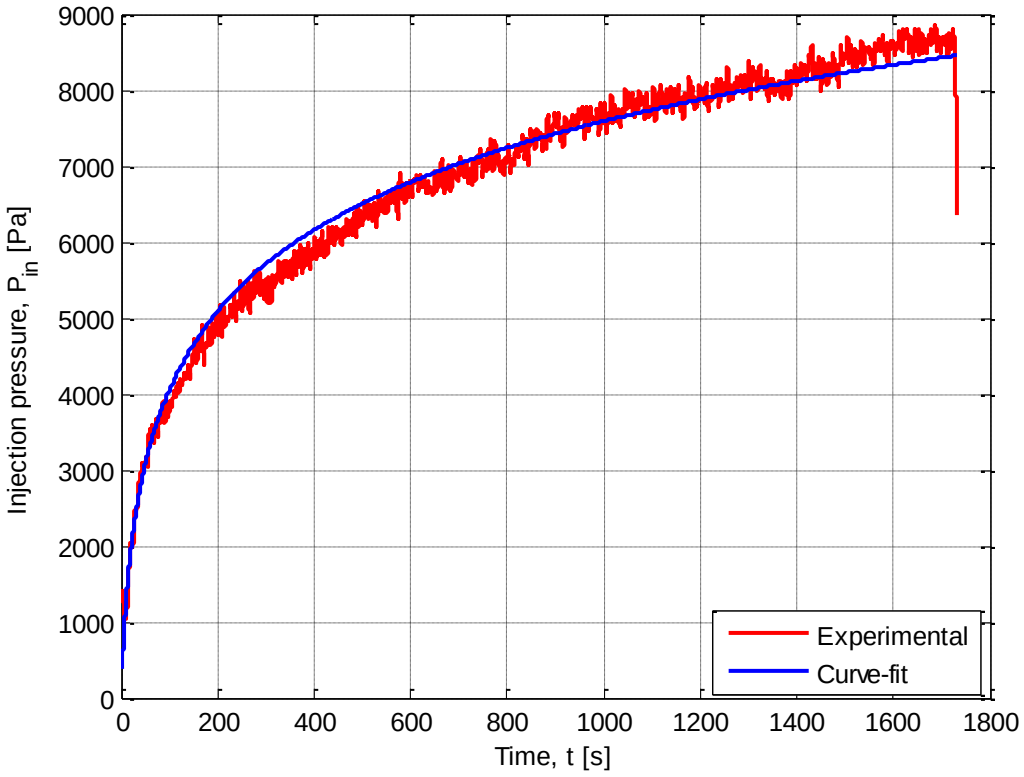

Figure 3.14 Injection pressure, P_{in} versus time, t for a typical 2D unsteady constant flow rate permeability measurement experiment for [8R] fabric at h = 6 mm. The curve fit constant was found as D = 1589 Pa / s by using Eq 1.16 curve fit to data.

Permeability of the fabric preform at 6 mm is calculated by using Eq 1.15 given in Chapter 1. The curve fit constant D is to be determined by using Eq 1.16 in Chapter 1. (Figure 3.11)

$$K \equiv \sqrt{K_{xx}\,K_{yy}} = \frac{(0.191)(1.67x10^{-7})}{4\pi\,(0.006)(1589)} = 2.66\,x10^{-10}\ m^2 \qquad (1.15)$$

CHAPTER 4

INVESTIGATION OF ERROR SOURCES IN PERMEABILIT MEASUREMENT EXPERIMENTS

In this chapter, anticipated sources of errors in permeability measurement experiments, and methods that are suggested and applied to minimize these errors are given.

4.1 Sources of Error and Methods to Minimize Them

All permeability measurement experiments are very sensitive to experimental error which can occur during sample preparation, experiments or post processing. In order to obtain more accurate and repeatable experimental results, some precaution should be taken. In our permeability characterization experiments, the following items contributed to the experimental error in the calculation of permeability.

4.1.1 Sample Preparation

Sample preparation process can be classified under two subtitles; (i) fabric preform, (ii) test fluid preparation. During cutting and placing operations, additional care should be

given to obtain samples with small dimensional tolerances so that they can perfectly fit in the mold cavity preventing racetracking. Moreover, cutting operations should be done with a very sharp cutter to avoid applying in-plane shear of the fiber bundles in the fabric plies which may change otherwise the permeability tensor of the material.

- *Superficial Density*

Before each experiment, superficial density of each fabric preform should be calculated and used for permeability calculation instead of using catalog value specified by the supplier. For random fabric, the catalog value of superficial density is given as 450 g/m^2. But as seen in Table 3.1 in Chapter 3, the difference between catalog value (450 g/m^2) and the minimum value (395 g/m^2) for superficial density of random fabric reaches up to 14 % in this study.

- *Viscosity of test fluids*

It was observed that the viscosity of glucose syrup shows some variations in the reservoir one hour after mixing the syrup and water. It can be explained as a result of sedimentation of glucose syrup with time. For example, in one of the observation, viscosity of diluted glucose syrup with water was measured as 202 mPa.s. just after mixing. After one hour, two viscosity measurements at different sections of the reservoir were made. One of them was close to the surface and measured as 218 mPa.s, and the other one was close to the bottom and measured as 231 mPa.s. After 2 hours, more than 5% variation was observed in the measured viscosity when compared with initial viscosity value and roughly 6% variation

was observed between different sections. It means homogeneity of the viscosity cannot be conserved for 1 hours. This variation is higher for more viscous mixtures of glucose syrup water. In order to minimize this variation, mixing operation should be done up to homogeneity is achieved at all parts of the reservoir, and experiments should be completed quickly, preferably within an hour or the test fluid should be mixed periodically.

4.1.2 Mold Deflection

Mold deflection is observed in our experiments, and it is the main issue in permeability measurement experiment. Mold deflection is more effective in constant flow rate boundary condition experiments which reach higher inlet pressure values than constant pressure experiments unless the flow rate is set to very low value. During experimental part of this study, up to 0.45 mm deflection was observed unless additional precautions (such as clamps) were taken. Especially, thickness reduction stages during a continuous permeability measurement experiment with constant flow rate boundary condition leads to a sudden pressure jump which triggers to such a high mold deflection. In the following case study, the effect of the mold deflection inside the mold cavity and contribution of the different component of injection machine (pipe, piston) which are not stiff enough to the total error are investigated.

Input data for the case study;

N = 8	Number of fabric layers
h = 3.5	[mm], thickness of the mold cavity
m = 102	[g], weight of 8 layers of random fabric
Q = 15	[cc/min], flow rate
w = 100	[mm], width of the fabric specimen
L = 300	[mm], length of the fabric specimen
ρ_f = 2540	[kg/m^3], density of the glass fiber
L_p = 1	[m], initial length of injection pipe

Before each experiment, we suggest calculating (i) the expected amount of injected test fluid which is sufficient to completely saturate the fabric preform, and (ii) fill time theoretically. Then compare these results with experimental results to reveal is there any considerable difference.

Theoretical calculations;

- Initially ρ_{sup} and V_f are calculated for this particular fabric specimen:

$$\rho_{sup} = \frac{m}{NwL} = \frac{0.102}{(8)(0.1)(0.3)} = 0.425\ kg/m^2$$

$$V_f = \frac{N\,\rho_s}{h\,\rho_f} = \frac{(8)(425)}{(3.5)(2540)} = 0.382$$

- Porosity ($\emptyset$), the total volume of the fabric specimen (V_{total}) , total pore volume inside it (V_{pore}), and expected fill time ($t_{fill(expected)}$) are calculated below.

$$\emptyset = 1 - V_f = 0.618$$

$$V_{total} = (0.35)(10)(30) = 105\ cc$$

$$V_{pore} = V_{total}\,\emptyset = (105)(0.617) = 64.9\ cc$$

$$t_{fill(expected)} = \frac{V_{pore}}{Q} = \frac{64.9}{15} = 4.33\ \text{min} = 259.6\ sec$$

Experimental results;

- Experimental fill time ($t_{fill\ (experimental)}$) for this case study is 338 sec. It is roughly 30 % higher than expected fill time. The experimental injected volume is calculated below and it is shown that there is 18 cc difference between theoretical and experimental injected volume.

$$V_{injected} = Q\ t_{fill\ (experimental)} = (15)(\frac{338}{60}) = 84.5\ cc$$

$$\Delta V = V_{injected} - V_{pore} = 84.5 - 64.5 = 20\ cc$$

All the items that may be expected lead to this variation should be checked out. This variation means that either the pore volume inside the mold cavity is higher than theoretical one, thus more test fluid is injected to completely fill it or the injection machine does not work appropriately. If the constant flow rate controlled injection machine is proven to work appropriately, such a high variation in ΔV can be explained with either mold deflection or

the other stretching of the resin reservoir in the injection equipment which may form this extra volume. The dial gages which were fixed at two sides (inlet and vent sides) of the mold showed up to 0.45 mm deflection at the inlet (because of high injection pressure) and nearly zero deflection at the vent (because it is open to the atmosphere) for this case study.

In Figure 4.1 extra volume forms on the fabric specimen because of 0.45 mm deflection at the inlet port. This extra volume is calculated below.

$$V_{extra} = (0.00392 + 0.0056)(30)(10) = 13.44 \text{ cc}$$

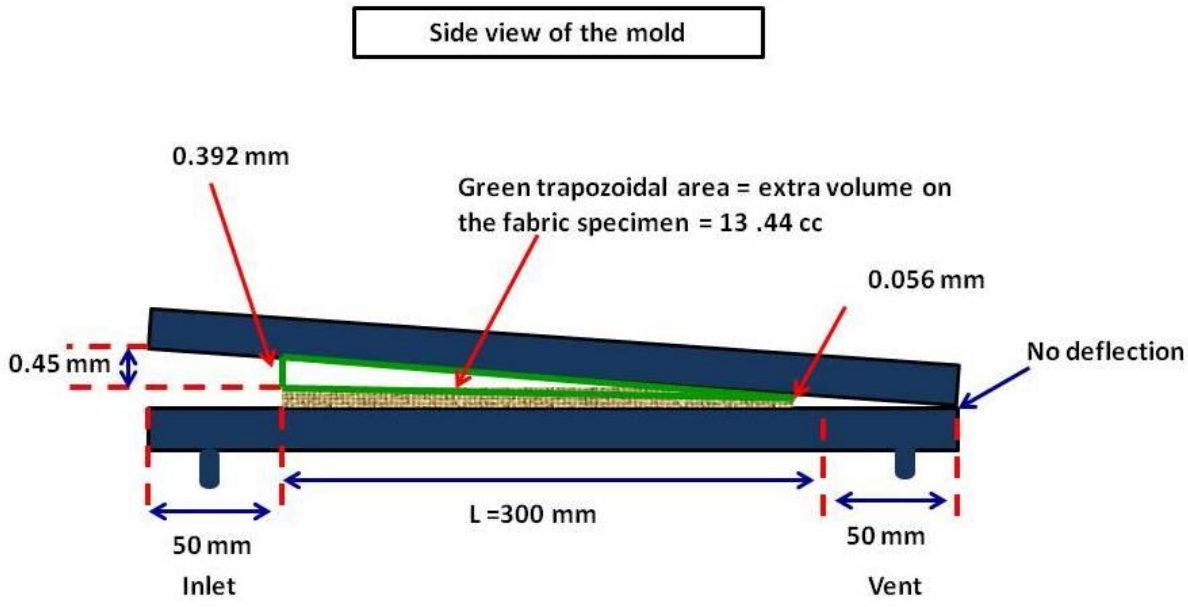

Figure 4.1 Side view of the mold during injection when deflection exists.

Now the majority of the extra injected volume (difference between experimental and theoretical injected volume) is explained, but still 6.56 cc remains. This is also explained in the following parts. Even though it is not possible to eliminate all of this deflection totally the following can useful to minimize it.

(i) Four additional latches are used near the four corner of the mold especially inlet side. If the deflection on the dial gage screen is significant, the latches are adjusted to rezero it.

(ii) This suggestion is for continuous permeability measurement experiments. The most significant deflection occurs during the thickness reduction stage because of a sudden injection pressure jump. Instead of starting at the high thickness and continuing towards to the lowest one, the experiment is started at the lowest thickness value and continues thought to the highest one to overcome this sudden deflection. This approach was used in this study, and it is proven that a significant improvement was observed in the deflection.

(iii) During thickness adjustment in the continuous experiments, injection can be paused until the thickness is adjusted to the next value, and then it is continued starts again. This suggestion was also applied in this study. Though the reduction of the deflection is not as significant as in the previous suggestion, it also helped reducing the error.

4.1.3 Injection pipe

Under high pressure such as 3.5-5 bars which is frequently encountered during constant flow rate permeability measurement experiments, the thermoplastic injection pipe is not stiff enough to resist to such a high pressure, and undergoes some enlargement. In order to reveal the magnitude of this enlargement, a pipe with a length of 1.5 m was cut and one end of it was closed. The other end was connected to the compressed air at 3.5 bars. The initial radius and the radius at 3.5 bar internal pressure were measured using vernier caliper. The amount of enlargement and volume change are calculated below.

- Initial Volume of the 1.5 m pipe with $r_{initial}$= 0.5 cm:

$$V_{initial} = \pi\, r^2\, h = \pi(\,0.5^2)(150) = 117.8\, cc$$

- After 3.5 bars compressed air was applied to it, the new radius became 0.505 mm, thus

$$V_{new} = \pi\, r_{new}^2\, h = \,\pi\,(0.505^2\,)(150) = 120.4\, cc$$

To calculate volume enlargement accurately, the radius was measured at several points along the pipe before and after the application of compressed air. As seen in the calculations above, 2.2 % volume enlargement was observed at 3.5 bars. Note that this change is expected to be independent of the length, L_p assuming that the internal pressure is uniform along the pipe length. It is supposed to reach higher enlargement at higher pressures. In order to minimize the effect of the injection pipe's enlargement, it is suggested to use it as short as possible. In this study, the length of the injection pipe is no more than 1 m, preferably 0.5 m for each type of experiments.

Recall that, in this case study given above, 6.56 cc differences between the theoretical and experimental test fluid exist. In the following, effect of injection pipe is investigated.

Initial volume of the injection pipe;

$$V_{initial} = \pi r^2 \mathrm{h} = \pi\,(0.5^2)\,(100) = 78.54 \text{ cc}$$

Extra volume of the injection pipe under 3.5 bars;

$$V_{extra=}\, V_{initial}\, 2.2\% = 1.73\ cc$$

Now, it is clarified that the extra 1.73 cc comes from the enlargement of the injection pipe under around 3.5 bars. But, still 4.83 cc extra volume remains unresolved yet and it will be explained in the following section.

4.1.4 Piston motion inside the injection machine

High pressure inside the injection machine affects the motion of the piston if it is not stiff enough. Compressed air at 3.5 bars was applied into the cylinder; and the movement of the piston was measured using a vernier caliper. Then, the volume change was calculated. The measurement of was repeated several times under 3.5 bars, and it was observed that the piston movement resulted in 2.5 - 4.5 cc extra volume formation.

As a summary, recall that

$$\Delta V = V_{injected} - V_{pore} = 18\ cc$$

And the error analysis indicated that

$$\Delta V_{error} = \Delta V_{deflection} + \Delta V_{pipe\ enlargement} + \Delta V_{piston\ movement}$$

$$\Delta V_{error} = 13.44cc + 1.73cc + (2.5 \sim 4.5)\text{cc}$$

$$\Delta V_{error} \cong 17.67 - 19.67\ \text{cc}$$

CHAPTER 5

RESULTS OF THE EXPERIMENTS

In this chapter, results of the permeability measurement experiments performed for [8R], [8B], [$8W_{warp}$] and [$8W_{weft}$] fabric configurations are investigated. The effects of suggestions given in the previous sections to minimize anticipated errors are discussed, and final comments which may allow one to performing more repeatable and accurate permeability measurements are given in this chapter. The coefficient of determination, R^2 which is a statistical term and represents the proportions of variability in the data sets (in this study K vs V_f) is calculated for each fabric type and experimental procedures. The calculation of R^2 is as follows [27]

$$R^2 = 1 - \frac{SS_{err}}{SS_{tot}} \tag{5.1}$$

where SS_{err} is residual sum of squares (where the residual is the difference between the observed and the predicted values) and SS_{tot} is the total sum of the squares, and they are calculated by using the formulas given below.

$$SS_{tot} = \sum_i (y_i - \bar{y})^2 \quad (5.2)$$

$$SS_{err} = \sum_i (y_i - f_i)^2 \quad (5.3)$$

here, y_i is the observed data of depended variable (in this study, K_{uns} or K_s), $\bar{y}$ is the mean of the observed data, and f_i is the predicted values of the depended variable which are obtained from curve fit. R^2 changes between 0 and 1. The closer the R^2 to 1, the correlation between data points and the model becomes stronger which results in lower residual. The determination of coefficient values and the curve fit constants for each fabric types are demonstrated in Table 5.1. For each fabric type, the largest residuals are observed in 1D steady permeability measurement experiments performed with constant pressure boundary condition. This error is expected to be because of the following two items: (i) The procedure is based on measuring dm/dt at the inlet reservoir. Under the pressure differential selected, the typical dm/dt values are in the order of 0.1 g/s or less. Using a digital balance that is not within the precision of the mass flow rate may have caused inaccurate permability result. (ii) The sink effect [7] may have caused a delay in the resin flow affecting the accuracy of dm/dt especially at low flow rate. For constant pressure 1D permeability measurement experiments, more than one order of magnitude variation in K_s is observed compared to the other types of experiments for random and biaxial fabrics. The results of K_s for the woven fabric under constant pressure were closer to the results of the other methods. Note that such a big variation between different experimental procedures was also observed in the permeability benchmark exercise [16], even though procedures are consistent in each other. Observing Figures 5.1-5.4, it is easily said that unsteady permeability of each fabric is higher than the

steady values for all measurement methods. Parnas et al. [13] found similar result between radial unsaturated flow and unidirectional saturated flow and explained this as a result of the capillary forces which are not taken into account during unsaturated flow. Another distinct result observed in Figures 5.1-5.4, is that, for all fabric types, both unsteady and steady K of 1D constant flow rate experiments are higher than the corresponding K's of constant pressure boundary conditions. It was also observed that the mold deflection, which is one of the main sources of error, is less effective in constant pressure permeability measurement experiments than the constant flow rate experiments. This is due to the lower levels of injection pressure in constant pressure experiments than constant flow rate experiments.

Even though all the issues and sources of error have not been eliminated totally, the suggestion given in this thesis will be helpful for the troubleshootings and minimizing error sources. The followings summarizes of the suggestion given in this study.

- During 1D experiments, it must be validated that the flow is almost 1D until the mold is completely filled with test fluid. Otherwise the experiments must be repeated.
- Before each experiment, superficial density should be calculated, and the viscosity of the test fluid should be measured.
- Fill time of an experiment performed at constant flow rate boundary condition must be checked. The difference between experimental and analytical expected fill time indicates the probable problems such as; (i) inaccurately running of injection machine due to high internal pressure, (ii) mold bending, (iii) inflation of injection tube. In order to minimize the total error, suggestions are given in Chapter 4.

- During continuous experiments, starting with the lowest thickness values and continuing towards to the highest one, or pausing the injection machine during thickness adjustment are effective ways of preventing sudden pressure jump which causes mold bending.
- It is also noteworthy that the novel mold used in this study is practical setup especially for continuous permeability measurement experiments, and it provides consistent measurements because of its robust thickness adjustment system.

Additionally, 2D (radial) permeability measurement experiments were performed only for [8R] fabric, because of the unexpected results obtained. Investigation to find reason of these irrelevant results still continues.

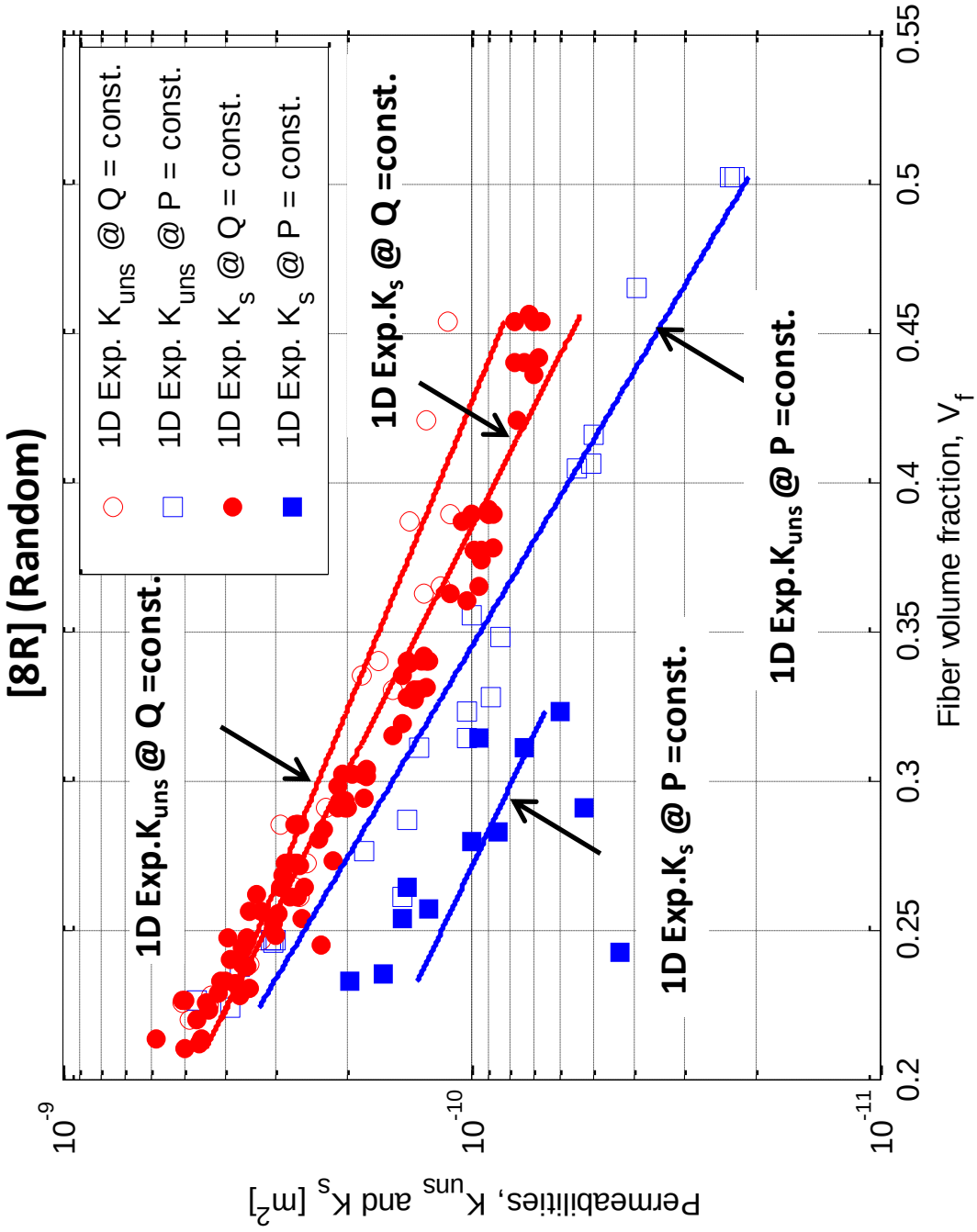

Figure 5. 1 Results of 1D permeability measurement experiments for [8R] (Random).

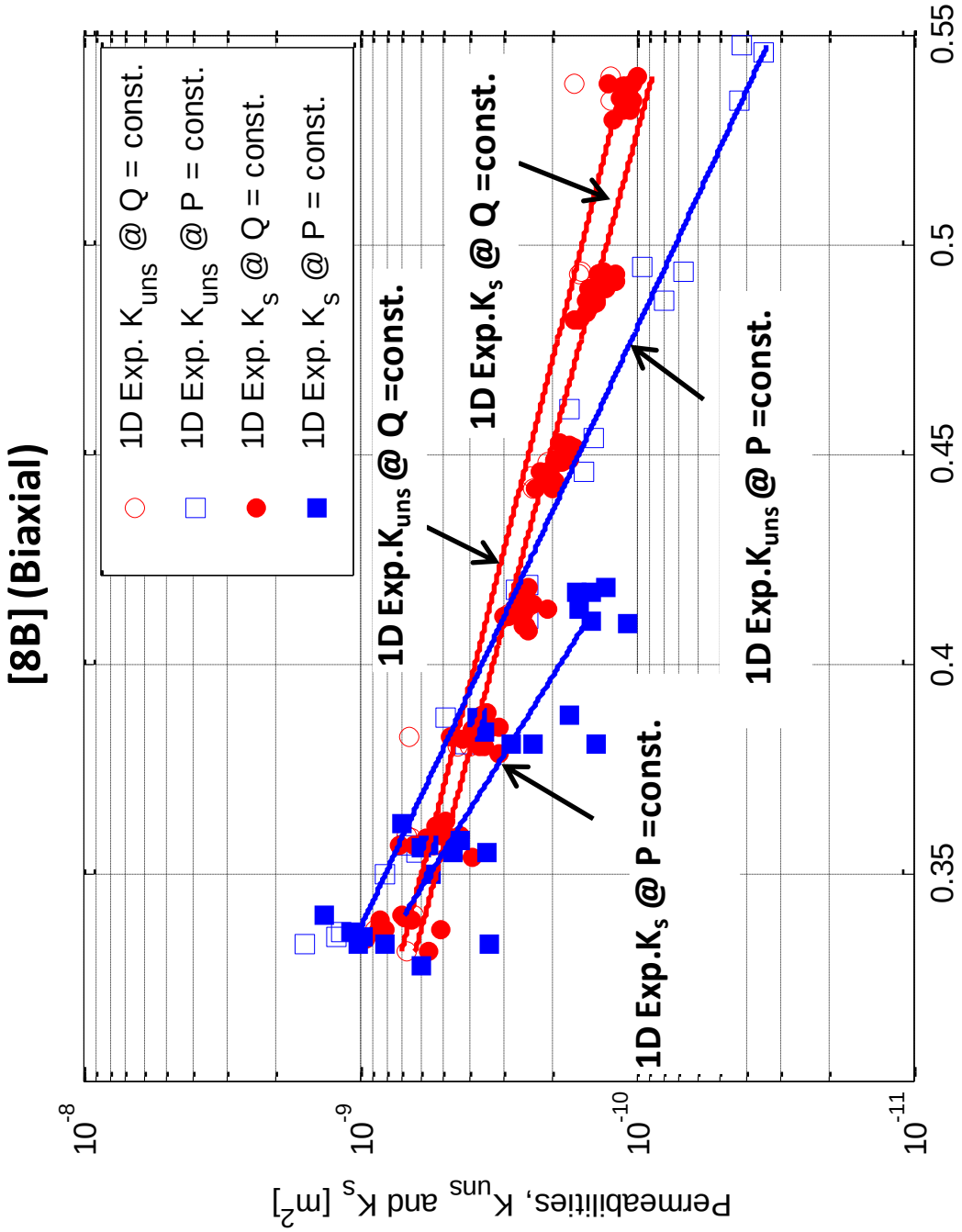

Figure 5. 2 Results of 1D permeability measurement experiments for [8B] (Biaxial).

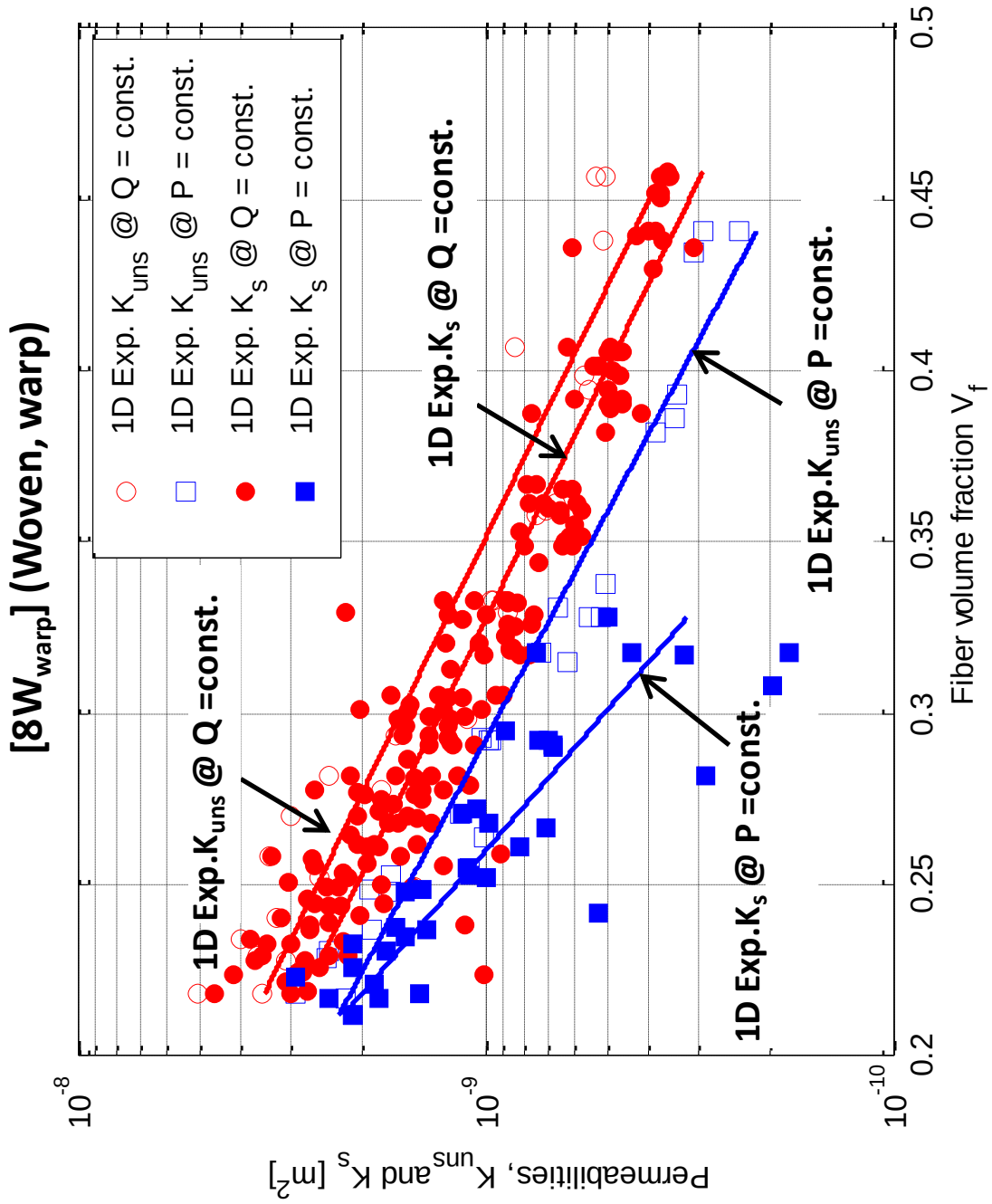

Figure 5. 3 Results of 1D permeability measurement experiments for [8W_{warp}] (Woven- Warp).

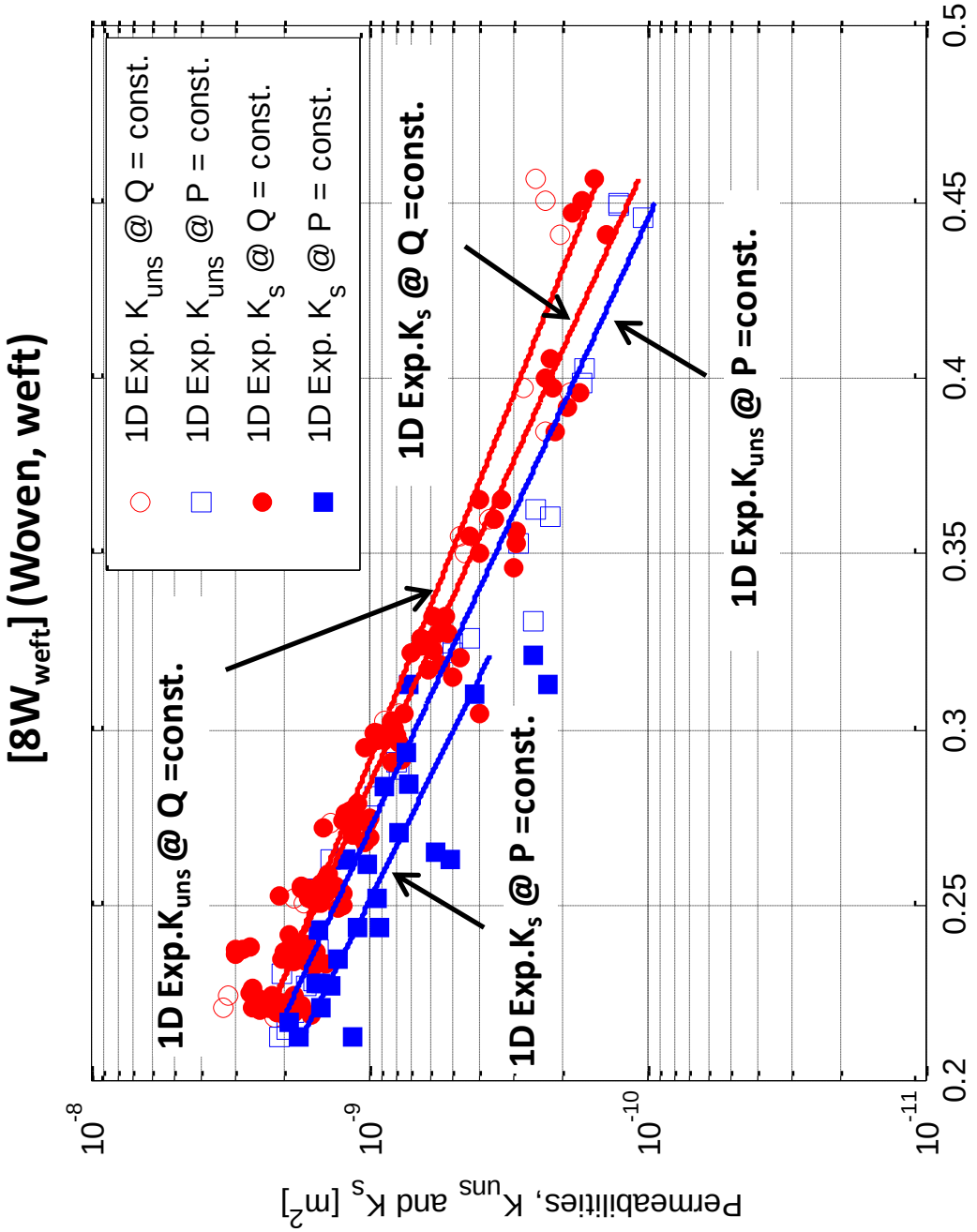

Figure 5. 4 Results of 1D permeability measurement experiments for [8W$_{weft}$] (Woven- Weft).

Table 5. 1 Results of curve fit (by using K =Ae^{-BV_f}) for 1D permeability measurement experiments for all fabric types.

[8R] (RANDOM)				
		$K = Ae^{-BVf}$		
Type of the Experiment	**V_f domain**	**A [m^2]**	**B**	**R^2**
1D Unsteady @ Q = const.	0.221 - 0.455	1.82E-09	6.80	0.8910
1D Steady @ Q = const.	0.221 - 0.455	2.73E-09	8.60	0.9270
1D Unsteady @ P = const.	0.224 - 0.503	3.06E-09	9.91	0.8735
1D Steady @ P = const.	0.224 - 0.503	8.58E-10	7.93	0.3676

[8B] (BIAXIAL)				
		$K = Ae^{-BVf}$		
Type of the Experiment	**V_f domain**	**A [m^2]**	**B**	**R^2**
1D Unsteady @ Q = const.	0.332 - 0.541	1.34E-08	8.88	0.8790
1D Steady @ Q = const.	0.332 - 0.541	1.43E-08	9.43	0.8589
1D Unsteady @ P = const.	0.333 - 0.548	2.22E-07	16.05	0.9060
1D Steady @ P = const.	0.333 - 0.548	1.08E-06	21.61	0.6210

[8W_{warp}] (WOVEN - Warp)				
		$K = Ae^{-BVf}$		
Type of the Experiment	**V_f domain**	**A [m^2]**	**B**	**R^2**
1D Unsteady @ Q = const.	0.218 - 0.457	2.69E-08	9.37	0.8259
1D Steady @ Q = const.	0.218 - 0.457	2.16E-08	9.39	0.7702
1D Unsteady @ P = const.	0.212 - 0.441	2.04E-08	10.31	0.8946
1D Steady @ P = const.	0.212 - 0.441	7.75E-08	16.72	0.7563

[8W_{weft}] (WOVEN - Weft)				
		$K = Ae^{-BVf}$		
Type of the Experiment	**V_f Domain**	**A [m^2]**	**B**	**R^2**
1D Unsteady @ Q = const.	0.218 - 0.457	2.79E-08	11.45	0.8645
1D Steady @ Q = const.	0.218 - 0.457	3.91E-08	12.92	0.8578
1D Unsteady @ P = const.	0.213 -0.450	3.65E-08	13.27	0.9552
1D Steady @ P = const.	0.213 -0.450	3.64E-08	14.31	0.7515

5.1 Summary and Conclusion

Permeabilities of three different types of fabrics (random, biaxial, woven) at different fiber volume fractions were measured by performing four different experimental procedures (unsteady, steady, with constant flow rate and constant pressure boundary conditions). The results obtained from each experimental procedure, $R^{2,}$ the highest amount of residuals are observed in the 1D steady experiments with constant pressure boundary conditions which was proposed in this study. In order to obtain more reliable and consistent measurement of permeability, all expected sources of errors should be minimized by taking precautions given as in this study.

Although the results of different methods (unsteady or steady; constant P or constant Q) have large scatters; one should not forget that the appropriate method should be selected by considering where the permeability data will be used. For example, if the permeability is used in modeling the mold filling stage in the VI process, then the appropriate one is to use unsteady K measured using constant pressure injection boundary condition by mimicking the process in the characterization experiments. However, if constant-flow rate injection machine is used in RTM process, then the appropriate permeability measurement method seems to be unsteady K measured using constant flow rate injection boundary condition. One may suitably use steady K values for the post-filling stages such as resin bleeding.

BIBLIOGRAPHY

[1] Airbus Military, http://www.airbusmilitary.com/A400M.aspx, retrieved on 10.02.2012.

[2] Sino Armor,http://www.sinoarmor.com, retrieved on 10.02.2012.

[3] CG Compositos, http://www.cgcomposites.com.au/MARINE.html, retrieved on 10.02.2012.

[4] TPI Composites**,** http://www.tpicomposites.com/, retrieved on 10.02.2012.

[5] Temsa Global, http://www.temsaglobal.com.tr/tr/otobus.aspx, retrieved on 10.02.2012.

[6] S. Kalpakjian and S. R. Schmid. 'Manufacturing Engineering and Tecnology'. Prentice Hall, 4^{th} Edition, 2001.

[7] E. M. Sozer, P. Simacek, S. G. Advani. Handbook of Polymer Matrix Composite Manufacturing. Chapter 9,September 2011.

[8] S. G. Advani, M. V. Bruschke, R. Parnas. Resin transfer molding. Flow and rheology in polymeric composite manufacturing,1994, Elsevier, Chapter 12, 465-516.

[9] S. G. Advani, E. M. Sozer. Process modeling in composites manufacturing. 2nd Edition, CRC Press.

[10] H. Darcy. Les fontaines publiques de la ville de Dijon. Dalmonti Paris, 1856.

[11] S. Sharma, D. A. Siginer. Permeability measurement methods in porous media of fiber reinforced composites. Applied Mechanics Reviews, 2010;63;1-19.

[12] K. Hoes, D. Dinescu, H. Sol, R. S. Parnas, S. Lomov. Study of nesting induced scatter of permeability values in layered reinforcement fabrics. Composites, 2004; 35:1407-1418.

[13] R. S. Parnas, K. M. Flynn, M. E. Dal-favero. A permeability database for composite manufacturing. Poly Compos,1997;18(5):623-633.

[14] T. S. Lundström, R. Stenber, R. Bergström, H. Partenen, P. A. Birkeland. In-Plane permeability measurement: a Nordic round –robin study. Composites Part A, 2000;31,29-43.

[15] B. R Gebart, P. Lidström. Measurement of in-plane permeability of anisotropic fiber reinforcements. Polymer Compos,1996;17(1):43-51.

[16] R. Arbter, J. M. Beraud, C. Binetruy, L. Bizet. Experimental determination of the permeability of textiles: A benchmark exercises. Composites Part A: Applied Science and Manufacturing, 2011;42(9):1157-1168.

[17] R. S. Parnas, Y. Cohen. Coupled parallel flows of power- law fluids in a channal and bounding porous medium. Chem Eng Commun, 1987;53:3-22.

[18] R. S. Parnas, J. G. Howard, T. L. Luce, S. G. Advani. Permeability characterisation. Part I: A proposed standart reference fabric for permeability. Polym Compos 1995;16(6): 429-45.

[19] C. Lekakou, M. A. K. Johari, D. Norman, M. G. Bader. Mesurement tecniques and effects on in plane permeability of woven cloths in resin transfer moulding. Composites A, 1996;27:401-408.

[20] C. M. Lawrence, J. Barr, R. Karmakar, S. G. Advani. Characterization of preform permeability in presence of race-tracking. Composites Part A,2004;35:1393-1405.

[21] Y. Luo, I. Verpoest, K. Hoes, M. Vanheule, H. Sol, A. Permeability measurement of textile reinforcements with several test fluids. Composites Part A,2001;(32): 1497-1504.

[22] V. H. Hommond, A. C. Loos. The effects of fluid type and viscosity on the steady-state and advancing front permeability behaviour of textile preforms. J. Reinf Plast Compos 1997;16(1):50-72.

[23] D. A. Steenkamer, D. J. Wilkins, V. M. Karbhari. Influence of test fluid on fabric permeability measurement and implications for processing of liquid molded composites. Mater. Sci,1993; 12(13): 971-973.

[24] J. G. Williams, C. E. M. Morris, B. C. Ennis. Liquid flow through fiber beds. Polymer Eng. Science 1974;14(6):413-419.

[25] M. R. Haboglu. Strain rate controlled compaction characterization of e-glass fabrics and investigation of the effects of process parameters on the results. M.Sc. Thesis, Koc University, Graduate School of Engineering, 2012.

[26] M. A. Yalcınkaya. Effect of part thickness variation on the mold filliing in vacuum infusion process. M.Sc. Thesis, Koc University, Graduate School of Engineering, 2012.

[27] R. G. D. Steel, and J. H. Torrie. Principles and Procedures of Statistics, New York: McGraw-Hill, 1960, pp. 187, 287.

VITA

Ayşen Sarıoğlu was born in Kocaeli, Turkey on November 28, 1986. She received her B.S. degree in Material Science and Engineering and also lateral degree from Chemical Engineering from Anadolu University, Eskişehir, in 2010. Since then, she has enrolled to the M.S. program in Mechanical Engineering at Koc University, Istanbul as both a teaching and research assistant. She has been studying in the "Permeability measurement experiments for fabric preform used in LCM processes" project since September 2010. She is planning to continue her career in the industry.

APPENDIX A

PERMEABILITY MEASUREMENT EXPERIMENTS

Abbreviation	**Preform configuration**
[8R]	8 Layer Random
[8S]	8 Layer Stitches (Biaxial)
[$8W_{warp}$]	8 Layer woven (warp direction)
[$8W_{weft}$]	8 Layer woven (weft direction)

Appendix A.1. Results of 1D permeability measurement experiments with constant flow rate for [8R].

						h [mm]		h [mm]		h [mm]		h [mm]		h [mm]		h [mm]		h [mm]	
						6.0		5.5		5.0		4.5		4.0		3.5		3.0	
Exp. Code	Viscosity [mPa.s]	Superficial Density [g/m ^{2}]	Initial Thickness h [mm]	Initial V_f	K_{uns} [m^2]	K_s [m^2]	V_f	K_s [m^2]	V_f	K_s [m^2]	V_f	K_s [m^2]	V_f	K_s [m^2]	V_f	K_s [m^2]	V_f	K_s [m^2]	V_f
8R_Q1	200	429	6	0.225	4.36E-10			2.33E-10	0.246										
8R_Q2	197	421	6	0.221	4.87E-10	4.67E-10	0.221	3.88E-10	0.241	2.90E-10	0.265	2.02E-10	0.294	1.34E-10	0.331	9.47E-11	0.378	7.84E-11	0.441
8R_Q3	191	435	6	0.228	4.32E-10	3.69E-10		3.01E-10	0.249	2.16E-10	0.274	1.80E-10	0.305	1.29E-10	0.343	9.07E-11	0.392	7.22E-11	0.457
8R_Q4	190	434	5	0.273	2.51E-10					2.70E-10	0.273	1.84E-10	0.303	1.28E-10	0.341	9.03E-11	0.390	7.00E-11	0.455
8R_Q5	190	421	5	0.265	2.70E-10					2.54E-10	0.265	1.83E-10	0.295	1.28E-10	0.332	8.85E-11	0.379	6.80E-11	0.442
8R_Q6	192	417	5	0.262	2.63E-10					2.64E-10	0.262	2.00E-10	0.291	1.38E-10	0.328	9.45E-11	0.374	7.01E-11	0.437
8R_Q7	190	428	4	0.336	1.85E-10	4.37E-10	0.336	3.61E-10	0.245	2.90E-10	0.269	2.12E-10	0.299	1.46E-10	0.336				
8R_Q8	190	421	4	0.331	1.55E-10									1.37E-10	0.331	9.81E-11	0.378	7.36E-11	0.441
8R_Q9	192	433	4	0.341	1.69E-10									1.43E-10	0.341	1.00E-10	0.390	7.82E-11	0.455
8R_Q10	190	396	5.5	0.226	5.10E-10			4.44E-10	0.226										
8R_Q11	191	418	5.5	0.239	3.46E-10			3.64E-10	0.239	3.34E-10	0.263	2.12E-10	0.292	1.42E-10	0.328				
8R_Q12	192	433	5.5	0.247	3.27E-10			3.51E-10	0.247	2.60E-10	0.272	1.80E-10	0.302	1.42E-10	0.340				
8R_Q13	191	408	4.5	0.286	2.90E-10	4.53E-10	0.286	4.06E-10	0.234	3.27E-10	0.257	2.67E-10	0.286						
8R_Q14	195	408	4.5	0.286	2.66E-10	5.90E-10	0.286	3.98E-10	0.234	3.46E-10	0.257	2.62E-10	0.286						
8R_Q15	197	417	4.5	0.291	2.25E-10			3.52E-10	0.238	2.76E-10	0.262	2.01E-10	0.291						
8R_Q16	195	433	3.5	0.390	1.12E-10	5.04E-10	0.390	3.91E-10	0.248	2.84E-10	0.273	2.07E-10	0.303	1.32E-10	0.341	8.84E-11	0.390		
8R_Q17	190	407	3.5	0.365	1.18E-10			3.79E-10	0.233	2.97E-10	0.256	2.29E-10	0.284	1.48E-10	0.320	9.58E-11	0.365		
8R_Q18	190	404	3.5	0.364	1.29E-10	4.61E-10	0.364	3.49E-10	0.231	2.59E-10	0.255					1.12E-10	0.364		
8R_Q20	200	401	3	0.421	1.29E-10	4.99E-10	0.421	4.13E-10	0.230	3.04E-10	0.253	2.34E-10	0.281	1.54E-10	0.316	1.02E-10	0.361	7.68E-11	0.421
8R_Q21	190	433	3	0.455	1.14E-10	4.99E-10	0.455	3.53E-10	0.248	2.64E-10	0.273	1.96E-10	0.303	1.26E-10	0.341	9.08E-11	0.390	6.75E-11	0.455
8R_Q22	193	400	3.25	0.388	1.41E-10													1.05E-10	0.388

Appendix A.2. Results of 1D permeability measurement experiments with constant flow rate for [8S].

						h [mm]		h [mm]		h[mm]		h [mm]		h [mm]		h[mm]		h [mm]	
						8.0		7.5		7.0		6.5		6.0		5.5		5.0	
Exp Code	Viscosity [mPa.s]	Superficial Density [g/m ^{2}]	Initial Thickness h [mm]	Initial V_f	K_{uns} [m^2]	K_s [m^2]	V_f	K_s [m^2]	V_f	K_s [m^2]	V_f	K_s [m^2]	V_f	K_s [m^2]	V_f	K_s [m^2]	V_f	K_s [m^2]	V_f
8S_Q1	191	843	8	0.332	6.77E-10	5.62E-10	0.332	3.87E-10	0.354	3.12E-10	0.379	2.47E-10	0.408	2.00E-10	0.442	1.69E-10	0.482		
8S_Q2	192	855	8	0.337	8.72E-10	8.12E-10	0.337	5.06E-10	0.359	3.46E-10	0.385	2.52E-10	0.414	1.89E-10	0.449	1.41E-10	0.490		
8S_Q3	200	863	8	0.340	6.38E-10	7.07E-10	0.340	4.87E-10	0.362	3.48E-10	0.388	2.45E-10	0.418	1.89E-10	0.453				
8S_Q4	192	855	7.5	0.359	6.73E-10			5.40E-10	0.359	3.32E-10	0.385	2.36E-10	0.414	1.74E-10	0.449	1.28E-10	0.490	1.03E-10	0.539
8S_Q5	197	850	7.5	0.357	5.43E-10			7.19E-10	0.357			2.56E-10	0.412			1.44E-10	0.487		
8S_Q6	190	853	7.5	0.358	6.49E-10			4.57E-10	0.358			2.08E-10	0.413						
8S_Q7	193	846	7	0.380	4.01E-10					3.55E-10	0.380	2.57E-10	0.409	2.03E-10	0.444	1.53E-10	0.484	1.13E-10	0.532
8S_Q8	195	846	7	0.380	4.43E-10					3.67E-10	0.380	2.53E-10	0.409	1.95E-10	0.444	1.52E-10	0.484	1.05E-10	0.532
8S_Q9	190	850	7	0.383	6.58E-10					4.73E-10	0.383	2.84E-10	0.412	2.21E-10	0.446	1.52E-10	0.487	1.13E-10	0.535
8S_Q10	190	854	6.5	0.414	2.44E-10							2.56E-10	0.414	1.85E-10	0.448	1.37E-10	0.489	1.11E-10	0.538
8S_Q11	193	850	6.5	0.411	2.94E-10							2.87E-10	0.411	2.05E-10	0.446	1.44E-10	0.486	1.03E-10	0.535
8S_Q12	195	850	6.5	0.412	2.89E-10							2.81E-10	0.412	2.10E-10	0.446	1.39E-10	0.487	1.06E-10	0.535
8S_Q13	195	843	6	0.442	2.36E-10									2.31E-10	0.442	1.60E-10	0.482	1.21E-10	0.530
8S_Q14	190	847	6	0.445	2.40E-10									2.12E-10	0.445	1.49E-10	0.485	1.06E-10	0.534
8S_Q15	190	854	6	0.448	2.10E-10	8.57E-10	0.336	5.74E-10	0.359	3.91E-10	0.384	2.57E-10	0.414	1.90E-10	0.448				
8S_Q16	198	862	5.5	0.494	1.59E-10	6.83E-10	0.339	5.03E-10	0.362	3.61E-10	0.388	2.49E-10	0.418	1.75E-10	0.453	1.30E-10	0.494		
8S_Q17	200	861	5.5	0.493	1.36E-10	8.42E-10	0.339	5.30E-10	0.362	3.54E-10	0.387	2.51E-10	0.417	1.68E-10	0.452	1.18E-10	0.493		
8S_Q18	199	861	5.5	0.493	1.61E-10	6.52E-10	0.339	5.14E-10	0.362	3.55E-10	0.387	2.58E-10	0.417	1.81E-10	0.452	1.38E-10	0.493		
8S_Q19	195	856	5	0.539	1.67E-10	5.11E-10	0.337	4.30E-10	0.359	3.14E-10	0.385	2.66E-10	0.414	1.98E-10	0.449	1.48E-10	0.490	1.26E-10	0.539
8S_Q20	197	849	5	0.535	1.25E-10	9.60E-10	0.334	6.38E-10	0.357	4.27E-10	0.382	3.02E-10	0.411	2.18E-10	0.446	1.40E-10	0.486	1.04E-10	0.535
8S_Q21	200	858	5	0.541	1.24E-10	8.45E-10	0.338	4.95E-10	0.360	3.62E-10	0.386	2.61E-10	0.416	1.75E-10	0.450	1.18E-10	0.491	9.88E-11	0.541

Appendix A.3. Results of 1D permeability measurement experiments with constant flow rate for [8 W_{warp}].

						h [mm]		h [mm]		h [mm]		h [mm]		h [mm]		h [mm]		h [mm]		h [mm]		h [mm]	
						4.0		3.75		3.5		3.25		3.0		2.75		2.5		2.25		2.0	
Exp Code	Viscosity [mPa.s]	Superficial Density [g/m 2]	Initial Thickness h [mm]	Initial V_f	K_{uns} [m^2]	K_s [m^2]	V_f	K_s [m^2]	V_f	K_s [m^2]	V_f	K_s [m^2]	V_f	K_s [m^2]	V_f	K_s [m^2]	V_f	K_s [m^2]	V_f	K_s [m^2]	V_f	K_s [m^2]	V_f
8W_Q1_warp	205	290	4	0.228	3.07E-09	2.98E-09	0.228	2.41E-09	0.244	1.94E-09	0.261	1.50E-09	0.281	1.13E-09	0.305	8.38E-10	0.332	6.15E-10	0.365	4.61E-10	0.406	3.59E-10	0.457
8W_Q2_warp	195	277	4	0.218	3.54E-09	3.68E-09	0.218	2.99E-09	0.233	2.29E-09	0.249	1.72E-09	0.268	1.38E-09	0.291	1.00E-09	0.317	8.01E-10	0.349	7.74E-10	0.388	6.09E-10	0.436
8W_Q3_warp	185	277	4	0.218	5.08E-09	4.60E-09	0.218	3.44E-09	0.233	2.45E-09	0.249	1.63E-09	0.268	1.20E-09	0.291	7.84E-10	0.317	6.44E-10	0.349				
8W_Q4_warp	195	287	3.75	0.240	3.23E-09			3.15E-09	0.240	2.67E-09	0.257	2.06E-09	0.277	1.55E-09	0.300	1.13E-09	0.328	7.01E-10	0.360	4.83E-10	0.400	3.72E-10	0.450
8W_Q5_warp	195	279	3.75	0.234	3.95E-09			3.76E-09	0.234	3.05E-09	0.251	2.05E-09	0.270	1.24E-09	0.293	8.73E-10	0.320	5.83E-10	0.352	4.97E-10	0.391	4.22E-10	0.439
8W_Q6_warp	196	273	3.75	0.229	3.63E-09			3.50E-09	0.229	2.71E-09	0.246	2.14E-09	0.265	1.55E-09	0.287	1.21E-09	0.313	7.39E-10	0.344	5.06E-10	0.382	3.89E-10	0.430
8W_Q7_warp	200	281	3.5	0.252	2.54E-09					2.18E-09	0.252	1.81E-09	0.271	1.38E-09	0.294	1.03E-09	0.321	6.01E-10	0.353	4.62E-10	0.392	3.84E-10	0.441
8W_Q8_warp	200	281	3.5	0.249	1.48E-09					1.50E-09	0.249	1.36E-09	0.268	1.06E-09	0.291	8.19E-10	0.317	6.08E-10	0.349	4.14E-10	0.388	3.08E-10	0.436
8W_Q9_warp	185	288	3.5	0.258	3.38E-09					3.33E-09	0.258	2.62E-09	0.278	2.04E-09	0.301	1.24E-09	0.329	7.80E-10	0.362	5.41E-10	0.402	3.72E-10	0.452
8W_Q10_warp	198	288	3.25	0.278	1.80E-09							1.44E-09	0.278	1.26E-09	0.301	9.89E-10	0.329	7.21E-10	0.362	5.28E-10	0.402	3.80E-10	0.452
8W_Q11_warp	185	292	3.25	0.282	2.41E-09							2.15E-09	0.282	1.71E-09	0.306	1.27E-09	0.333	7.48E-10	0.367	4.95E-10	0.407	3.56E-10	0.458
8W_Q12_warp	200	280	3.25	0.270	2.99E-09							1.55E-09	0.270	1.23E-09	0.293	8.56E-10	0.320	6.17E-10	0.352	4.58E-10	0.391		
8W_Q13_warp	195	281	3	0.294	1.65E-09									1.60E-09	0.294	1.25E-09	0.321	8.19E-10	0.353	6.02E-10	0.392	4.00E-10	0.441
8W_Q14_warp	190	283	3	0.296	1.58E-09									1.56E-09	0.296								
8W_Q15_warp	205	284	3	0.298	1.10E-09	1.01E-09	0.298	1.12E-09	0.239	1.26E-09	0.256	1.44E-09	0.275	1.64E-09	0.298								
8W_Q16_warp	205	292	2.75	0.333	9.52E-10			2.63E-09	0.244	1.86E-09	0.262	1.35E-09	0.282	9.05E-10	0.306	8.97E-10	0.333						
8W_Q17_warp	205	292	2.75	0.333	9.61E-10	2.17E-09	0.333	1.76E-09	0.244	1.46E-09	0.262	1.18E-09	0.282	9.45E-10	0.306	8.75E-10	0.333						
8W_Q18_warp	190	288	2.75	0.330	8.83E-10					9.12E-10	0.259	1.09E-09	0.279	1.54E-09	0.302	2.21E-09	0.330						
8W_Q19_warp	195	285	2.5	0.359	7.07E-10	2.80E-09	0.359					1.99E-09	0.276	1.37E-09	0.299	8.85E-10	0.326	6.58E-10	0.359				
8W_Q20_warp	198	284	2.5	0.358	7.45E-10	4.16E-09	0.358	2.70E-09	0.239	2.63E-09	0.256	1.80E-09	0.275	1.21E-09	0.298	8.45E-10	0.325	6.58E-10	0.358				
8W_Q21_warp	200	287	2.5	0.362	6.71E-10	2.55E-09	0.362	2.03E-09	0.241	1.62E-09	0.258	1.27E-09	0.278	1.02E-09	0.301	7.59E-10	0.329	5.97E-10	0.362				
8W_Q22_warp	192	283	2.25	0.395	5.60E-10	3.07E-09	0.395	2.69E-09	0.237	2.24E-09	0.254	1.68E-09	0.273	1.23E-09	0.296	8.90E-10	0.323	6.01E-10	0.355	4.98E-10	0.395		
8W_Q23_warp	195	285	2.25	0.399	5.72E-10	2.86E-09	0.399	2.42E-09	0.239	1.95E-09	0.257	1.48E-09	0.276	1.12E-09	0.299	7.72E-10	0.326	5.77E-10	0.359	4.69E-10	0.399		
8W_Q24_warp	190	292	2.25	0.407	8.47E-10	2.42E-09	0.407			2.06E-09	0.262	1.67E-09	0.282	1.31E-09	0.306	1.06E-09	0.333	7.87E-10	0.367	6.30E-10	0.407		
8W_Q25_warp	200	290	2	0.457	5.35E-10	2.76E-09	0.457	2.26E-09	0.244	1.82E-09	0.261	1.48E-09	0.281	1.23E-09	0.305	8.78E-10	0.332	6.48E-10	0.365	4.98E-10	0.406	3.70E-10	0.457
8W_Q26_warp	210	290	2	0.457	5.08E-10													6.44E-10	0.365	4.75E-10	0.406	3.54E-10	0.457
8W_Q27_warp	198	279	2	0.438	5.12E-10	2.71E-09	0.438	2.23E-09	0.234	1.79E-09	0.250	1.47E-09	0.269	1.22E-09	0.292	8.69E-10	0.318	6.41E-10	0.350	4.94E-10	0.389	3.66E-10	0.438

Appendix A.4. Results of 1D permeability measurement experiments with constant flow rate for [$8W_{weft}$].

						h [mm]		h [mm]		h [mm]		h [mm]		h [mm]		h [mm]		h [mm]		h [mm]		h [mm]	
						4.0		3.75		3.5		3.25		3.0		2.75		2.5		2.25		2.0	
Exp Code	Viscosity [mPa.s]	Superfcial Density [g/m2]	Initial Thickness h [mm]	Initial V_f	$K_{uns\,[m^2]}$	K_s [m^2]	V_f	K_s [m^2]	V_f	K_s [m^2]	V_f	K_s [m^2]	V_f	K_s [m^2]	V_f	K_s [m^2]	V_f	K_s [m^2]	V_f	K_s [m^2]	V_f	K_s [m^2]	V_f
8W_Q1_weft	200	283	2.75	0.324	6.50E-10			2.98E-09	0.238	1.74E-09	0.255	1.23E-09	0.274	9.25E-10	0.297	6.50E-10	0.324						
8W_Q2_weft	190	283	2.75	0.324	6.18E-10			2.83E-09	0.238	1.65E-09	0.255	1.17E-09	0.274	8.78E-10	0.297	6.17E-10	0.324						
8W_Q3_weft	196	285	2.75	0.325	5.92E-10			2.68E-09	0.239	1.75E-09	0.256	1.22E-09	0.275	8.22E-10	0.298	6.12E-10	0.325						
8W_Q4_weft	197	285	3	0.299	9.52E-10	2.24E-09	0.224	1.86E-09	0.239	1.48E-09	0.257	1.22E-09	0.276	9.56E-10	0.299								
8W_Q5_weft	195	285	3	0.298		2.50E-09	0.224	1.76E-09	0.239	1.31E-09	0.256	9.83E-10	0.275	7.97E-10	0.298								
8W_Q6_weft	195	289	3	0.302	8.79E-10	2.60E-09	0.227	1.94E-09	0.242	1.39E-09	0.259	1.10E-09	0.279	8.25E-10	0.302								
8W_Q7_weft	197	277	4	0.218	2.18E-09	1.98E-09	0.218	1.57E-09	0.233	1.29E-09	0.249	1.04E-09	0.268	8.21E-10	0.291	6.12E-10	0.317						
8W_Q8_weft	190	281	4	0.221	3.32E-09			3.03E-09	0.236	2.08E-09	0.253	1.46E-09	0.272	1.04E-09	0.295	7.03E-10	0.322						
8W_Q9_weft	200	285	4	0.224	3.17E-09	1.86E-09	0.224	1.68E-09	0.239	1.42E-09	0.257	1.16E-09	0.276	9.38E-10	0.299	6.52E-10	0.326						
8W_Q10_weft	190	281	3.5	0.252	1.84E-09	2.45E-09	0.221	2.03E-09	0.235	1.64E-09	0.252												
8W_Q11_weft	194	279	3.5	0.251	1.70E-09	1.85E-09	0.220	1.66E-09	0.234	1.49E-09	0.251												
8W_Q12_weft	190	283	3.5	0.254	1.47E-09			2.02E-09	0.237	1.57E-09	0.254												
8W_Q13_weft	194	281	2.5	0.355	4.70E-10	1.73E-09	0.222	1.54E-09	0.237	1.23E-09	0.254	1.00E-09	0.273	7.75E-10	0.296	5.82E-10	0.323	4.30E-10	0.355				
8W_Q14_weft	200	279	2.5	0.350	4.46E-10	1.59E-09	0.219	1.43E-09	0.234	1.24E-09	0.250	9.91E-10	0.269	7.60E-10	0.292	5.48E-10	0.318	3.98E-10	0.350				
8W_Q15_weft	198	286	2.5	0.360	3.70E-10	2.66E-09	0.225	1.91E-09	0.240	1.43E-09	0.257	1.17E-09	0.277	8.11E-10	0.300	5.24E-10	0.328	3.54E-10	0.360				
8W_Q16_weft	196	282	3.25	0.273	1.38E-09	2.33E-09	0.222	1.89E-09	0.237	1.44E-09	0.254	1.11E-09	0.273										
8W_Q17_weft	200	279	3.25	0.270	1.10E-09	2.15E-09	0.220	1.85E-09	0.234	1.54E-09	0.251	1.13E-09	0.270										
8W_Q18_weft	197	283	3.25	0.274	1.04E-09	2.05E-09	0.223	1.59E-09	0.238	1.28E-09	0.255	1.05E-09	0.274										
8W_Q19_weft	190	290	3,0	0.305	7.84E-10									7.49E-10	0.305	5.90E-10	0.332	3.99E-10	0.365				
8W_Q20_weft	200	282	3.75	0.237	1.71E-09	2.32E-09	0.222	1.91E-09	0.237														
8W_Q21_weft	195	281	3.75	0.236	1.71E-09	2.62E-09	0.221	1.95E-09	0.236														
8W_Q22_weft	192	283	3.75	0.237	1.69E-09	2.58E-09	0.222	1.92E-09	0.237														
8W_Q23_weft	200	280	2.25	0.398	2.75E-10															2.20E-10	0.398	1.84E-10	0.447
8W_Q24_weft	200	284	2.25	0.396	1.89E-10											6.38E-10	0.324	2.97E-10	0.357	1.75E-10	0.396		
8W_Q25_weft	199	275	2.25	0.385	2.31E-10											5.01E-10	0.315	3.02E-10	0.347	2.14E-10	0.385		
8W_Q26_weft	190	285	2	0.441	2.04E-10											4.67E-10	0.321	2.97E-10	0.353	1.92E-10	0.392	1.39E-10	0.441
8W_Q27_weft	195	290	2	0.457	2.52E-10											5.28E-10	0.332	3.29E-10	0.365	2.23E-10	0.406	1.55E-10	0.457
8W_Q28_weft	196	286	2	0.450	2.32E-10											5.63E-10	0.328	3.56E-10	0.360	2.31E-10	0.400	1.71E-10	0.450

Appendix A.5. Results of 1D permeability measurement experiments with constant pressure for [8R] .

						h [mm]		h [mm]		h [mm]		h [mm]	
						6		5.5		5		4.5	
Exp Code	Viscosity [mPa.s]	Superficial Denstiy [g/m2]	Initial Thickness h [mm]	Initial V_f	K_{uns} [m^2]	K_s [m^2]	V_f	K_s [m^2]	V_f	K_s [m^2]	V_f	K_s [m^2]	V_f
8R_P1	192	433	6	0.227	4.67E-10								
8R_P2	192	454	6	0.238	3.65E-10								
8R_P3	194	427	6	0.224	3.89E-10								
8R_P4	195	432	5.5	0.247	3.09E-10								
8R_P5	198	432	5.5	0.247	3.01E-10								
8R_P6	194	430	5.5	0.246	3.04E-10								
8R_P7	196	456	5	0.287	1.43E-10								
8R_P8	192	440	5	0.277	1.82E-10								
8R_P9	196	415	5	0.261	1.48E-10								
8R_P10	190	445	4.5	0.311	1.34E-10	1.96E-10	0.234	1.47E-10	0.255	9.99E-11	0.280	7.35E-11	0.312
8R_P11	190	464	4.5	0.324	1.02E-10	4.31E-11	0.243	1.44E-10	0.265	5.26E-11	0.292	6.07E-11	0.324
8R_P12	195	450	4.5	0.315	1.01E-10	1.64E-10	0.236	1.27E-10	0.258	8.59E-11	0.283	9.55E-11	0.315
8R_P13	199	418	4	0.329	8.89E-11								
8R_P14	194	426	4	0.348	8.42E-11								
8R_P15	191	452	4	0.356	9.89E-11								
8R_P16	192	453	3.5	0.407	5.10E-11								
8R_P17	191	451	3.5	0.405	5.46E-11								
8R_P18	198	463	3.5	0.417	4.99E-11								
8R_P19	195	445	3	0.466	3.93E-11								
8R_P20	210	479	3	0.503	2.31E-11								
8R_P21	200	479	3	0.503	2.27E-11								

Appendix A.6. Results of 1D permeability measurement experiments with constant pressure for [8S].

							h [mm]		h [mm]		h [mm]		h [mm]		h [mm]		h [mm]	
							h[mm]		h[mm]		h[mm]		h[mm]		h[mm]		h[mm]	
							4		3.75		3.5		3.25		3		2.75	
Exp Code	Exp Code	Viscosity [mPa.s]	Superficial Density [g/m^{2}]	Initial Thickness h [mm]	Initial V_f	K_{uns} [m2]	K_s [m^2]	V_f	K_s [m^2]	V_f	K_s [m^2]	V_f	K_s [m^2]	V_f	K_s [m^2]	V_f	K_s [m^2]	V_f
8S_P	8W_P1_warp	199	275	4	0.217	2.20E-09												
8S_P	8W_P2_warp	188	269	4	0.212	2.12E-09	2.11E-09	0.212	2.11E-09	0.226	5.24E-10	0.242	8.23E-10	0.261	2.89E-10	0.282	1.97E-10	0.308
8S_P	8W_P3_warp	185	277	4	0.218	2.90E-09	1.44E-09	0.218	2.11E-09	0.233	1.43E-09	0.249	9.76E-10	0.268	6.79E-10	0.291	3.23E-10	0.317
8S_P	8W_P4_warp	184	283	3.75	0.237	1.90E-09	2.93E-09	0.223	1.65E-09	0.238								
8S_P	8W_P5_warp	183	275	3.75	0.231	2.41E-09	2.43E-09	0.217	1.75E-09	0.231								
8S_P	8W_P6_warp	182	273	3.75	0.229	2.44E-09												
8S_P	8W_P7_warp	180	276	3.5	0.248	1.71E-09					1.57E-09	0.248	7.08E-10	0.267	6.81E-10	0.290		
8S_P	8W_P8_warp	186	281	3.5	0.253	1.69E-09					1.09E-09	0.253	1.04E-09	0.272	8.93E-10	0.295		
8S_P	8W_P9_warp	190	277	3.5	0.249	1.93E-09												
8S_P	8W_P10_warp	190	263	3.25	0.255	1.09E-09			1.88E-09	0.221	1.40E-09	0.237	1.10E-09	0.255				
8S_P	8W_P11_warp	187	280	3.25	0.271	1.15E-09	1.83E-09	0.217	1.58E-09	0.235	9.91E-10	0.252	1.13E-09	0.271				
8S_P	8W_P12_warp	191	272	3.25	0.264	1.01E-09												
8S_P1	8W_P13_warp	192	278	3	0.292	9.66E-10									6.99E-10	0.292	4.36E-10	0.318
8S_P1	8W_P14_warp	191	278	3	0.292	9.82E-10									7.38E-10	0.292	7.46E-10	0.318
8S_P1	8W_P15_warp	193	279	3	0.293	1.02E-09												
8S_P1	8W_P16_warp	194	286	2.75	0.328	5.53E-10											1.78E-10	0.328
8S_P1	8W_P17_warp	197	278	2.75	0.318	7.33E-10											4.97E-10	0.318
8S_P1	8W_P18_warp	194	275	2.75	0.315	6.26E-10												
8S_P1	8W_P19_warp	215	268	2.5	0.338	5.06E-10												
8S_P1	8W_P20_warp	192	263	2.5	0.331	6.60E-10												
8S_P1	8W_P21_warp	188	260	2.5	0.328	5.23E-10												
8S_P1	8W_P22_warp	192	276	2.25	0.386	3.44E-10												
8S_P1	8W_P23_warp	193	273	2.25	0.382	3.80E-10												
8S_P1	8W_P24_warp	195	281	2.25	0.393	3.39E-10												
8S_P2	8W_P25_warp	195	280	2	0.441	2.40E-10												
8S_P2	8W_P26_warp	190	280	2	0.441	2.90E-10												
8S_P2	8W_P27_warp	194	276	2	0.435	3.06E-10												

Appendix A.8. Results of 1D permeability measurement experiments with constant pressure for [8 W_{weft}]

						h [mm]		h [mm]		h [mm]		h [mm]		h [mm]		h [mm]	
						4.0		3.75		3.5		3.25		3.0		2.75	
Exp Code	Viscosity [mPa.s]	Superficial Density [g/m^2]	Initial Thickness h [mm]	Initial V_f	K_{uns} [m^2]	K_s [m^2]	V_f	K_s [m^2]	V_f	K_s [m^2]	V_f	K_s [m^2]	V_f	K_s [m^2]	V_f	K_s [m^2]	V_f
8W_Q1_weft	192	280	4	0.220	1.87E-09	1.48E-09	0.221	1.28E-09	0.235	9.31E-10	0.252	7.82E-10	0.271	7.32E-10	0.294	4.16E-10	0.321
8W_Q2_weft	196	271	4	0.215	1.98E-09							5.78E-10	0.265	6.32E-11	0.287	2.26E-10	0.313
8W_Q3_weft	199	271	4	0.213	2.10E-09	1.79E-09	0.213	1.49E-09	0.228	9.06E-10	0.244	1.22E-09	0.263	7.20E-10	0.285	7.19E-10	0.313
8W_Q4_weft	194	270	3.75	0.227	1.68E-09			1.38E-09	0.227	1.52E-09	0.243	1.02E-09	0.262	8.75E-10	0.284	2.54E-10	0.310
8W_Q5_weft	180	275	3.75	0.231	2.04E-09	1.91E-09	0.217	1.53E-09	0.228								
8W_Q6_weft	180	273	3.75	0.229	1.59E-09												
8W_Q7_weft	185	264	3.5	0.238	1.51E-09												
8W_Q8_weft	186	283	3.5	0.255	1.61E-09												
8W_Q9_weft	190	281	3.5	0.253	1.58E-09												
8W_Q10_weft	195	271	3.25	0.263	1.22E-09	1.15E-09	0.213			1.10E-09	0.244	5.10E-10	0.263				
8W_Q11_weft	188	271	3.25	0.263	1.38E-09												
8W_Q12_weft	190	275	3.25	0.267	1.18E-09												
8W_Q13_weft	190	275	3	0.289	7.81E-10												
8W_Q14_weft	185	277	3	0.291	7.91E-10												
8W_Q15_weft	190	268	3	0.281	9.50E-10												
8W_Q16_weft	182	285	2.75	0.326	4.36E-10												
8W_Q17_weft	180	284	2.75	0.325	4.96E-10												
8W_Q18_weft	195	281	2.75	0.322	4.95E-10												
8W_Q19_weft	198	288	2.5	0.363	2.50E-10												
8W_Q20_weft	190	280	2.5	0.353	2.86E-10												
8W_Q21_weft	192	263	2.5	0.331	2.55E-10												
8W_Q22_weft	193	288	2.25	0.403	1.66E-10												
8W_Q23_weft	198	285	2.25	0.399	1.70E-10												
8W_Q24_weft	192	258	2.25	0.361	2.21E-10												
8W_Q25_weft	205	283	2	0.446	1.04E-10												
8W_Q26_weft	185	285	2	0.449	1.26E-10												
8W_Q27_weft	190	286	2	0.450	1.27E-10												

APPENDIX B

MATLAB CODES

App B.1. Matlab code (**rtmstart.m**) for data transfer of injection pressure (P_{in}) and time (t) from RTM radius injection machine to the computer and online drawing of P_{in} versus t.

```
clear all; close all; clc;
delete(instrfindall);

s=serial('COM4','Baudrate',1000000);
fid=fopen('','w');
start=tic;
tt=[];dd=[];
fopen(s);
fscanf(s);
s.BytesAvailableFcn='tt=[tt toc(start)];dd=[dd str2num(fscanf(s))];
fprintf(fid,''%.2f\t%.0f\n'',tt(end),dd(end))
plot(tt,(dd-2000)/93*10);';
```

App B.2. Matlab code (**perm_Qconstant.m**) for calculating K_{uns} and K_s for 1D continuous permeability measurement experiments with constant flow rate boundary condition.

```
clear all,close all,clc
A = load('1m.txt');
tshift  = A(1,1);
P       = A(:,2);
P       =
P*6894.8;
  %% Pressure [Pa]
t       = A(:,1) - tshift;
tadjust =[400 600,900 1050  1250 1440 1800 1900 2100 2400] ;


%% Filter to loaded data

[fa,fb]=besself(3,.1);
[fa,fb]=bilinear(fa,fb,1);
P=filtfilt(fa,fb,P);
P=filtfilt(fa,fb,P);

figure(1)
plot(t,P,'b-','linewidth',2),grid, ylabel('Pressure(kPa)'),xlabel('time(second)')
hold on
title('8R_Q2 Pressure vs Time')

for i = 1:length(tadjust)
plot([tadjust(i),tadjust(i)], [min(P),max(P)], 'r--')
end

%% Input data for permeability calculations

Mu =0.200;                                  %% viscosity of the fluid (Pa.s)
Q    =1.67e7;                               %% Volumetric flow rate (m3/s)
N    = 8;                                   %% number of plies
ds   = 0.283;                               %% superficial density (kg/m2)
d    = 2540;                                %% density of the glass fiber (kg/m3)
w    = 0.10;                                %% width of the fabric preform (meter)
xf   = 0.30;                                %% Length of the fabric preform (meter)

h    = [2.75 3 3.25 3.5 3.75]*1e-3;         %% thickness ranges

for i  = 1:1:length(h)
    Vf(i) = ( N * ds)/(d * h(i));
end

for i=1:1:length(Vf)
    p(i)= (1-Vf(i)) ;                       %% Porosity (1-Vf)

end
```

```
t1 = t(1:tadjust(1));           %% Time of unsteady part at thickness h1 (sec)
t2 = ( tadjust(1)) :tadjust(2); %% Time of first steady part at thickness h1(sec)
t3 = ( tadjust(3)) :tadjust(4); %% Time of second steady part at thickness h2 (sec)
t4 = ( tadjust(5)) :tadjust(6); %% Time of second steady part at thickness h3 (sec)
t5 = ( tadjust(7)) :tadjust(8); %% Time of second steady part at thickness h4 (sec)
t6 = ( tadjust(9)) :tadjust(10);%% Time of second steady part at thickness h5 (sec)
t7 = ( tadjust(11)):tadjust(12);%% Time of second steady part at thickness h5 (sec)
t8 = ( tadjust(13)):tadjust(14); %% Time of second steady part at thickness h5(sec)


%%  First order curve fit to data (Pin(t))
figure(2)
P1   =  P(1:tadjust(1));
tt1  = linspace(t1(1),t1(end),300);
PP1  = polyfit(t1,P1,1);
dPdt = PP1(1);
PP   = polyval(PP1,tt1);
plot(t1,P1,'r',tt1,PP,'g-','linewidth',2),grid,
xlabel('time (min)'),ylabel('Pressure(Pa)')
legend('experimental data''Curve fit data')
title('Curve Fit')
print -djpeg fig_time_vs_pressure_curvefit_5

%%   K1u (K1 unsteady  @ h (1))
K1u  = ((Q/(w*h(1)))^2 * (mu/(p(1)))  *
(1/dPdt))                                          %% K1 Unsteady (m2)
uf   = (Q /
(p(1)*w*h(1)))  ;
    %% Linear velocity (m/s)
tf   = (p(1)*h(1)*w*xf) / Q                        %% Time to fill (sec)

%% K1s( K1 steady @ h1)

P1_avr = mean(P(tadjust(1):tadjust(2)))
K1s = (Q * mu)/(w * h(1))* (xf
/P1_avr)                                           %% K1 steady permeability

%% K2s (K2 steady @ h2)

P2_avr = mean(P(tadjust(3):tadjust(4)))
K2s = (Q * mu)/(w * h(2))* (xf
/P2_avr)                                           %% K2 steady permeability

%% K3s (K3 steady @ h3)

P3_avr = mean(P(tadjust(5):tadjust(6)))
K3s = (Q * mu)/(w * h(3))* (xf /P3_avr)            %% K3 steady permeability

%% K4s (K4 steady @ h4)

P4_avr = mean(P(tadjust(7):tadjust(8)))
K4s = (Q * mu)/(w * h(4))* (xf /P4_avr)            %% K4 steady permeability

%% K5s (K5 steady @ h5)

P5_avr = mean(P(tadjust(9):tadjust(10)))
K5s = (Q * mu)/(w * h(5))* (xf /P5_avr)            %% K5 steady permeability
```

```
figure(3)
K   = [K1s K2s K3s K4s K5s K6s K7s];
semilogy(Vf,K,'ro-','linewidth',2),grid,
xlabel('Fiber Volume Fraction [Vf]'), ylabel(' Permeability [m2]')

xlabel('Fiber Volume Fraction'), ylabel('Permeability [m2]')
print -djpeg fig_permeability_vs_Vf
```

App B.3. Matlab code (**load_cell_amp.m**) for data transfer of mass of test fluid in reservoir (m) from digital weighting machine to the computer and online drawing of m versus t (time).

```
function load_cell_amp()

port = 'COM5';

close all;

delete(instrfindall('Name',['Serial-' port]));

SP = serial(port,'BaudRate',9600);
SP.Terminator={'CR/LF' 'CR/LF'};
fid = fopen('14Wh.txt','a+');
fopen(SP);
c = onCleanup(@()fclose(fid));
tic;
i=0;

tOld  = rem(now,1)*1e5;
fOld = 0;

while 1
    i=i+1;
    dispnum=[];
    while isempty(dispnum)
        dispnum=fscanf(SP,[2 43 '%f' 13 10]);
    end
    force=dispnum/1e4;
    time=rem(now,1)*1e5;

    if rem(i,8) == 0
        fprintf(fid,'%.2f\t%.3f\n',time,force(end));
    end
    plot([tOld time],[fOld force(end)],'-r','linewidth',2),  grid on,hold on
    xlabel('Time [s]'), ylabel('Mass [kg]')

    tOld  = time;
    fOld = force(end);

    drawnow;
end
end
```

App B.4. Matlab code (**constantP_unsteady.m**) for x_f (t) first order curve fit to data and K_{uns} permeability calculation for 1D continuous permeability measurement experiment with constant P.

```
clear all,close all,clc
disp('8R_1 experiment result')
%%% x(t) = A*t.^2  is expected
%%% for the following experimental data:
ts = 107;
x = [0 2 4 6 8 10 12 14 16 18 20 22 24 26 28]'*1e-2;
t = [107 109 111 115 120 125 132 142 152 166 180 194 208 224 246]'-ts;
C  = [x.^2];
d  = (C'*C)\(C'*t);
A  = d;
xx  = linspace(x(1),x(end),1000);
tt  = A*xx.^2;
figure(1)
plot(t,x,'ro', tt,xx,'b-', 'linewidth',2)
grid on, xlabel('t'), ylabel('x')
legend('Experimental Data','Curve fit: x(t) = A*t^2',0)

%% Permeability Calculation
%%% t = A*x^2;
%%% A = (mu*po)/(2*K*Pin);
%%% K = (mu*po)/(2*A*Pin);
N   = 8;                  % Number of fiber layer
mu  = 0.199;              % Pa.s
Pin = 20000;              % Pa
w   = 100;                % mm
h   = 4;                  % mm
L   = 300;                % mm
qs  = 275;                % Superficial density of fiber [kg/m^2]
qf  = 2540;               % Density of fiber [kg/m^3]

Vf =((qs*N)/(qf*h));
po = 1-Vf;
Kuns = (mu*po)/(2*A*Pin)
fprintf('When Vf is %5.5f, permeability is %g\n',Vf,Kuns)
```

App B.5. Matlab code (**constantP_steady.m**)for Ks (steady permeability) calculation for 1D permeability measurement experiments with constant pressure.

```
clear all,close all,clc
disp('1D Permeability Experiment at Constant Pressure')
A = load('10R.txt');
t  = A(:,1);
m  = A(:,2);

 figure(1)
 plot(t,m,'b-', 'linewidth', 2)
 grid on, xlabel('Time, t [s]'), ylabel('Mass of resin, m [kg]')
 ylim([-5 5])
 legend('raw data',0)

%%%%%%%%%%%%%%%%%%%%%%%%%%%%%%%%%%%%%%%%%%%%%%%%%%%%
I = find(m>0.6 & m<1.7);
%%%%%%%%%%%%%%%%%%%%%%%%%%%%%%%%%%%%%%%%%%%%%%%%%%%%

T = t(I);
M = m(I);
T = T - T(1);         %% Absolute time
M = M - M(1);         %% Absolute mass

%% Data filtering
[fa,fb]=besself(3,.1);
[fa,fb]=bilinear(fa,fb,1);
mfiltered = filtfilt(fa,fb,M);
NN = 10000;
tt        = linspace(T(1),T(end),NN);
mm        = spline(T,mfiltered,tt);


 figure(2)
 plot(T,M,'b-',  'linewidth', 2)
 grid on, xlabel('Time, t [s]'), ylabel('Mass of resin, m [g]')
 ylim([-0.5 0.5])
 legend('raw data','filtered','equally-spaced data',0)


 MR = -M;
 mfilteredr = -mfiltered;
 mmr = -mm;
 figure(3)
 plot(T,MR,'b-o', T,mfilteredr,'r-',tt,mmr,'k-', 'linewidth', 2)
 grid on, xlabel('Time, t [s]'), ylabel('Mass of resin, m [g]')
 ylim([-0.1 0.2])
 legend('raw data','filtered','equally-spaced data',0)
 hold on
```

APPENDIX B

```
%%%%%%%%%%%%%%%% In each thickness experiment, enter these data:
 mu = 0.190;                              % Pa.s
 w  = 0.1;                                % m
 L =  0.3                                 % m
 DP = 100e3;                              % Pa
 rho = 1250;                              % kg/m^3
 N   = 8;
 qs  = 0.395                              % kg/m^2
 qf  = 2540 ;                             % kg/m^3
 h   = 0.0045;                            % m
 T1  = 500;
 T2  = 1250;
 Vf =((qs*N)/(qf*h));
 po = 1-Vf;

%%%%%%curve fit to m(t)data

 J = find(T>T1 & T<T2);
 P = polyfit(T(J),MR(J),1);
 TTT = linspace(T1,T2,100);
 MMM = polyval(P,TTT);
 dMdt = P(1)                            % kg/s
 Q = dMdt/rho                           % m^3/s
 plot(TTT,MMM,'g-','linewidth',3)
 hold off
 K = (Q*mu*L)/(w*h*DP)                  % m^2 (Steady permeability)

 fprintf('When Vf is %5.5f, permeability is %g\n',Vf,K)
```

APPENDIX C

EXPERIMENTAL EQUIPMENTS & SPECIMENS

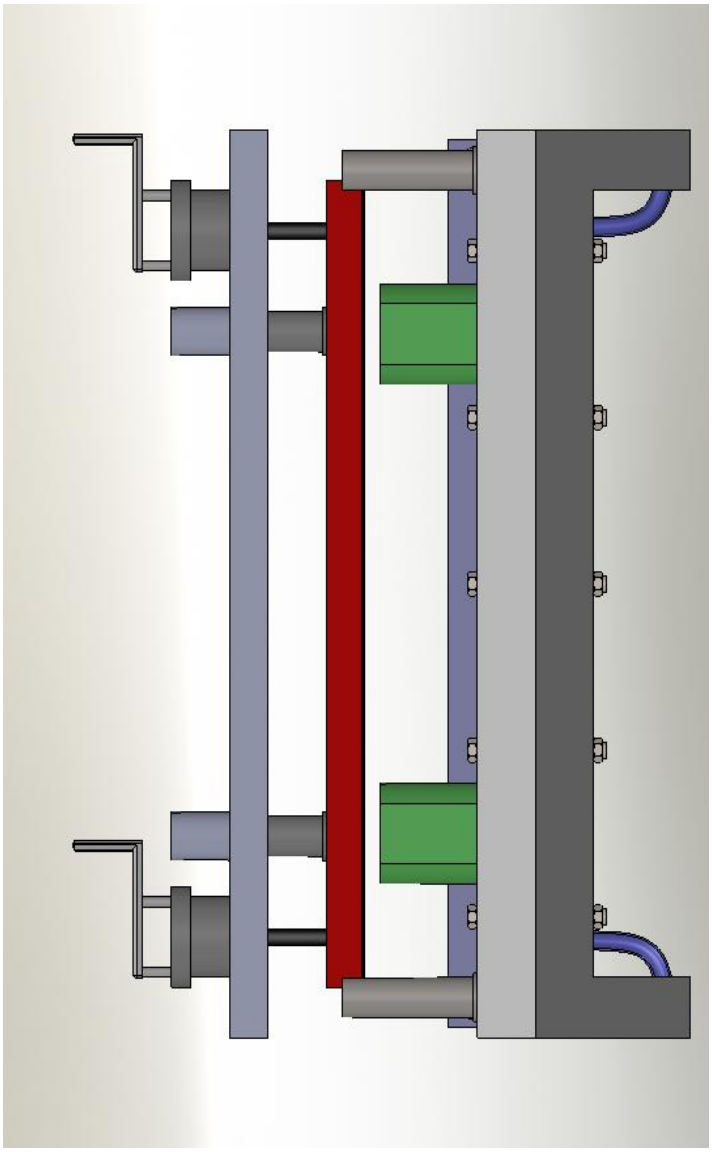

App C.1. 3D visualization of side view of the1D mold [26].

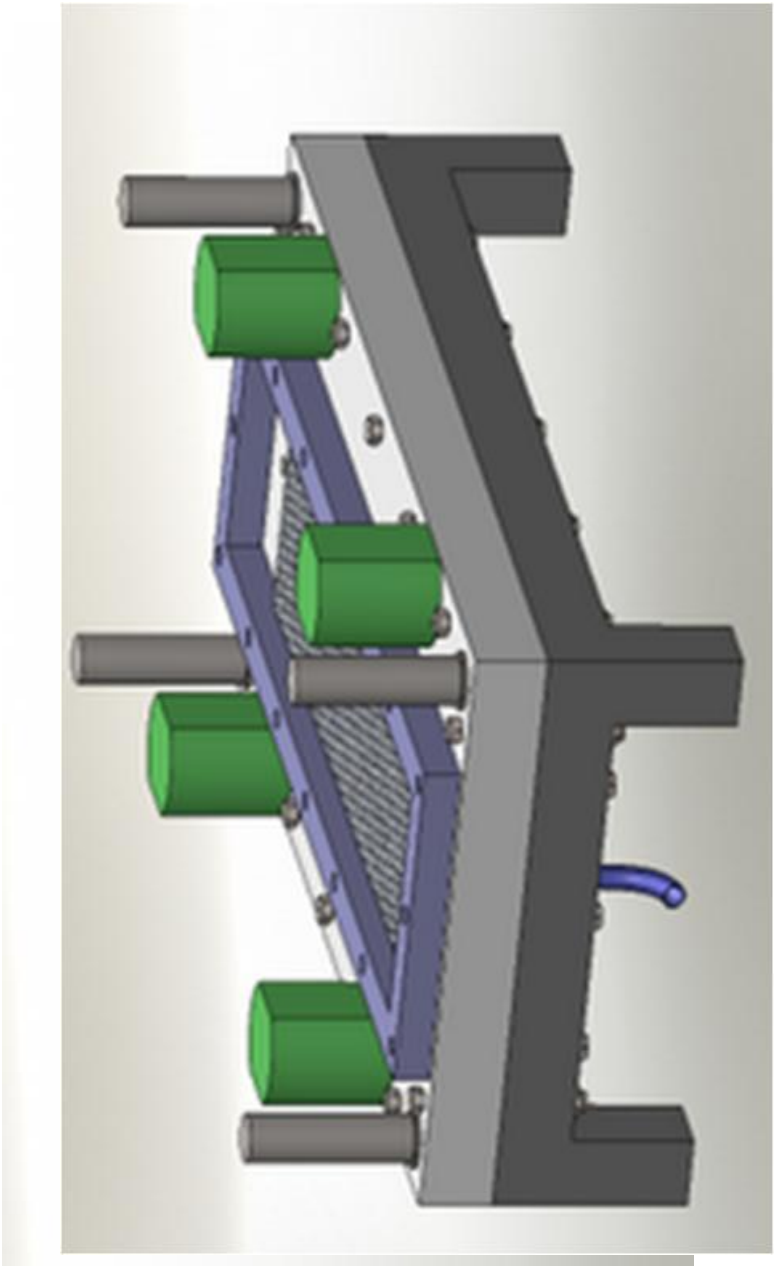

App C.2. 3D Visualization of male plate of the 1D mold [26].

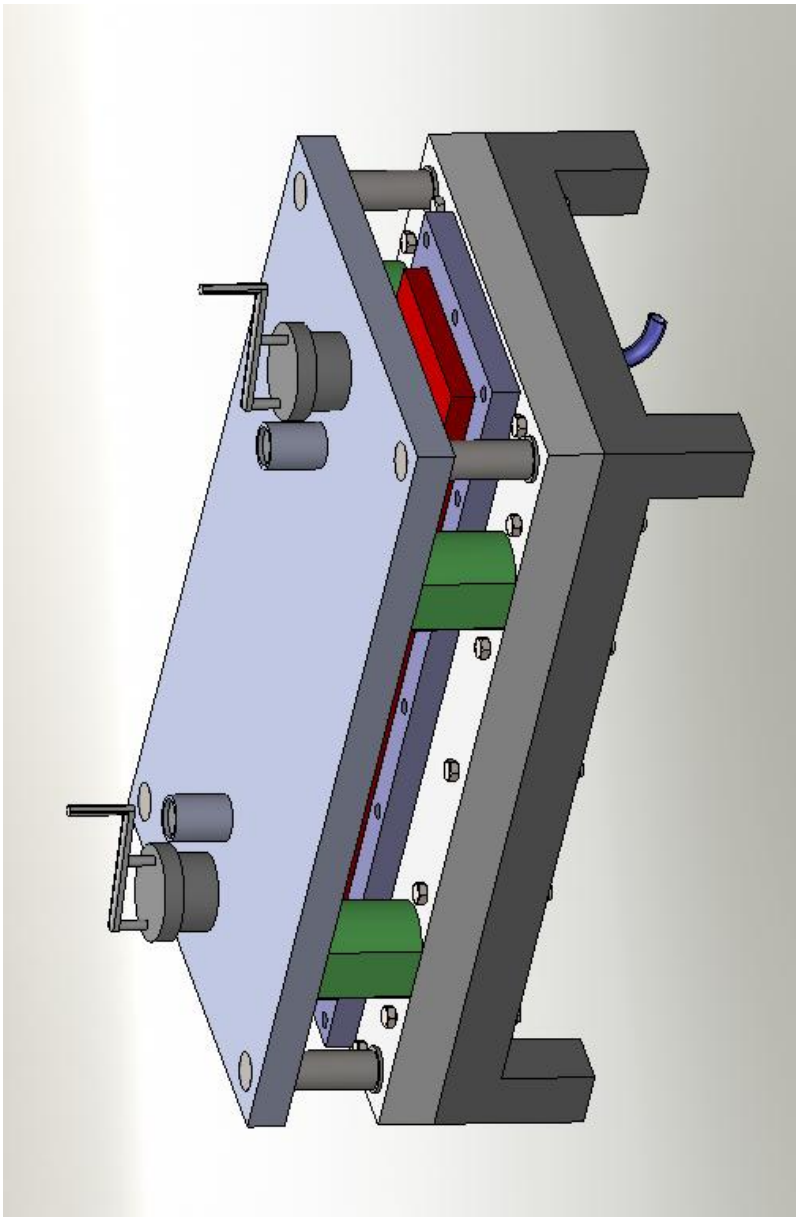

App C.3. 3D visualization of top view of the 1D mold [26].

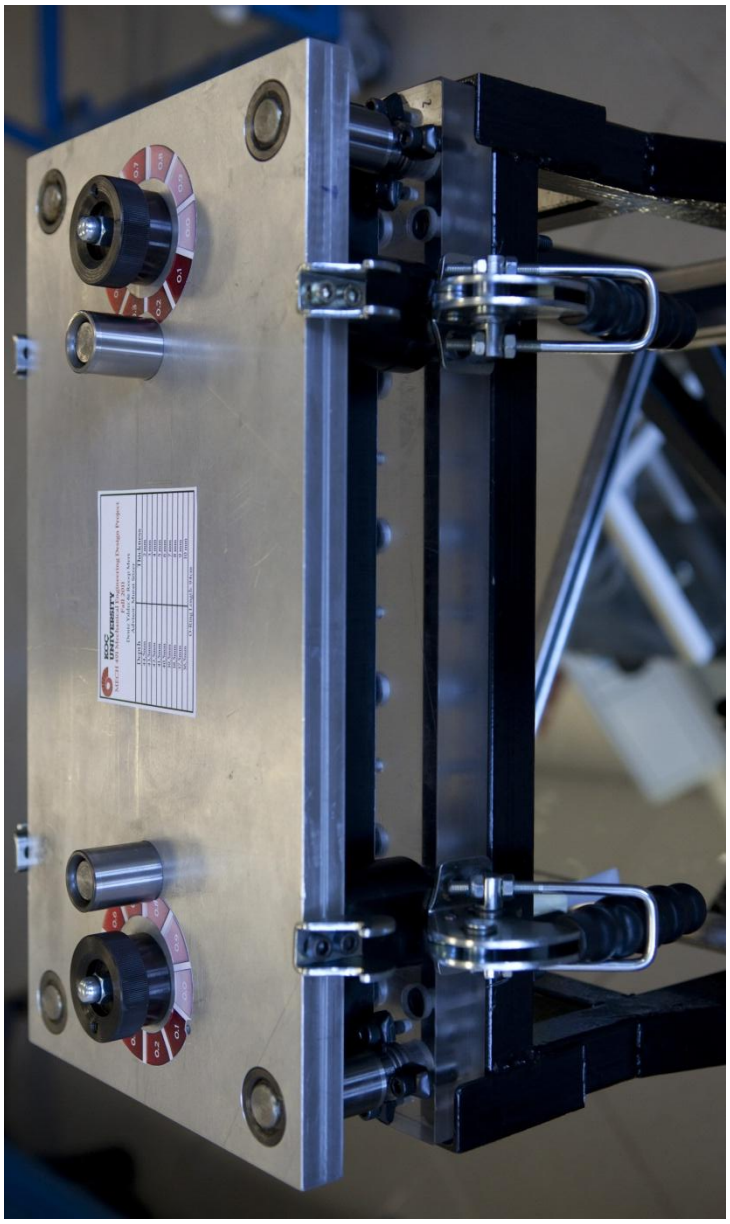

App C.4. Top view of the 1D mold .

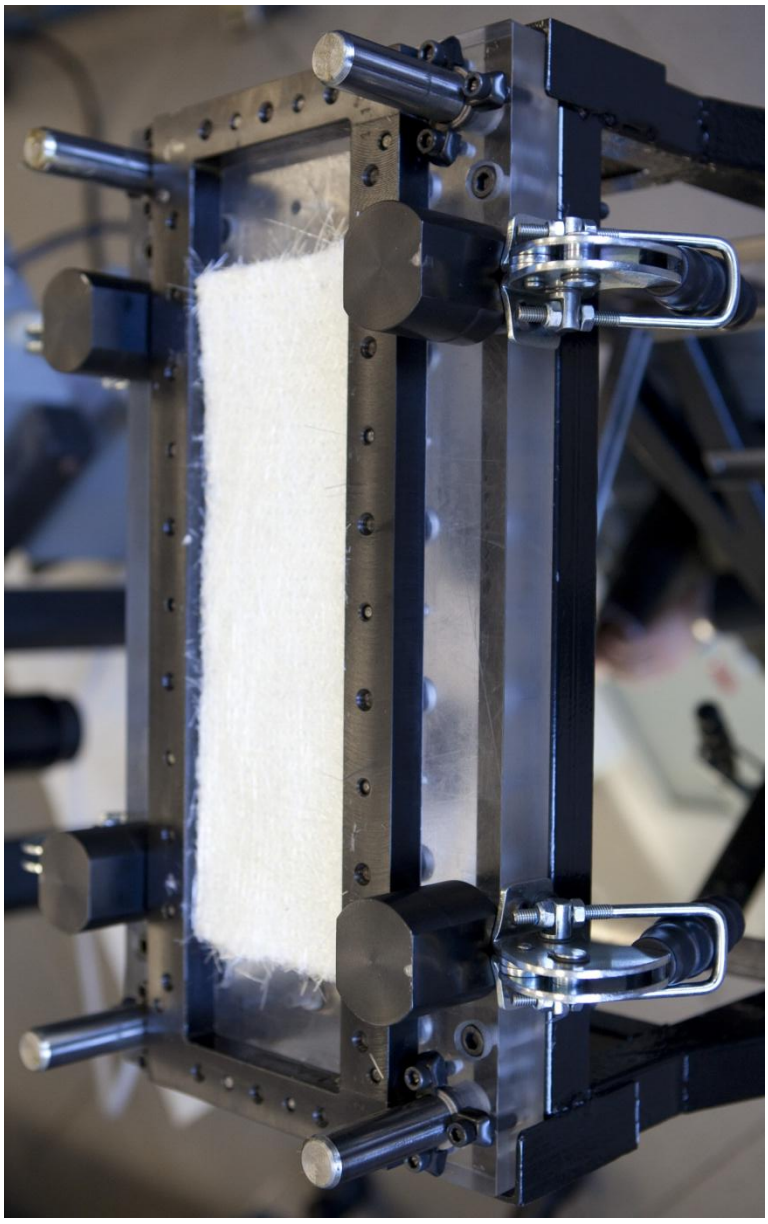

App C.5. Mold cavity of the 1D mold.

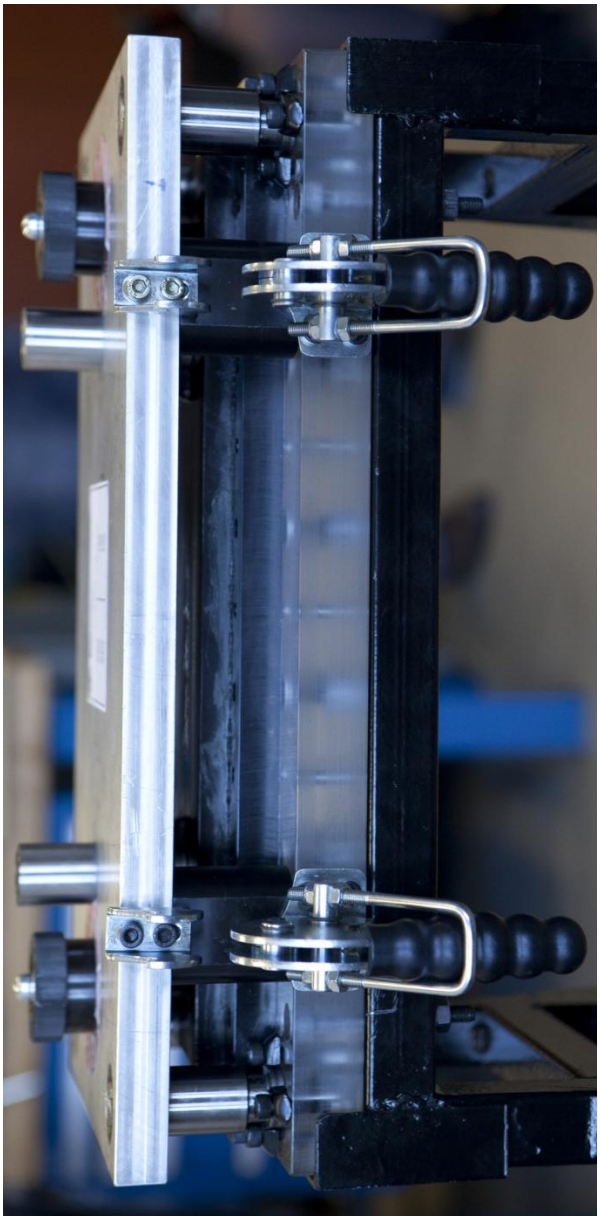

App C.6. Side view of 1D mold

App C.7. Metallic lower plate for 2D experiments.

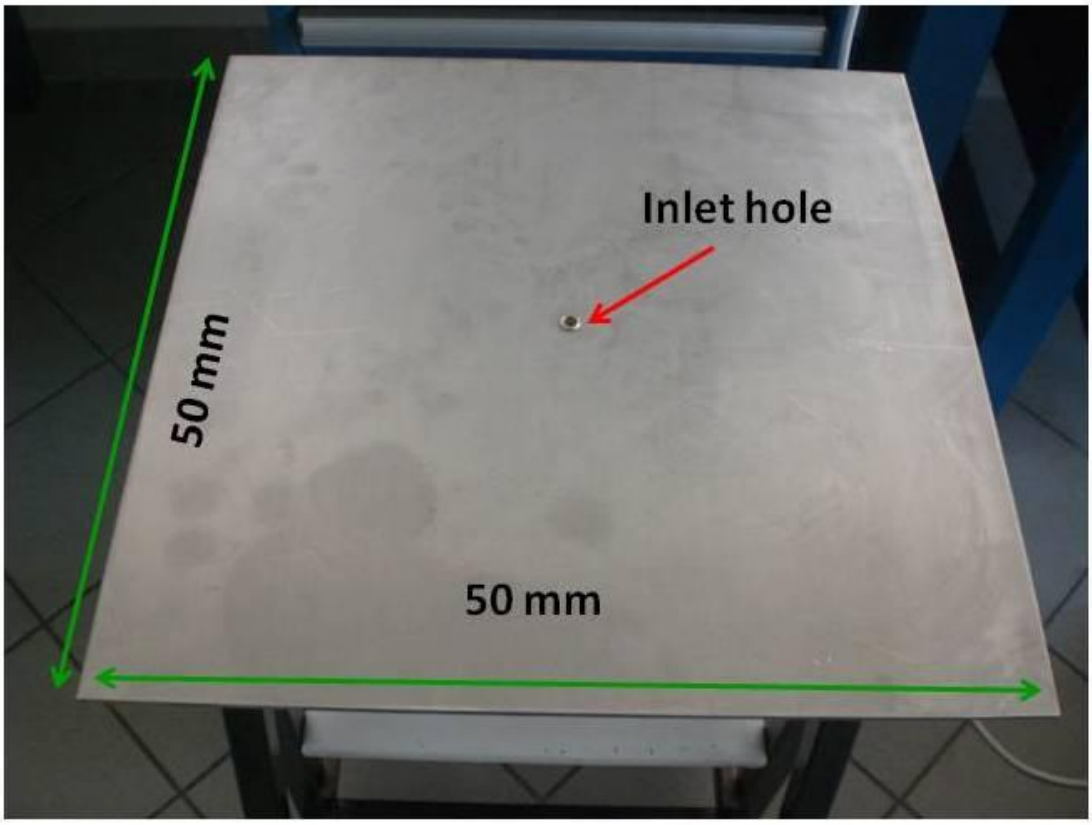

App C.8. Glass upper plate for 2D experiments.

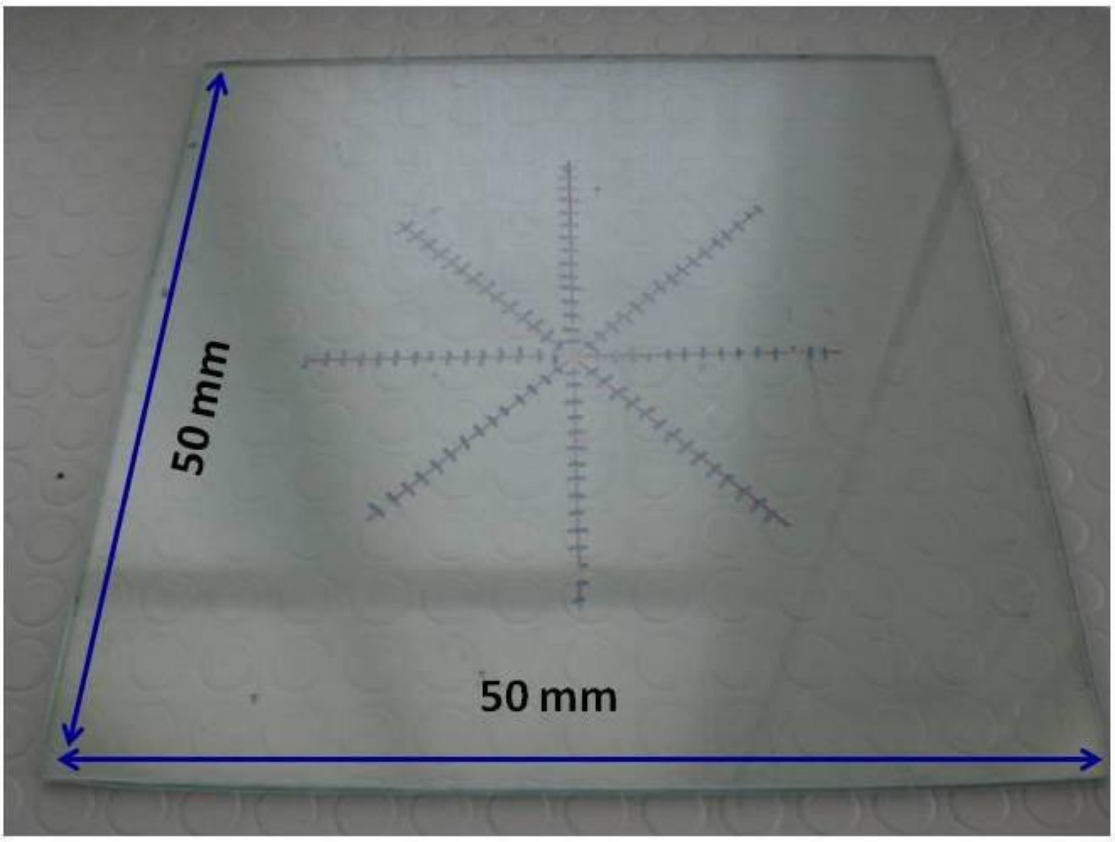

App C.9. Radius Engineering 2100cc, flow rate-controlled injection machine

Manufacturer:	Radius Engineering Inc., Utah, A.B.D. (RADIUS)
Model:	Radius 2100 cc Electric RTM Injection Cylinder
	Version 5.17.2001
Capacity of polymer:	2100 cc
Polymer types:	Thermoset (applicable to RTM)
Maximum injection pressure:	27.5 bar (= 2.7 MPa = 400 psi)
Heating system:	Electrical heater around injection cylinder and tubes
Maximum temperature:	176°C (= 350°F)
Control:	PID temperature control
	Flowrate control
	Injection pressure set points
Power:	4.8 kW (240 V, 20 amp)

App C.10. ALCATEL PASCAL 2100 SD vacuum pump

App C.11. NDJ-5S digital rotary viscometer

Range of Measurement of Viscosity	10- 100000 mPa.s (cP)
Rotors to be used to measure	Four rotors of NO. 1-4
Rotate speed	6r/min, 12r/min,30r/min,60r/min
Meterage error	± 5% (Newtonian fluids)
Electrical power	220V/50Hz
Weight	10 kg
Dimensions	308mmx30mmx450mm (LxWxH)

App C.12 Dial gages

Range (mm)	Resolution (mm)	A (mm)	Dia (mm)	Accuracy (mm)
0 - 10	0.01 / 0.001	8.00	2.50	0.03

App C.13. Digital caliper (Produced by Mitutuyo U.S.A.)

App C.14. Latches

App C.15. Punch

App C.16. Cutter

App C.17. Glucose syrup used in this study.

Trade Name	**Brand**
GF40 Glucose Fructose Blend	Doğal Katkı Malzemeleri, Bayrampaşa, İstanbul.

App C.18. Specimens used in the 1D permeability measurement experiments.

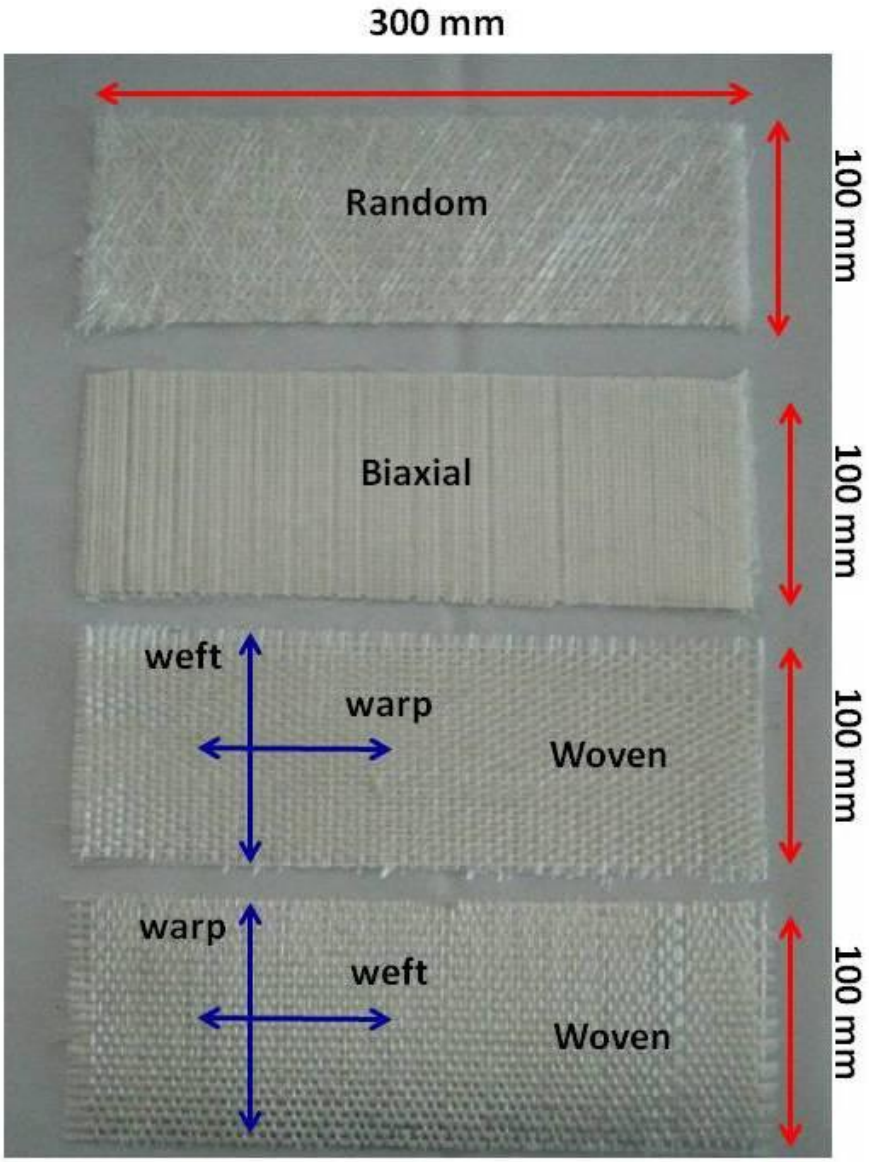

App C.19. Specimens used in the 2D permeability measurement experiments.